A FUNCTIONAL DESIGN METHODOLOGY WITH GENETIC ALGORITHM OPTIMIZATION TO A DOOR ACTUATION MECHANISM

A THESIS SUBMITTED TO
THE GRADUATE SCHOOL OF NATURAL AND APPLIED SCIENCES
OF
MIDDLE EAST TECHNICAL UNIVERSITY

BY

HASAN AKMAN

IN PARTIAL FULFILLMENT OF THE REQUIREMENTS
FOR
THE DEGREE OF MASTER OF SCIENCE
IN
MECHANICAL ENGINEERING

SEPTEMBER 2019

Approval of the thesis:

A FUNCTIONAL DESIGN METHODOLOGY WITH GENETIC ALGORITHM OPTIMIZATION TO A DOOR ACTUATION MECHANISM

submitted by **HASAN AKMAN** in partial fulfillment of the requirements for the degree of **Master of Science in Mechanical Engineering Department, Middle East Technical University** by,

Prof. Dr. Halil Kalıpçılar
Dean, Graduate School of **Natural and Applied Sciences** _____

Prof. Dr. M.A. Sahir Arıkan
Head of Department, **Mechanical Engineering** _____

Assist. Prof. Dr. Ali Emre Turgut
Supervisor, **Mechanical Engineering, METU** _____

Dr. Hakan Çalışkan
Co-Supervisor, **Mechanical Engineering, METU** _____

Examining Committee Members:

Assist. Prof. Dr. Gökhan Osman Özgen
Mechanical Engineering, METU _____

Assist. Prof. Dr. Ali Emre Turgut
Mechanical Engineering, METU _____

Assist. Prof. Dr. Kıvanç Azgın
Mechanical Engineering, METU _____

Assist. Prof. Dr. Selçuk Himmetoğlu
Mechanical Engineering, Hacettepe University _____

Assist. Prof. Dr. Yiğit Taşçıoğlu
Mechanical Engineering, TOBB ETU _____

Date: 04.09.2019

I hereby declare that all information in this document has been obtained and presented in accordance with academic rules and ethical conduct. I also declare that, as required by these rules and conduct, I have fully cited and referenced all material and results that are not original to this work.

Name, Surname: Hasan Akman

Signature:

ABSTRACT

A FUNCTIONAL DESIGN METHODOLOGY WITH GENETIC ALGORITHM OPTIMIZATION TO A DOOR ACTUATION MECHANISM

Akman, Hasan
Master of Science, Mechanical Engineering
Supervisor: Assist. Prof. Dr. Ali Emre Turgut
Co-Supervisor: Dr. Hakan Çalışkan

September 2019, 123 pages

In this thesis, the preliminary design of an in-flight refueling door actuation mechanism is designed. A novel design methodology is introduced to create and evaluate different mechanism design alternatives systematically. The design is divided into two sub-problems. For each sub-problem, different conceptual design alternatives and evaluation criteria are created considering the design requirements. Suitable concepts are systematically selected among the alternatives based on the evaluation criteria. Then, detailed synthesis and analysis are performed on the selected concepts. After synthesis and analysis, selected concepts are optimized by using Genetic Algorithm. For each sub-problem, optimized mechanism concepts are compared one more time based on different criteria, and a suitable mechanism concept is selected. Lastly, mechanism concepts of each sub-problem are combined to obtain the best design of the in-flight refueling door actuation mechanism.

Keywords: Mechanism Synthesis, Mechanism Analysis, Mechanism Optimization, Genetic Algorithm

ÖZ

KAPI HAREKETLENDİRME MEKANİZMASI İÇİN GENETİK ALGORİTMA YÖNTEMİ İLE OPTİMİZASYONU YAPILAN BİR FONKSİYONEL TASARIM METODOLOJİSİ GELİŞTİRME

Akman, Hasan
Yüksek Lisans, Makina Mühendisliği
Tez Danışmanı: Doç. Dr. Ali Emre Turgut
Ortak Tez Danışmanı: Dr. Hakan Çalışkan

Eylül 2019, 123 sayfa

Bu tezde, havada yakıt ikmal kapağı hareketlendirme mekanizmasının ön tasarımı sunulmuştur. Farklı tasarım alternatiflerinin sistematik bir şekilde oluşturulması ve değerlendirilmesi amacı ile bir tasarım metodolojisi geliştirilmiştir. Tasarım iki alt probleme ayrılmıştır. Her bir alt problem için kavramsal olarak farklı tasarım konseptleri ve değerlendirme kriterleri tasarım gereksinimlerine göre oluşturulmuştur. Oluşturulan mekanizma konseptleri arasından, uygun mekanizma çözümleri belirlenen kriterlere göre sistematik olarak seçilmiştir. Seçilen mekanizma alternatifleri üzerinde detaylı sentez ve analiz çalışmaları yapılmıştır. Sentez ve analiz çalışmaları yapılan mekanizmalar Genetik Algoritma kullanılarak optimize edilmiştir. Her bir alt problem için, optimizasyonu yapılan mekanizmalar belirlenen farklı kriterlere göre karşılaştırılmıştır ve bu kriterlere göre en uygun mekanizma alternatifi seçilmiştir. Alt problemlerin seçilen mekanizma çözümleri birbirleri ile birleştirilerek havada yakıt ikmal kapağı hareketlendirme mekanizması için en uygun tasarım elde edilmiştir.

Anahtar Kelimeler: Mekanizma Sentezi, Mekanizma Analizi, Mekanizma Optimizasyonu, Genetik Algoritma

To my mother…

ACKNOWLEDGEMENTS

I would like to thank my supervisor, Assist. Prof. Dr. Ali Emre Turgut and my co-supervisor Dr. Hakan Çalışkan for their support, guidance, patience, knowledge and suggestions throughout the research.

I would like to express my sincere gratitude to Prof. Dr. Eres Söylemez for his guidance and insight throughout the research.

I would like to express my thanks to my manager Dr. Özkan Altay and my colleagues Sinan Küçük, Burak Güzeller, Çağatay Koyuncuoğlu, Mark Chalmers, Talha Öz, Ali Akçay and Fatih Yıldız for their supports and presences during this study.

I am grateful to my family for their love and support throughout my life.

I would also like to thank my dear friends Doğacan Bahan, Baran Özmen and Ersin Altın for their supports.

Finally, I am severely grateful to Tuğba for her support and patience.

TABLE OF CONTENTS

LIST OF TABLES

TABLES

LIST OF FIGURES

FIGURES

CHAPTER 1

INTRODUCTION

1.1. General

Mechanisms are mechanical devices that are being used intensively in aerospace industry. The design of a mechanism is an activity in which the engineer faces difficult tasks. Experience and ingenuity are applied to combine a wide variety of mechanical elements with different functions to satisfy space restrictions and functional requirements. Designing of a mechanism is a recurring and iterative process. In the first stage, several types of mechanisms are synthesized and analyzed iteratively to reach an acceptable optimum solution that satisfies the requirements. The synthesis step can be divided into two main parts, which are type synthesis and dimensional synthesis. Type synthesis is performed to find different suitable configurations, which are combinations of different types of mechanisms (such as cams, linkages, gear-trains) for the desired function. Then, dimensional synthesis is applied to determine the dimensions of the mechanism, which satisfies the desired motion characteristic.

In dimensional synthesis, different methods are available such as graphical and analytical methods. One of the most common analytical methods is prescribed position synthesis. Additionally, different optimization methods can be applied for synthesis purposes. In the optimization process, the error function is defined to minimize the error between realized output and the desired output. On the other hand, prescribed position synthesis determines the mechanism dimensions exactly satisfying some prescribed positions of the desired motion.

In the kinematic synthesis of mechanisms, designer’s intuition and experience play a significant role compared to the other design stages, although synthesis problems require the solution of mathematical or geometrical systems as well. The calculation

procedure does not provide a unique solution; therefore, engineers have to use their intuition and experience to select the most suitable mechanism among the possible combinations.

In the synthesis stage, computers are extensively used. The computer programs can reach the best solutions with user interaction. Systematizing the synthesis problem stages using computer programs reduces engineer's efforts and design time.

1.2. Aim of the Study

The aim of this thesis is to synthesize an in-flight refueling door actuation mechanism with a systematic and general design methodology to determine suitable mechanism options. The mechanism should provide the desired motion to get the required clearance when the in-flight refueling door is open. Additionally, the mechanism should be optimized based on different criteria.

1.3. Outline of the Thesis

In this thesis, the development of an in-flight door actuation mechanism for aircraft is presented. The details of the design process are discussed in the following chapters. In Chapter 2, the literature survey is presented. In Chapter 3, the method used for the design process is explained. In Chapter 4, the conceptual design stage of the mechanism is presented. Firstly, different mechanisms are created conceptually. A concept evaluation criteria will then be defined. Lastly, each concept, in turn, is evaluated against the concept evaluation criteria by experienced mechanical design engineers to obtain the most suitable concept systematically among the created alternatives. In Chapter 5, the detailed design of the selected concepts is described. Firstly, the kinematic synthesis is performed to obtain the required door positions concerning geometric restrictions. Next, kinematic analysis is done to analyze the motion of concepts. Finally, force analysis is performed to obtain the required forces during the motion. In Chapter 6, mechanism optimization is done by using a Genetic Algorithm Method. Firstly, objective functions and constraints are determined. Then, the optimization process is performed to find the optimum solution. Additionally,

results are discussed, and different optimized concepts are compared to select one of them. In Chapter 7, the thesis is concluded, and some recommendations for future work and future improvements are given.

CHAPTER 2

LITERATURE SURVEY

2.1. State of the Art

Different door opening mechanisms are studied in the literature. One of the opening mechanisms is a swing plug door [1], which is detailed in Figure 2.1. This four-bar mechanism consists of only revolute joints. Additionally, the door is opened laterally. Therefore, the door requires little space in the open position. The same mechanism type is used for luggage door mechanisms on commercial vehicles as detailed by Baykus, Anli, and Ozkol [2]. They mentioned that the parallel-hinged system has a narrow and safe trajectory and takes up less space when fully open.

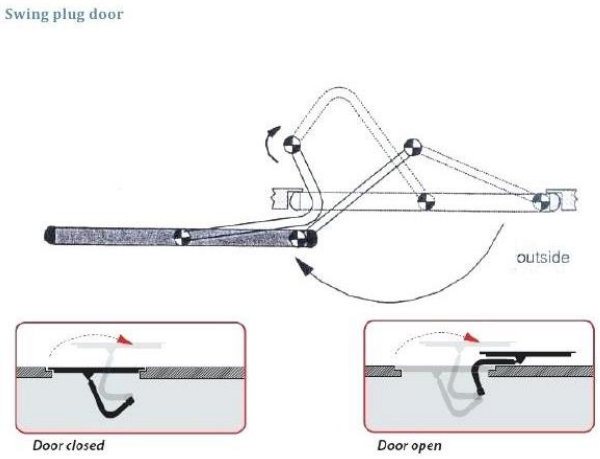

Figure 2.1. Swing plug door mechanism of bus door [1]

N.D. Thang designed different multi-link door hinge mechanisms for several purposes [3]. Some of N.D. Thang's designs are given in Figure 2.2.

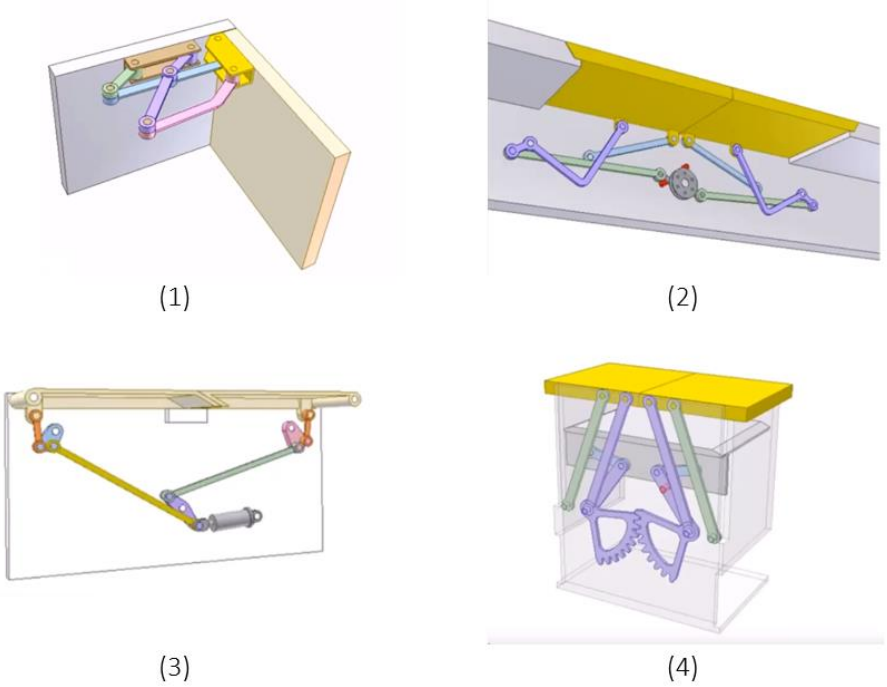

Figure 2.2. Thang's designs

Another multi-link door mechanism is an invisible hinge introduced by Joseph Soss in 1921 [4]. His original drawings are shown in Figure 2.3. As can be seen, this hinge is partly contained inside the thickness of the door and partly inside the thickness of the frame. This design allows the door to open up to 180° and meanwhile does not exhibit the hinge externally when the door is in the closed position. Toropov and Robertis [5] improved an analytical approach that can be used as a tool for the design of the concealed hinge which allows having a desirable trajectory of the door movement. The schematic presentation of the 5-axis invisible hinge is given in Figure 2.4.

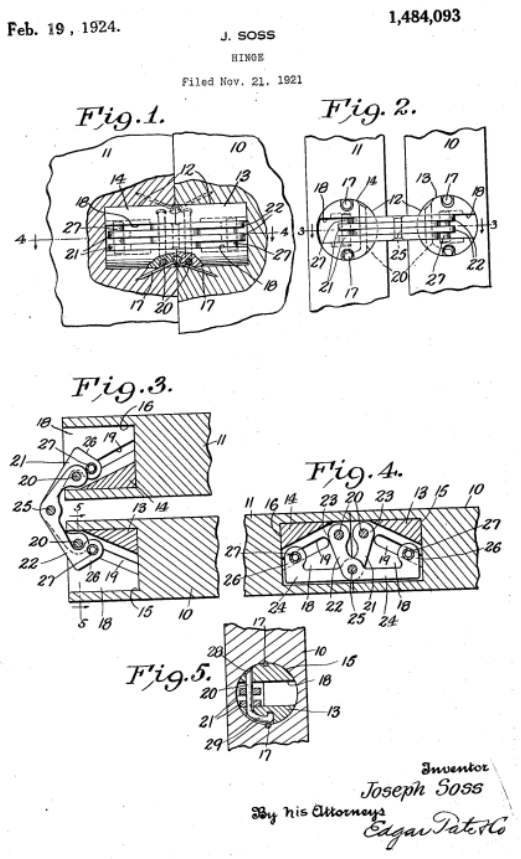

Figure 2.3. Drawings of invisible hinge invented by Joseph Soss in 1924 [4]

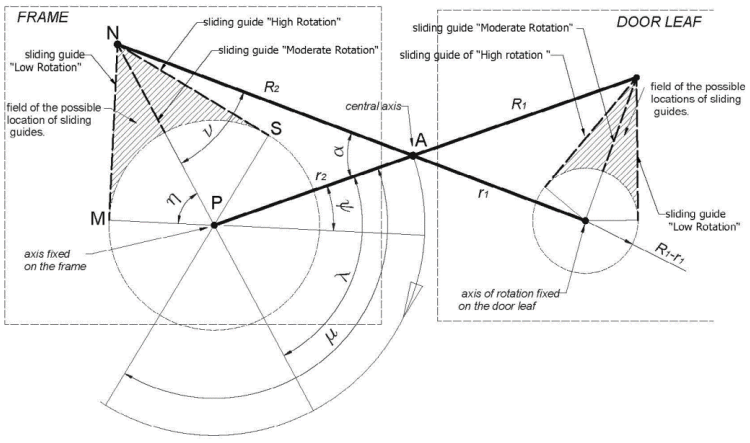

Figure 2.4. The schematic presentation of the invisible hinge mechanism [5]

Different types of mechanisms are also used to obtain symmetric motion. Gripper mechanisms are one of the examples of this type of mechanism. Lanni and Ceccarelli used industrial two-finger gripper, which is powered and controlled by one actuator in their corresponding study [6]. Details of the gripper mechanism is shown in Figure 2.5. A prismatic joint and revolute joints are combined to actuate the gripper mechanism symmetrically.

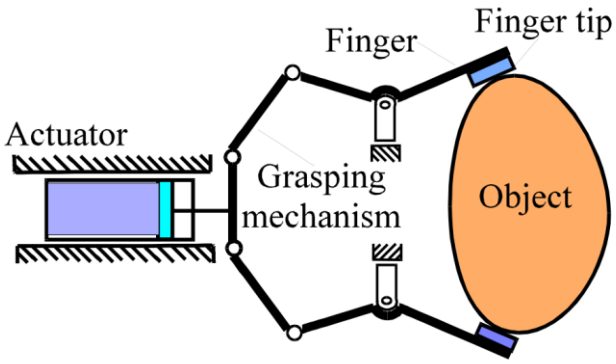

Figure 2.5. Two-finger gripper representation [6]

Another two-finger gripper mechanism is introduced by Nuttall and Breteler [7]. One inverted-crank mechanism is used in a piston-cylinder arrangement, and two four-bar mechanisms is used to transmit the motion two sides of the gripper. One actuator is used to control and actuate the gripper mechanism. Representation of the corresponding mechanism is shown in Figure 2.6.

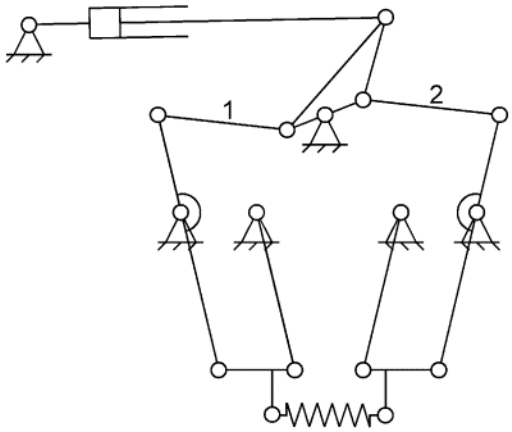

Figure 2.6. Schematic of two-finger gripper mechanism [7]

2.2. Synthesis and Optimization of Mechanism

Different mechanism synthesis and optimization methods are presented with the following sections.

Graphical approaches are one of the synthesis methods of the mechanisms. These methods are quick and relatively easy, but parameters cannot be easily manipulated to create new solutions[8]. Graphical approaches are simple to synthesize a four-bar mechanism with two and three prescribed positions [9]. However, these methods are not enough to find an optimal solution in the case that has constraints on ground and moving point locations, link length ratio, mechanical advantage, or transmission angle. A graphical approach is a simple method; however, the iterative process is needed to find a suitable solution [9].

Analytical methods are alternative to graphical approaches. The solution procedure usually consists of several mathematical techniques to prepare the analytical formulation. These mathematical techniques are algebraic methods, matrix methods, and complex number technique. The complex number technique is the simplest and most versatile method in order to synthesize the planar mechanism [9].

Optimization methods are alternative solutions to synthesize and optimize mechanisms. In the recent years, optimization algorithms have become popular. Many

researchers have focused on the development and application of optimization algorithms to synthesize and optimize mechanisms. One of the optimization methods is Genetic Algorithm (GA), which is an evolutionary search method that is inspired by natural evaluation. Genetic Algorithms constitute a class of search algorithms especially suited to solving complex optimization problems. The main advantages of GA are its simplicity in implementing the algorithms and low computational time/cost. GA manages a population of solutions to a problem by its genetic operators and allocates a fitness value to each individual. Better solutions are combined, and then new individuals of the populations are created. This procedure drives the individuals to a better point in the search space of the problem. GA consists of four subroutines, which are evolution, selection, crossover, and mutation [10], [11].

Kunjur and Krishnamurty (KK) used a modified GA to synthesize 18-point path generation with prescribed timing [10]. They compared their results with Finite Difference (FDM) and Exact Gradient (EGM) Methods as shown in Figure 2.7.

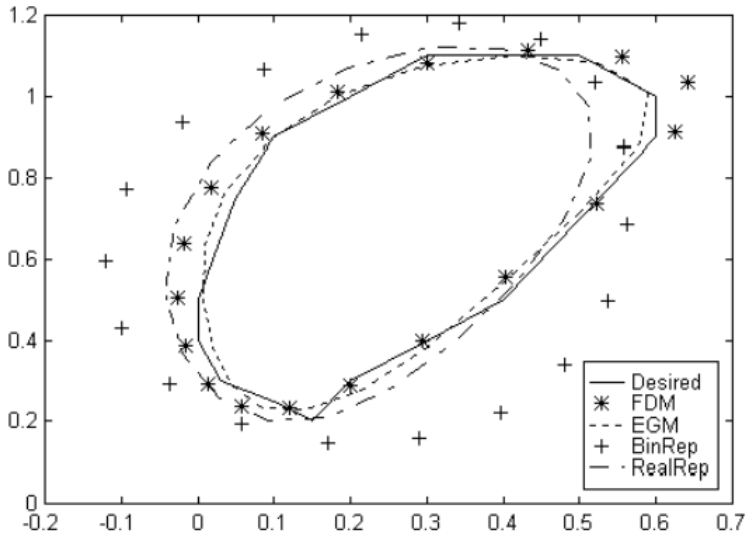

Figure 2.7. Comparison of desired and generated paths (18 point synthesis) [10]

Cabrera, Simon, and Prado [11] modified the definition of the objective function, by using penalty factors and use individual genetic operators to obtain a faster process and to improve the accuracy of the final solution compared to Kunjur and Krishnamurty study. Their proposed algorithm scheme is depicted in Figure 2.8.

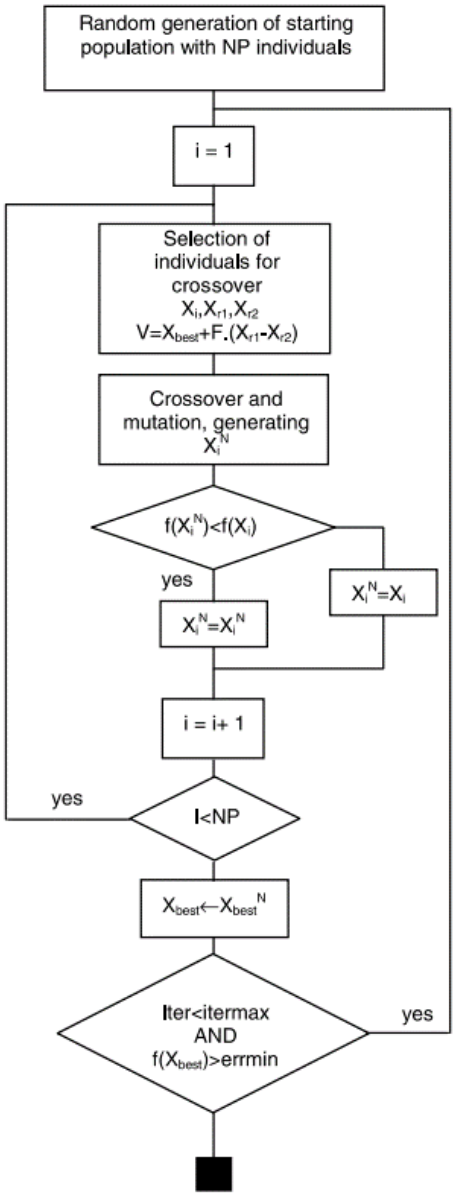

Figure 2.8. J.A. Cabrera, A. Simon, and M. Prado GA Algorithm [11]

Their result are detailed in Table 2.1, and the tracked path of the couplers of the resulting mechanisms from the different methods are shown in Figure 2.9. Results show that the exact gradient method gives better results compared to other methods. However, gradient-based methods involve the computation of the first-order derivative; therefore, a time cost penalty will be a disadvantage of the gradient-based methods. In this paper, the proposed algorithm is better than the GA-KK algorithm [10].

Table 2.1. *Results of the different optimization methods* [11]

	Central difference	Exact gradient	Genetic algorithm KK	Proposed algorithm
$N°$ evaluations	505	240	5000	5000
Final error	2.66×10^{-2}	1.68×10^{-2}	4.30×10^{-2}	2.45×10^{-2}
r_1	2.80000	2.85452	1.879660	3.057878
r_2	0.36000	0.36355	0.274853	0.237803
r_3	2.91000	2.91374	1.180253	4.828954
r_4	0.49845	0.49374	2.138209	2.056456
r_{cx}	1.023716	1.031223	−0.833592	0.767038
r_{cy}	1.718140	1.717471	−0.378770	1.850828
x_0	0.95000	0.95928	1.132062	1.776808
y_0	−1.18289	−1.19645	0.663433	−0.641991
θ_0	0.75999	0.76398	4.354224	1.002168
θ_2^1	0.51000	0.51172	2.558625	0.226186

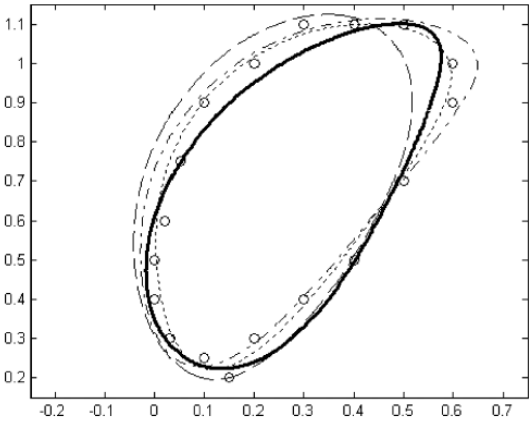

Path tracked by the solutions to case 3 from different methods along with target points. (· · ·): exact gradient method; (—): KK algorithm; (▬): proposed method; (– · – · –): central difference; (○): target points.

Figure 2.9. Results of the different optimization methods [11]

Another study is a combined Genetic Algorithm–fuzzy logic method (GA–FL) in mechanisms synthesis [12]. This optimization method is based on the classical GA.

Additionally, the fuzzy logic controller evaluates different variables during optimization and adjusts the boundary conditions of each design variable to increase the accuracy of the final result. They showed that different runs with different boundary conditions provide different results. Therefore, they improved this method to find the best choice of the bounding interval. Figure 2.10 shows the modified GA-FL optimization scheme.

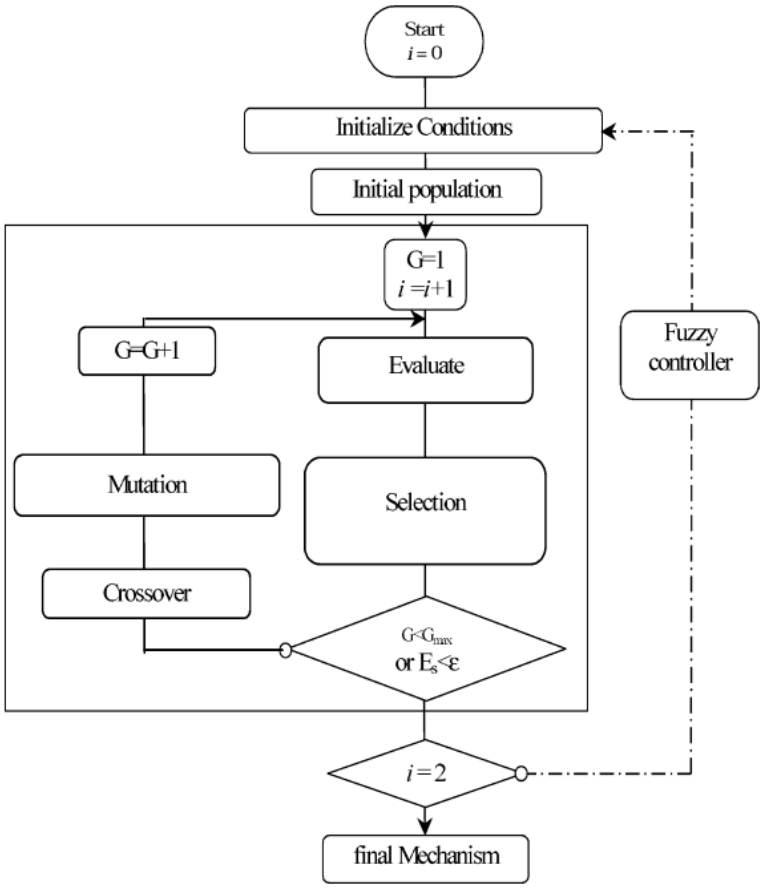

Figure 2.10. The GA-FL Optimization Scheme [12]

Figure 2.11 shows a comparison of the different GA optimization methods. The figure shows that the GA-FL method gives better results than other methods.

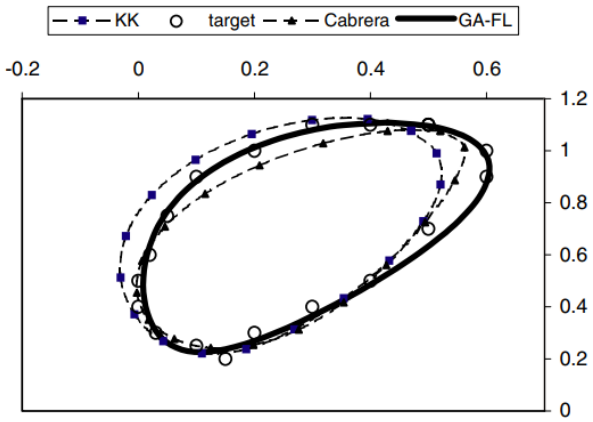

Figure 2.11. Comparison of the different GA optimization methods [12]

A Multi-objective optimization approach using the Genetic Algorithm is explained in [13]. In this study, the backhoe-loader mechanism, which is a complex mechanism with 11 linkages and two degrees of freedom was optimized. The optimized parameters are, dump height, digging depth, location, and interface of joints and, bucket and arm breakout forces and lift capacity. The corresponding mechanism, dump height, and digging depth are shown in Figure 2.12.

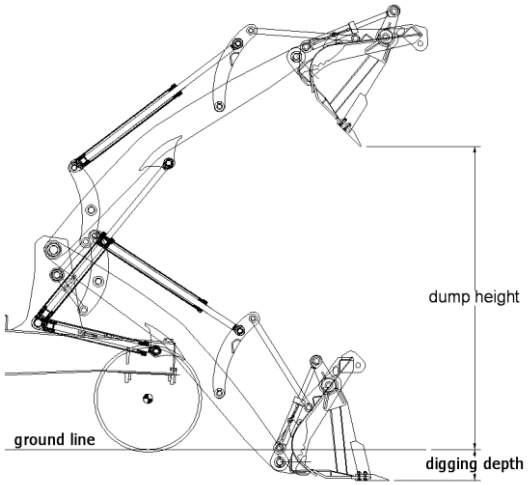

Figure 2.12. Dump height and digging depth [13]

In this study, the Genetic Algorithm was applied by using MS EXCEL. The developed optimization scheme is given in Figure 2.13.

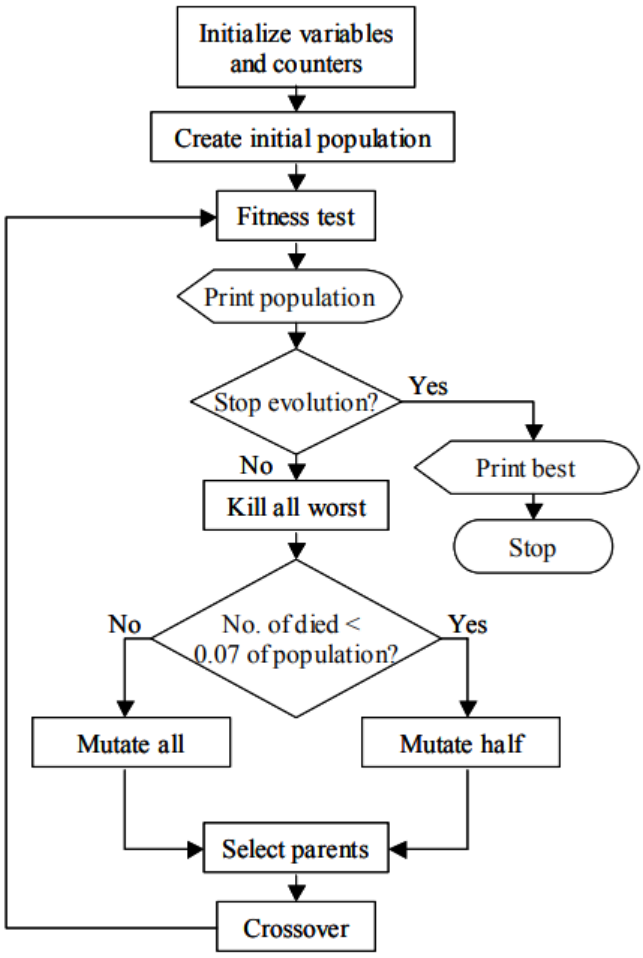

Figure 2.13. The GA Optimization Scheme [13]

After optimization, there are significant percent improvements in the breakout forces and lift capacity are detailed in Table 2.2. Results show that using GA improves the complex Backhoe-Loader Mechanism. Therefore, multi-objective GA can be applied to different complex mechanism problems.

Table 2.2. *Percent of improvements in breakout forces and lift capacity [13]*

	#1	#2	#3	#4
Arm Breakout Force	13.1 %	9.0 %	4.6 %	13.7 %
Bucket Breakout Force	6.2 %	2.5 %	-1.0 %	6.8 %
Lifting Capacity	3.1 %	1.2 %	3.0 %	2.7 %

CHAPTER 3

METHOD

3.1. Introduction

In this thesis, the approach to design consists of concept generation, evaluation, kinematic synthesis and analysis of mechanism, and optimization processes as listed as follows:

- Problem is defined and subdivided into sub-problems
- Concepts and evaluation criteria are created for each sub-problem
- Each concept is evaluated by the designer based on the determined evaluation criteria
- Best two or three concepts are chosen according to evaluation results
- This procedure is repeated till two or three concepts are chosen for each sub-problem
- Kinematic synthesis for each concept is performed
- Position and force analysis for each concept is performed, and the
- Optimization of each concept is performed based on defined objective functions by using a Genetic Algorithm optimization method
- Different design alternatives are created by combining one of the selected concepts from each sub-problem for the defined problem
- Created design alternatives are compared based on different criteria such as power requirement, weight, cost space requirement, and then the optimum design solution is selected accordingly.

Figure 3.1 shows the schematic of the method using in the design process.

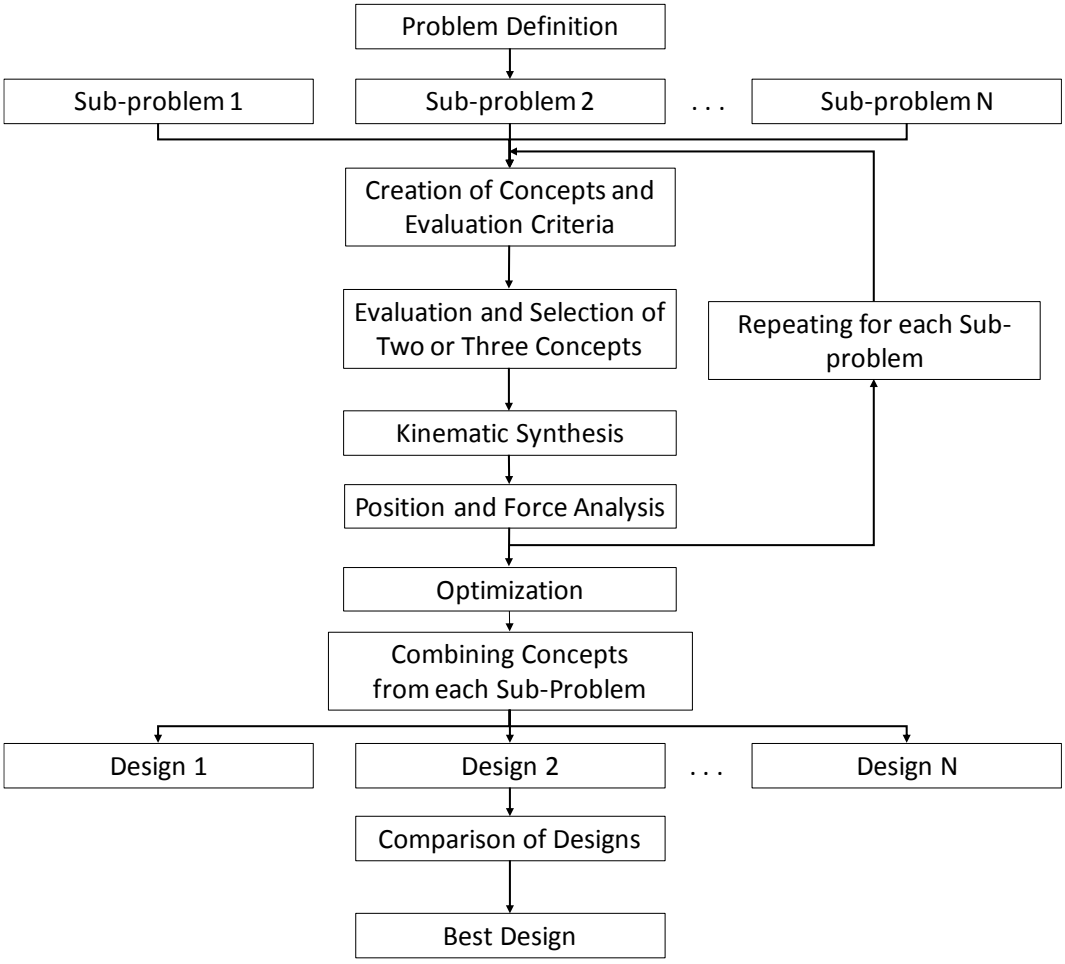

Figure 3.1. Schematic of Method

In this thesis, it is required to design a door drive mechanism for aircraft's in-flight refueling doors. This problem is divided into two sub-problems. The first sub-problem is the door opening/closing function. The second sub-problem is the actuation function. After the problem and sub-problems are defined, different suitable concepts are developed. Based on design requirements, concept evaluation criteria are defined. The concepts for both sub-problems are then evaluated and selected subjectively based on defined criteria. The selected concepts are synthesized by using different approaches and methods. The first approach is a graphical method [9] explained in Appendix A. The second approach is another graphical method explained in Reifschneider's study [14]. Another method is an analytical method, which is three-

position synthesis with specified fixed pivots [9] and is explained in Appendix B. After synthesis of the mechanisms, position and force analyses are performed. For position analysis, Freudenstein's equation [15] given in Appendix C is used. On completion of the position and force analyses, the optimization process starts. For the optimization process, the Multi-Objective Genetic Algorithm optimization method is used. MATLAB software is used to apply the Genetic Algorithm. Optimized mechanisms of each sub-problems are combined to create different designs of the door drive mechanism. Finally, these different designs are also evaluated based on different criteria, and the optimum solution is selected.

CHAPTER 4

CONCEPTUAL DESIGN

4.1. Introduction

In the conceptual design stage, the problem is separated into two parts, which are the door mechanism, and the actuation mechanism. Different concepts are generated for each part, and these concepts are selected according to different design requirements. The subjective evaluation process is performed at the selection stage. The flow chart of the generation concepts is given in Figure 4.1.

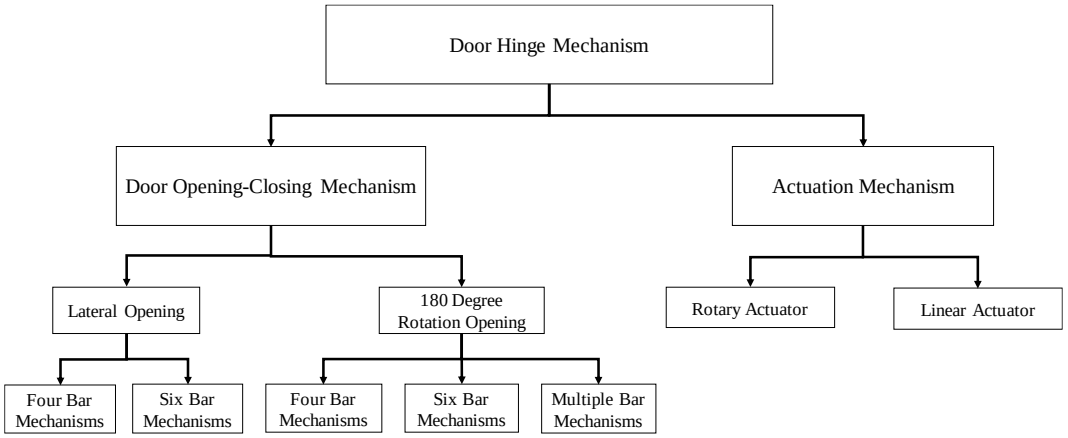

Figure 4.1. Flow chart of the generation concepts

Firstly, different concepts of door mechanisms and actuation mechanisms are presented, then the concept evaluation criteria are specified according to different requirements. Finally, a selection procedure is applied to both door mechanisms and actuation mechanisms separately. The best concepts are chosen by using specified concept evaluation criteria. In this stage, a simpler version of the evaluation procedure defined by Pahl, Beitz, Feldhusen, and Grote [16], [17] is used.

4.2. Concepts

In this section, the concept development procedure is separated into two parts. The first part is the door mechanism concept generation. In this part, different concepts of a door mechanism are developed. The second part is the actuation mechanism concept generation. Different actuation mechanism concepts are created in this part. These actuation mechanisms are used to actuate developed door mechanisms.

4.2.1. Door Mechanism Concepts

In this section, synthesized door opening mechanisms are presented. Nine different planar mechanisms are developed for door opening purposes.

4.2.1.1. Concept D1

In this concept, a four-bar mechanism is synthesized. All joints are selected as revolute joints. This mechanism is opened laterally. The door is rigidly connected to the coupler link. Figure 4.2 shows the sketch of Concept D1.

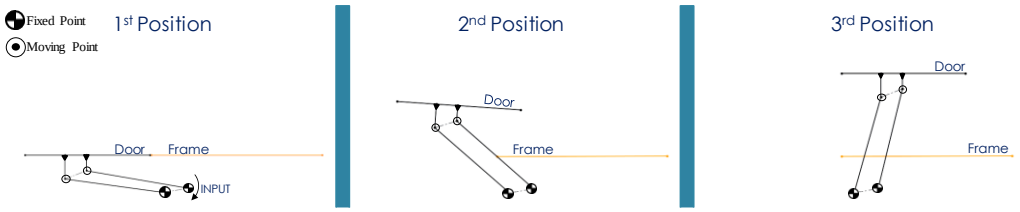

Figure 4.2. Concept D1 schematic

4.2.1.2. Concept D2

In this concept, a Watt I type six-bar mechanism is synthesized. All joints are selected as revolute joints. This mechanism is opened laterally. Figure 4.3 shows the sketch of Concept D2.

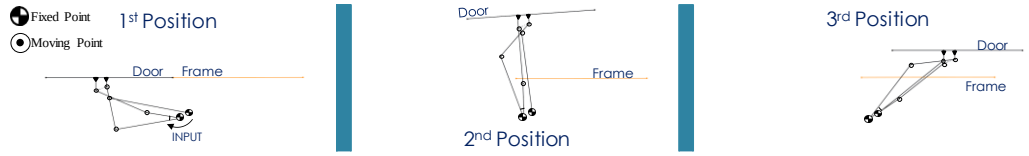

Figure 4.3. Concept D2 schematic

4.2.1.3. Concept D3

In this concept, a Stephenson III type six-bar mechanism is synthesized. All joints are selected as revolute joints. This mechanism is opened laterally. Figure 4.4 shows the sketch of Concept D3.

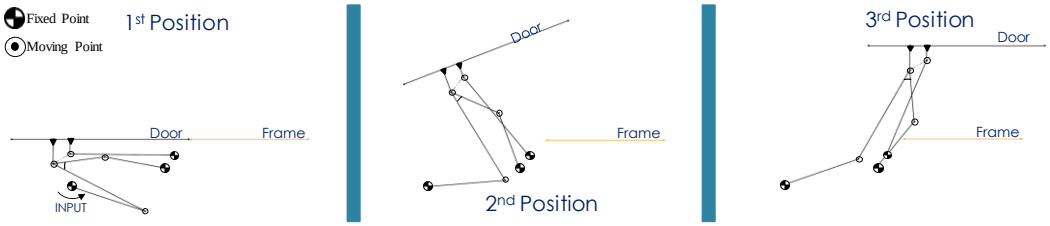

Figure 4.4. Concept D3 schematic

4.2.1.4. Concept D4

In this concept, a four-bar mechanism is synthesized. All joints are selected as revolute joints. This mechanism is opened with 180-degree door rotation. The door is rigidly connected to the follower link. Figure 4.5 shows the sketch of Concept D4.

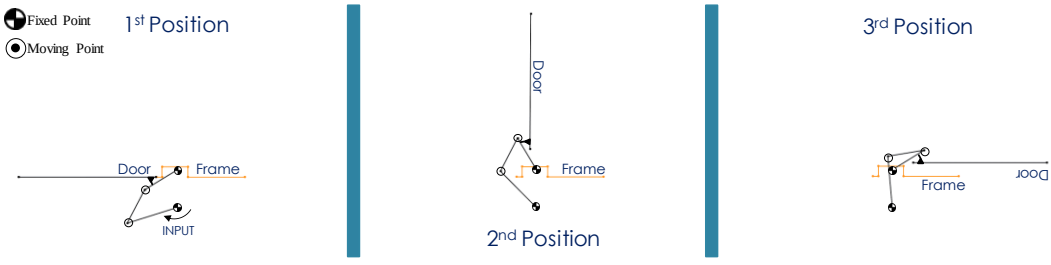

Figure 4.5. Concept D4 schematic

4.2.1.5. Concept D5

In this concept, a four-bar mechanism is synthesized. All joints are selected as revolute joints. This mechanism is opened with 180-degree door rotation. The door is rigidly connected to the coupler link. Figure 4.6 shows the sketch of Concept D5.

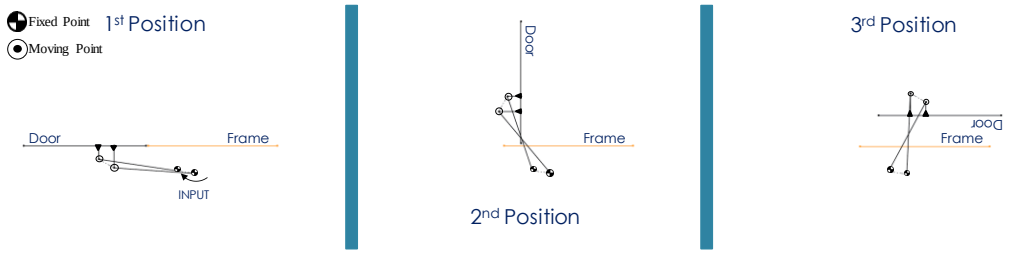

Figure 4.6. Concept D5 schematic

4.2.1.6. Concept D6

In this concept, a Watt I type six-bar mechanism is synthesized. All joints are selected as revolute joints. This mechanism is opened with 180-degree door rotation. Figure 4.7 shows the sketch of Concept D6.

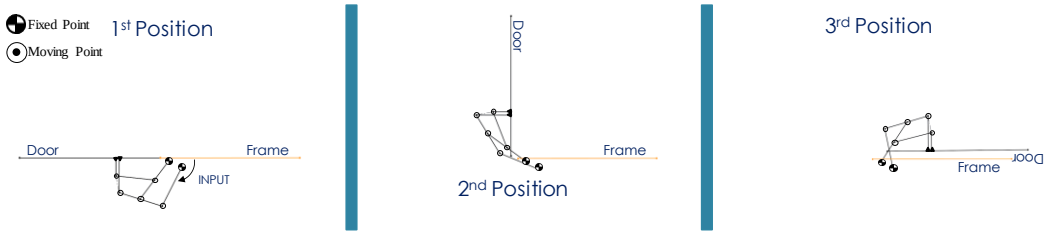

Figure 4.7. Concept D6 schematic

4.2.1.7. Concept D7

In this concept, a different configuration of Watt I type six-bar mechanism is synthesized. All joints are selected as revolute joints. This mechanism is opened with 180-degree door rotation. Figure 4.8 shows the sketch of Concept D7.

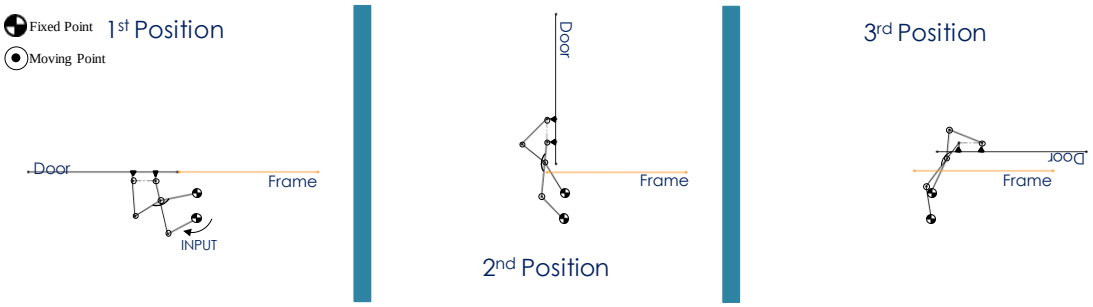

Figure 4.8. Concept D7 schematic

4.2.1.8. Concept D8

In this concept, a Watt II type six-bar mechanism is synthesized. All joints are selected as revolute joints. This mechanism is opened with 180-degree door rotation. Figure 4.9 shows the sketch of Concept D8.

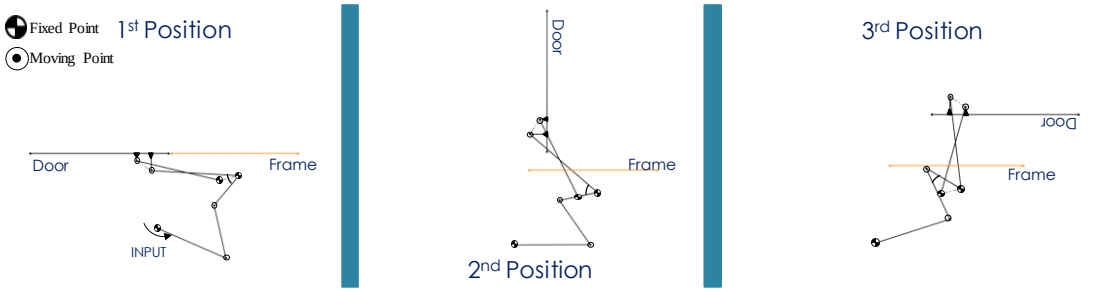

Figure 4.9. Concept D8 schematic

4.2.1.9. Concept D9

In this concept, an invisible hinge mechanism [4], [5] is synthesized. Revolute and sliding joints are used. The degrees of freedom of mechanism is one. This mechanism is opened with 180-degree door rotation. Figure 4.10 shows the sketch of Concept D9.

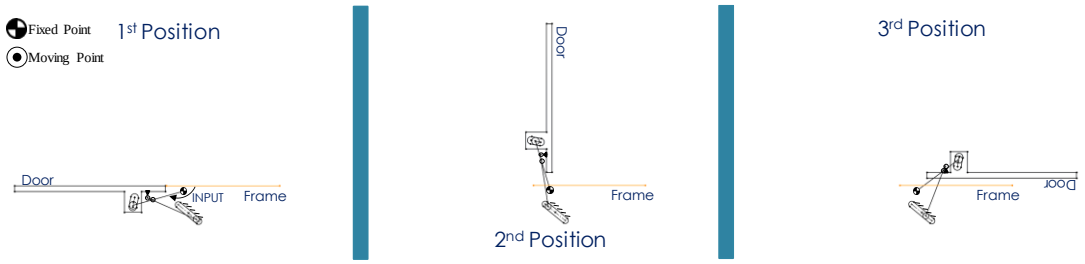

Figure 4.10. Concept D9 schematic

4.2.2. Actuation Mechanism Concepts

In this section, developed actuation mechanism concepts are presented. Twelve different actuation mechanism concepts are developed. Developed actuation mechanisms are integrated into Concept D5 of the door mechanism to represent clearly. Only Concept A5 of the actuation mechanism is integrated into Concept D8. In this section, actuation mechanisms are shown in blue color, and door-opening mechanisms are shown in green color.

4.2.2.1. Concept A1

In this concept, a slider-crank mechanism is used. The sliding joint is in the form of a piston-cylinder arrangement. Revolute and slider joints are selected in this planar mechanism. The follower of the actuation mechanism is rigidly connected to the door opening mechanisms driving link to transmit the motion as seen in Figure 4.11.

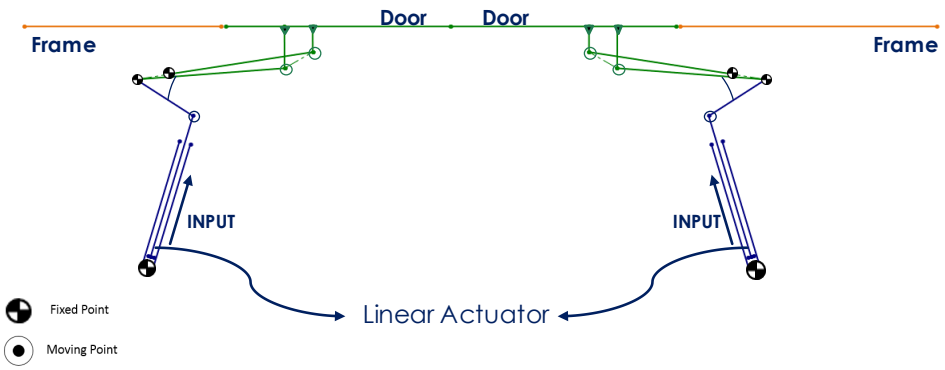

Figure 4.11. Concept A1 schematic

4.2.2.2. Concept A2

In this concept, a planar mechanism, which is actuated by a linear actuator by using revolute and slider joints, is developed. The sliding joint is in the form of a piston-cylinder arrangement. A similar concept is used in the Lanni and Ceccarelli study [6]. The follower of the actuation mechanism is rigidly connected to the door opening mechanisms crank to transmit the motion, as seen in Figure 4.12.

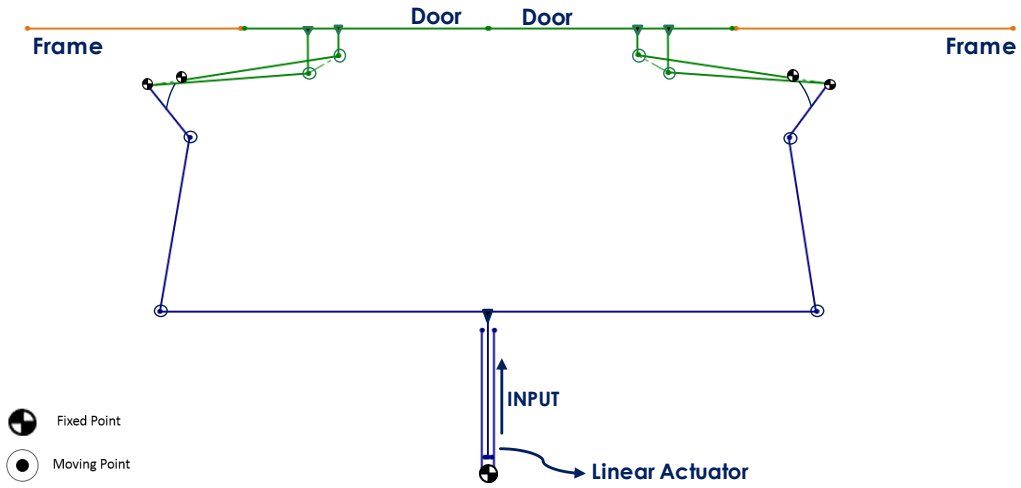

Figure 4.12. Concept A2 schematic

4.2.2.3. Concept A3

In this concept, a planar mechanism, which is actuated by a linear actuator by using revolute and slider joints, consists of two four-bar and inverted slider-crank mechanisms. The slider-crank mechanism is in the form of a piston-cylinder arrangement similar to Concept A2. A similar concept is used in the Nuttall and Klein Breteler study [7]. The followers of the four-bar mechanisms are rigidly connected to the door opening mechanisms cranks to transmit the motion, as seen in Figure 4.13.

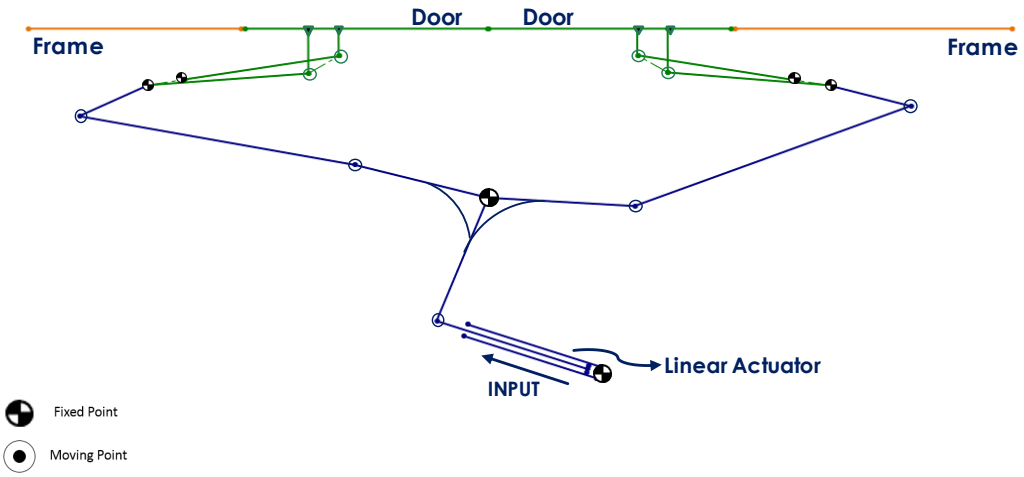

Figure 4.13. Concept A3 schematic

4.2.2.4. Concept A4

In this concept, a planar mechanism, which actuated by a linear actuator by using revolute and slider joints, consists of a Watt II type six-bar and inverted slider-crank mechanisms. The slider-crank mechanism is in the form of a piston-cylinder arrangement similar to Concept A2 and Concept A3. The six-bar mechanism transmits the motion to the other side in order to provide symmetrical motion. The followers of the mechanisms are rigidly connected to the door opening mechanisms cranks to transmit the motion, as seen in Figure 4.14.

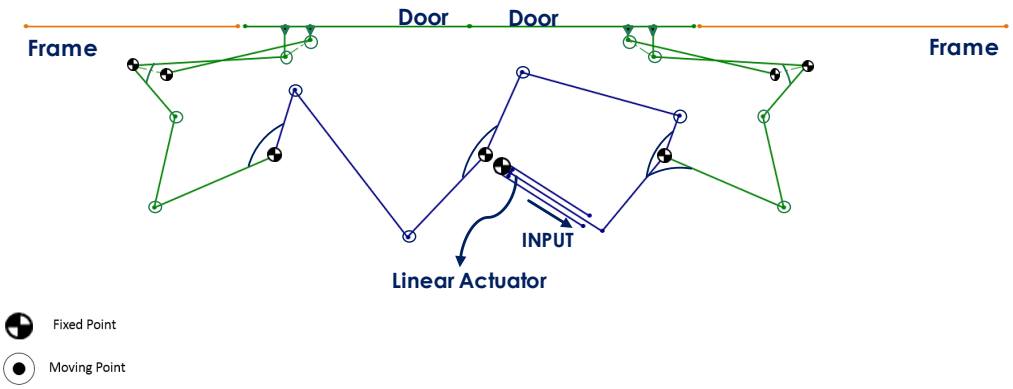

Figure 4.14. Concept A4 schematic

4.2.2.5. Concept A5

In this concept, a planar mechanism, which is actuated by a linear actuator by using revolute and slider joints, consists of a four-bar, Watt II type six-bar and inverted slider-crank mechanisms. The slider-crank mechanism is in the form of a piston-cylinder arrangement similar to previous concepts. The six-bar mechanism transmits the motion to the other side in order to provide symmetrical motion. The follower of the four-bar and six-bar mechanisms are rigidly connected to the door opening mechanisms crank to transmit the motion as seen in Figure 4.15.

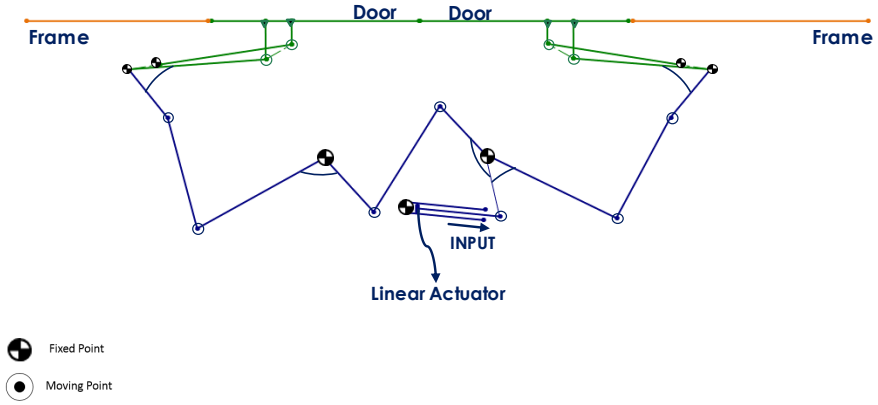

Figure 4.15. Concept A5 schematic

4.2.2.6. Concept A6

In this concept, a planar mechanism, which is actuated by a linear actuator by using revolute and slider joints, consists of a multi-bar mechanism. The double slider-crank mechanism is in the form of a piston-cylinder arrangement. Symmetrical motion is provided through the two sides of the slider-crank mechanism. Other slider-crank mechanisms transfer the motion to door mechanisms. The output links of the slider-crank mechanisms are rigidly connected to the door opening mechanisms crank to transmit the motion as seen in Figure 4.16.

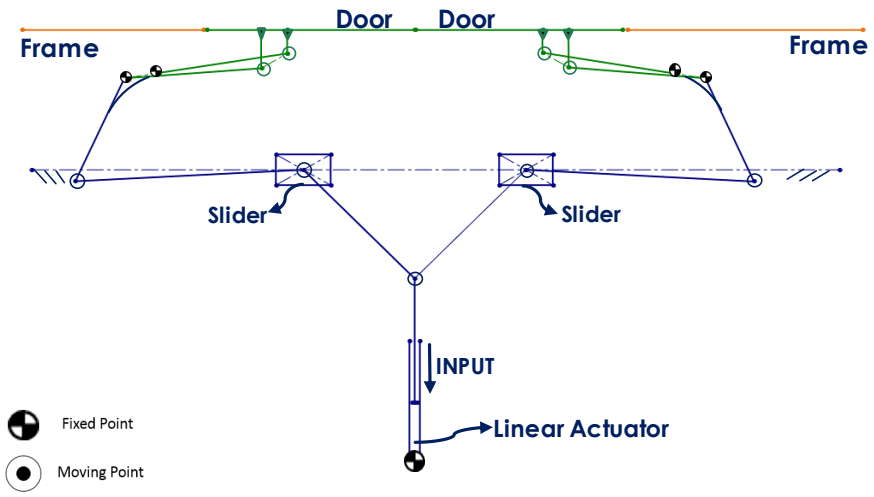

Figure 4.16. Concept A6 schematic

4.2.2.7. Concept A7

In this concept, two linear actuators are used to operate both sides of the mechanism. These linear actuators are directly connected to a rack and pinion system. Pinions are connected to the door opening mechanisms driving links to transmit the motion as seen in Figure 4.17.

Figure 4.17. Concept A7 schematic

4.2.2.8. Concept A8

In this concept, two rotary actuators are used to operate both sides of the mechanism. These rotary actuators are directly connected to the door opening mechanisms driving links to transmit the motion as seen in Figure 4.18.

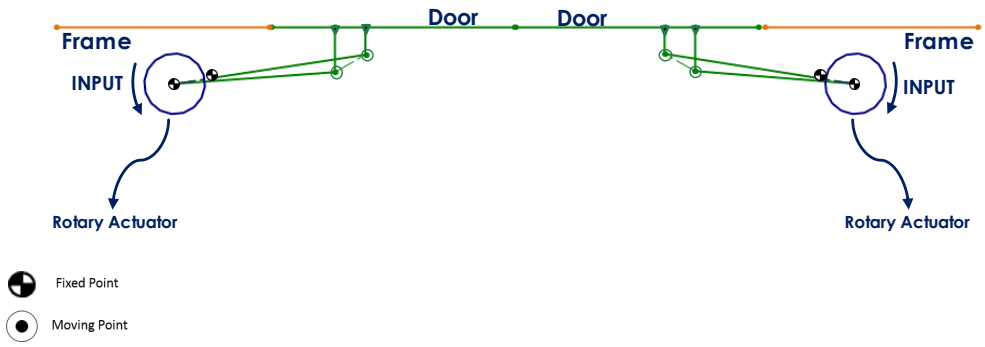

Figure 4.18. Concept A8 schematic

4.2.2.9. Concept A9

In this concept, one rotary actuator is used to drive the right side of the mechanism. The motion is transmitted to the left side by using a pulley and belt system. The rotary actuator and pulley are directly connected to the door opening mechanisms driving links to transmit the motion as seen in Figure 4.19.

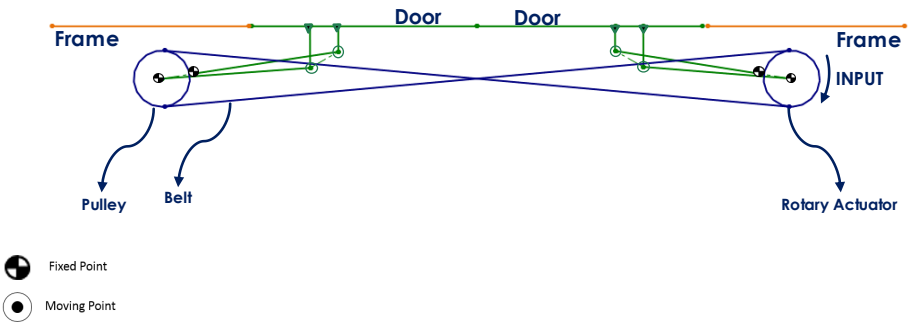

Figure 4.19. Concept A9 schematic

4.2.2.10. Concept A10

In this concept, one rotary actuator is used for the actuation of the mechanism. A rack-and-pinion system transmits the actuator motion to linkages. The motion is transferred to linkages, which are rigidly connected to the door opening mechanisms driving links. Figure 4.20 shows the sketch of Concept A10.

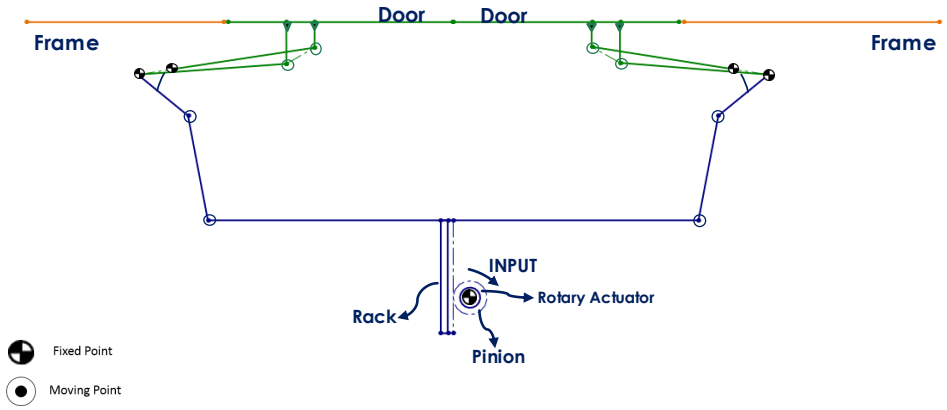

Figure 4.20. Concept A10 schematic

4.2.2.11. Concept A11

In this concept, one rotary actuator is used for the actuation of the mechanism. A screw-and-nut system transmits the actuator motion to linkages. The motion is transferred to linkages, which are rigidly connected to the door opening mechanisms driving links. Figure 4.21 shows the sketch of Concept A11.

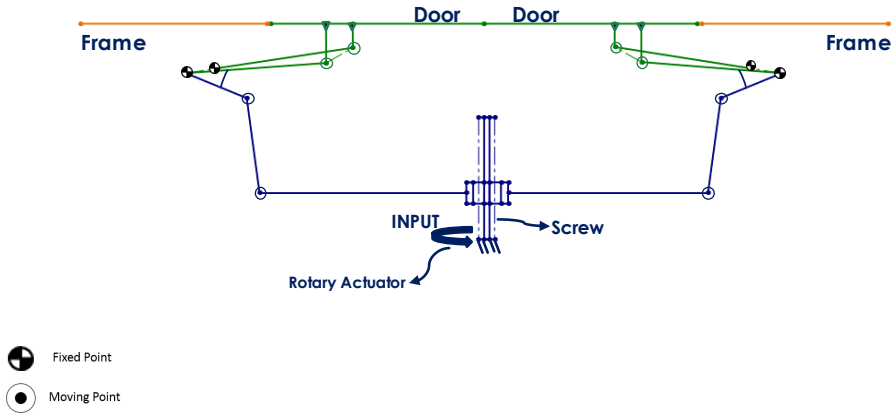

Figure 4.21. Concept A11 schematic

4.2.2.12. Concept A12

In this concept, one rotary actuator is directly connected to a gear used for the actuation of the mechanism. A gear system transmits the motion to the other side. Gears are rigidly connected to four-bar mechanisms driving linkages. These four-bar mechanisms transmit the motion to door opening mechanisms. Followers of these four-bar mechanisms are rigidly connected to the door opening mechanisms driving links. Figure 4.22 shows the sketch of Concept A12.

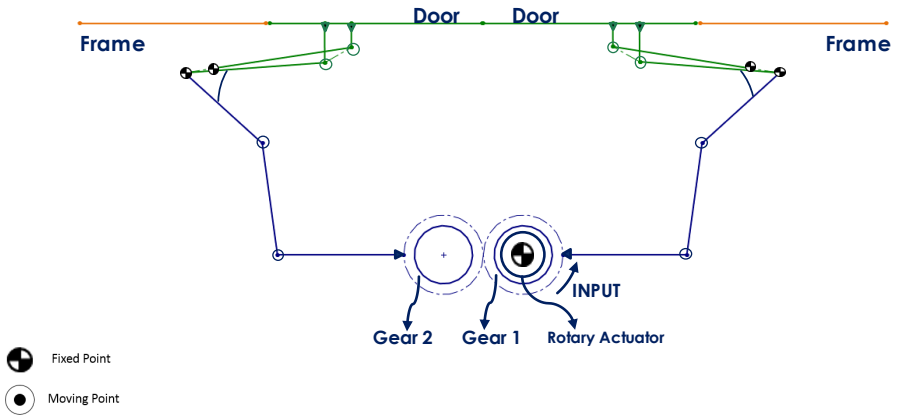

Figure 4.22. Concept A12 schematic

4.3. Evaluation of Concepts

In this section, the concept evaluation criteria of developed door mechanism and actuation mechanism concepts are clarified. The door mechanism and actuation mechanism concepts are evaluated separately according to different concept evaluation criteria. These criteria are selected by considering different requirements, such as technical and economic.

Once the concept evaluation criteria are defined, the concepts can be evaluated subjectively to choose the best concepts for the defined problem. The procedure of the evaluation is subjective; therefore, the experiences of the designer are important for the evaluation step. Six different design engineers evaluate concepts to reduce the

deviation of values because of this subjective approach. To reduce subjectivity in this method, six engineers were used to evaluate the concepts.

In Table 4.1, the value scale used for the evaluation of concepts is given with their meanings.

Table 4.1. *The value scale for the evaluation of concepts* [16]

Points	Meaning
0	Absolutely useless solution
1	Very inadequate solution
2	Weak solution
3	Tolerable solution
4	Adequate solution
5	Satisfactory solution
6	Good solution with few drawbacks
7	Good solution
8	Very good solution
9	Solution exceeding requirement
10	Ideal solution

4.3.1. Concept Evaluation Criteria of Door Mechanism Concepts

The chosen evaluation criteria for door mechanism design are simplicity of concept, maintainability, simplicity of assembly process, reliability, rigidity, mobility and design flexibility, space utilization, and force characteristic.

Simplicity of concept directly influences the design process of the product. The number of components, simplicity of components, and overall simplicity are essential parameters to reduce the total cost of the design.

Maintainability directly affects the service life and maintenance cost of the product.

Simplicity of assembly process is also an important factor affecting the integration effort of the product.

Reliability is the probability that the given system or product will perform its required function or mission under specified conditions for a specified period without failure.

Rigidity affects design performance under different load conditions.

Mobility and design flexibility of a product influences the design phase. These criteria affect the effort of the designing process.

Space utilization of the design is an area required in both the non-operation and operation stages.

Force characteristic is the last criteria. Force characteristic directly affects the component's size and weights.

4.3.2. Evaluation of Door Mechanism Concepts

Initially, weights of each criterion are assigned from zero to ten according to its importance for the defined problem. It is noted that this assignment is also subjective. Weights factors are then calculated by dividing weights to the sum of the assigned weights. Assigned weights and calculated weight factors are given in Table 4.2.

Table 4.2. *Weight and calculated weight factors of evaluation criteria*

Evaluation Criterion	Weight (1-10)	Weight Factor
Simplicity of Concept	9	0,161
Maintainability	7	0,125
Simplicty of Assembly Process	5	0,089
Reliability	8	0,143
Rigidity	7	0,125
Mobility and Design Flexibility	5	0,089
Space Utilization	6	0,107
Force Characteristic	9	0,161
Total	56	1,000

Finally, concepts are evaluated by assigning values according to defined criteria, and obtained results are given in Table 4.3. It is noted that the required space and driving force of each concept are calculated then space utilization and force characteristic criteria are assigned according to these calculations. As seen in Table 4.3, concept D1 and Concept D5 are selected to be the best concepts among alternatives for door mechanism concepts. In the later chapters, these two selected concepts are compared one more time to select the suitable concept of the door mechanism.

Table 4.3. *Evaluation of door mechanism concepts*

Evaluation Criterion	**Weight Factor**	**Concept D1**	**Concept D2**	**Concept D3**	**Concept D4**	**Concept D5**	**Concept D6**	**Concept D7**	**Concept D8**	**Concept D9**
Simplicity of Concept	0,161	8,75	6,00	5,50	7,50	8,08	5,33	5,08	4,67	3,00
Maintainability	0,125	8,83	5,33	6,33	7,83	8,17	5,67	5,33	4,58	3,33
Simplicty of Assembly Process	0,089	8,83	5,33	5,67	8,33	8,08	5,08	5,17	5,17	4,00
Reliability	0,143	8,83	7,00	6,67	8,67	7,92	5,75	6,33	6,00	4,58
Rigidity	0,125	8,17	5,92	6,08	7,00	6,75	5,83	5,50	5,50	3,83
Mobility and Design Flexibility	0,089	5,33	7,67	7,42	5,67	5,83	7,58	7,83	7,17	6,33
Space Utilization	0,107	2,13	3,92	8,36	4,70	2,83	8,27	9,36	1,00	10,00
Force Characteristic	0,161	9,14	9,85	1,00	6,05	7,71	10,00	7,76	2,35	9,80
Total	1	**7,76**	6,53	5,61	7,02	**7,08**	6,74	6,49	4,45	5,60

4.3.3. Concept Evaluation Criteria of Actuation Mechanism Concepts

The chosen evaluation criteria for the actuation mechanism concept are the simplicity of concept, maintainability, cost, long service life, simplicity of assembly process, reliability, rigidity, design flexibility, space utilization.

Cost is a critical parameter and directly influences the design stage of the product.

Long service life of a product reduces the maintenance effort of the product.

4.3.4. Evaluation of Actuation Mechanism Concepts

As previous, the evaluation of concepts procedure is performed on the actuation mechanism concepts. Weights are assigned to criteria, and weight factors are calculated for each criterion. In Table 4.4, the assigned weights and calculated weight factors are given.

Table 4.4. *Weight and calculated weight factors of evaluation criteria*

Evaluation Criterion	Weight (1-10)	Weight Factor
Simplicity of Concept	9	0,148
Maintainability	7	0,115
Cost	6	0,098
Long Service Life	8	0,131
Simplicty of Assembly Process	5	0,082
Reliability	8	0,131
Rigidity	7	0,115
Design Flexibility	5	0,082
Space Utilization	6	0,098
Total	61	1

The next step is the evaluation of actuation mechanism concepts. The values given previously with their meanings in Table 4.1 are assigned to criteria for each actuation mechanism concept as done before. In Table 4.5 the result of the evaluation is presented. As seen in Table 4.5, Concept A1, Concept A3, and Concept A8 are selected to be the best concepts among alternatives of the actuation mechanism. In the later chapters, these selected concepts are compared one more time to select the suitable concept of the actuation mechanism.

Table 4.5. *Evaluation of actuation mechanism concepts*

Evaluation Criterion	**Weight**	**Concept A1**	**Concept A2**	**Concept A3**	**Concept A4**	**Concept A5**	**Concept A6**
Simplicity of Concept	0,148	8,50	8,00	7,00	5,00	5,17	5,17
Maintainability	0,115	7,83	7,33	7,00	5,17	5,33	4,67
Cost	0,098	6,50	6,50	7,42	5,50	5,50	4,67
Long Service Life	0,131	8,17	7,00	7,67	5,67	6,00	4,83
Simplicty of Assembly Process	0,082	8,17	7,83	7,33	4,83	4,83	4,50
Reliability	0,131	8,17	7,17	7,17	6,00	5,83	4,83
Rigidity	0,115	8,17	6,50	6,83	5,17	5,17	5,50
Design Flexibility	0,082	7,33	6,50	6,67	6,00	6,17	5,67
Space Utilization	0,098	7,33	5,67	6,33	5,17	4,83	4,67
Total	1	**7,86**	7,00	**7,07**	5,39	5,44	4,95
Evaluation Criterion	**Weight**	**Concept A7**	**Concept A8**	**Concept A9**	**Concept A10**	**Concept A11**	**Concept A12**
Simplicity of Concept	0,148	6,33	9,00	6,67	5,50	5,83	5,83
Maintainability	0,115	4,17	8,00	5,67	5,17	5,25	5,00
Cost	0,098	3,17	6,17	5,50	5,08	5,08	5,00
Long Service Life	0,131	4,50	7,33	5,17	4,83	4,17	4,50
Simplicty of Assembly Process	0,082	4,83	8,83	5,67	5,00	5,17	4,83
Reliability	0,131	5,17	8,50	5,33	5,17	5,00	5,33
Rigidity	0,115	5,50	9,00	5,17	5,50	5,67	5,83
Design Flexibility	0,082	6,00	8,00	6,17	5,33	5,33	5,50
Space Utilization	0,098	7,33	9,17	6,83	4,67	5,33	5,50
Total	1	5,23	**8,24**	5,79	5,15	5,20	5,27

CHAPTER 5

KINEMATIC SYNTHESIS AND ANALYSIS

5.1. Introduction

In this chapter, selected door mechanisms and actuation mechanism concepts are separately synthesized by considering design criteria and restrictions.

After the synthesis part is completed, kinematic analysis is carried out to check motion and geometric limitations. In addition to kinematic analysis, force analysis is performed to obtain necessary forces acting on the system. The external forces acting on the doors are estimated.

5.2. Kinematic Synthesis and Analysis of Selected Door Mechanisms

In this part, selected door mechanism concepts are synthesized by using the graphical approach and analytical methods given in Appendix A and Appendix B. After synthesized studies are completed, kinematic analysis and force analysis are performed. Only one side of the door mechanisms is considered because both sides are considered symmetrical.

5.2.1. Kinematic Synthesis and Analysis of Concept D1

The schematic view of Concept D1 and variables are shown in Figure 5.1. The fixed link is A_0B_0. The door is rigidly connected to coupler link AB.

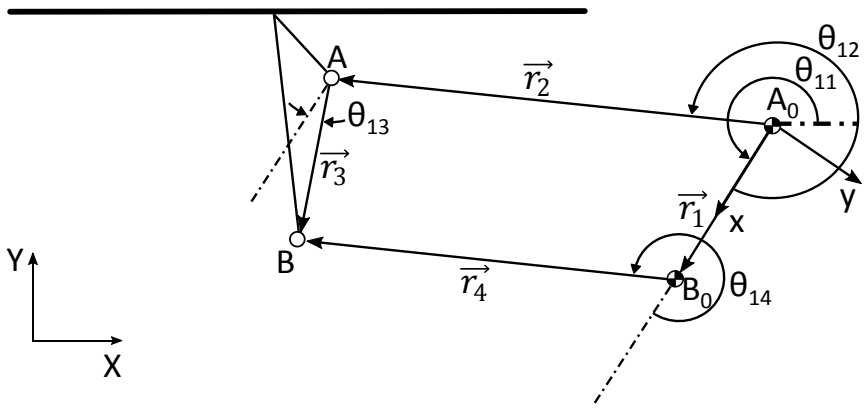

Figure 5.1. Schematic of Concept D1

5.2.1.1. Kinematic Synthesis

i. Graphical Approach

In this part, the graphical approach for the two-position synthesis given in Appendix A is applied to Concept D1 to find a solution. Figure 5.2 shows the initial and final positions of the door.

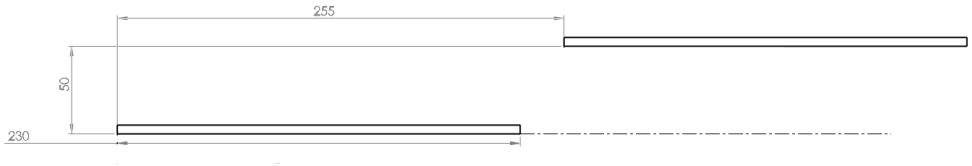

Figure 5.2. Initial and final positions of the door

After applying the graphical approach, a suitable mechanism shown in Figure 5.3 is synthesized.

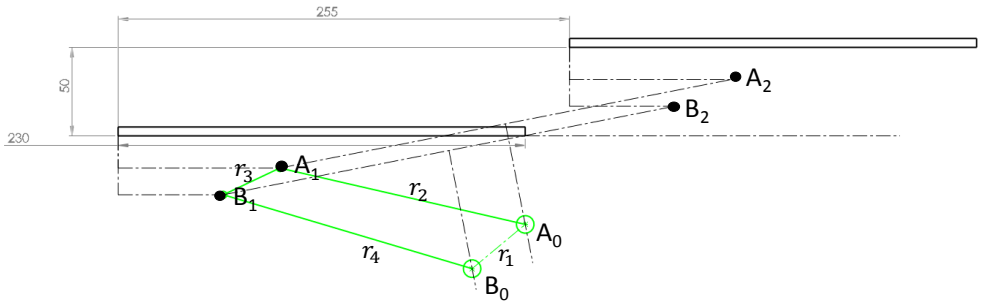

Figure 5.3. Synthesized Concept D1 schematic (Graphical Approach)

Calculated parameter values are given in Table 5.1.

Table 5.1. *Calculated parameter values for Concept D1 (Graphical Approach)*

1	2	3	4	5	6
r_1(mm)	r_2(mm)	r_3(mm)	r_4(mm)	θ_{12} (deg)	θ_{11} (deg)
39,05	142,24	35,32	146,65	-52,73	219,81

ii. Analytical Method

An analytical method, three-position synthesis with specified fixed pivots is applied to synthesize Concept D1. Equations given in Appendix B are used to calculate unknown parameters.

The three-position of the door are given in Figure 5.4. Unlike the first and final position, mid-position is arbitrarily selected because there is no restriction for this position.

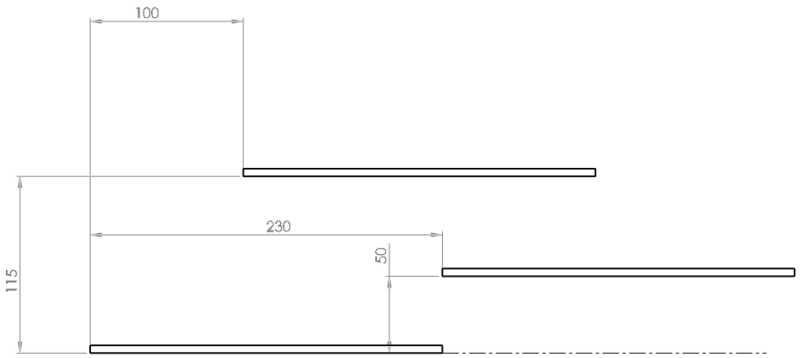

Figure 5.4. Three-Position of the Door

Figure 5.5 shows the dyads of Concept D1.

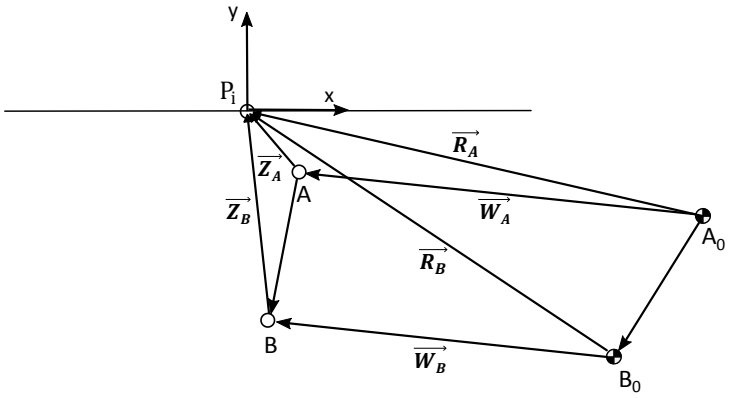

Figure 5.5. Dyads of Concept D1

Specified input parameters, which are positions and orientations of the door and positions of fixed points, are given in Table 5.2.

Table 5.2. *Input parameters of Concept D1*

Inputs								
	mm			**deg**	**rad**		**mm**	
δ_2	115	100	α_2	0	0	$\mathbf{R_A}$	115	-50
δ_3	230	50	α_3	0	0	$\mathbf{R_B}$	65	-80

Then, Vectors **W** and **Z** can be found by using Eqs. set (A.1) to (A.13). Calculated unknown parameters are given in Table 5.3.

Table 5.3. *Results of Concept D1*

	x	**y**
$\mathbf{W_A}$	-126,920	29,833
$\mathbf{Z_A}$	11,920	20,167
$\mathbf{W_B}$	-126,920	29,833
$\mathbf{Z_B}$	61,920	50,167
AB	-50,000	-30,000
$\mathbf{A_oB_o}$	-50,000	-30,000

The link lengths and orientation of the first position can now be determined by using vectors **W** and **Z**. The results are given in Table 5.4.

Table 5.4. *Calculated parameters of Concept D1 by using the analytical method*

1	**2**	**3**	**4**	**5**	**6**
r_1**(mm)**	r_2**(mm)**	r_3**(mm)**	r_4**(mm)**	θ_{12} **(deg)**	θ_{11} **(deg)**
58,31	130,38	58,31	130,38	-44,19	210,96

The synthesized mechanism is given in Figure 5.6.

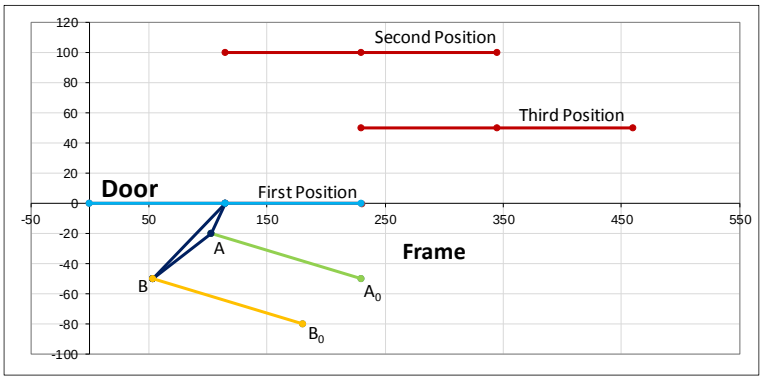

Figure 5.6. Representation of Concept D1 (Analytical Method)

5.2.1.2. Kinematic Analysis

After the synthesis study of Concept D1, Freudenstein's equation explained in Appendix C is used to perform kinematic analysis and to obtain positions of the mechanism for every specified input joint variable. The loop closure equation of the Concept D1 is given in the Eq. (5.1).

$$\vec{r_2} + \vec{r_3} - \vec{r_4} - \vec{r_1} = 0 \tag{5.1}$$

Complex number notation is given in the Eq. (5.2).

$$r_2 e^{i\theta_{12}} + r_3 e^{i\theta_{13}} - r_4 e^{i\theta_{14}} - r_1 = 0 \tag{5.2}$$

By solving the Eq. (5.2), the unknown joint variables are θ_{13} and θ_{14} can be found by using the below equations.

$$\theta_{13} = 2 \times atan\left(\frac{-B + \sigma\sqrt{B^2 - 4AC}}{2A}\right) \tag{5.3}$$

$$\theta_{14} = \text{atan}\left(\frac{r_2 sin\theta_{12} + r_3 sin\theta_{13}}{r_2 cos\theta_{12} + r_3 cos\theta_{13} - r_1}\right) \tag{5.4}$$

Where;

$$A = (K_1 + K_2 cos\theta_{12} - K_3 + cos\theta_{12}) \tag{5.5}$$

$$B = -2sin\theta_{12} \tag{5.6}$$

$$C = K_1 + K_2 cos\theta_{12} + K_3 - cos\theta_{12} \tag{5.7}$$

$$K_1 = \frac{r_4^2 - r_1^2 - r_2^2 - r_3^2}{2r_3 r_2} \tag{5.8}$$

$$K_2 = \frac{r_1}{r_3} \tag{5.9}$$

$$K_3 = \frac{r_1}{r_2} \tag{5.10}$$

$$\sigma = -1 \tag{5.11}$$

These equations are used to find joint variables for every crank angle and check the motion of the synthesized mechanism.

5.2.1.3. Static Force Analysis

Static force analysis is performed for Concept D1 to calculate the required driving torque. The free-body diagram of each link is drawn, and unknown forces are identified. Force equilibrium equations are written for each link. Free body diagrams and equations are given below.

The system given in Figure 5.7 is in equilibrium under the action of the external force F and driving torque, T_{input}. The magnitude and direction of external force F are estimated and known. Driving torque and the forces acting at joints can be determined.

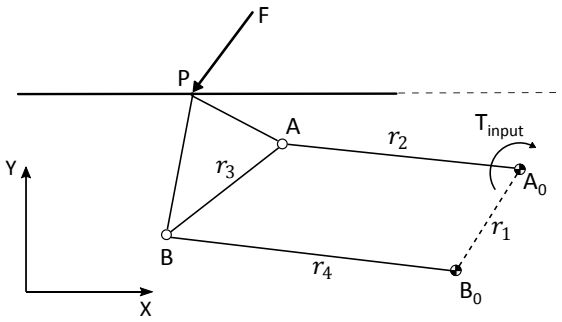

Figure 5.7. External force, F and driving torque, T_{input} acting on Concept D1

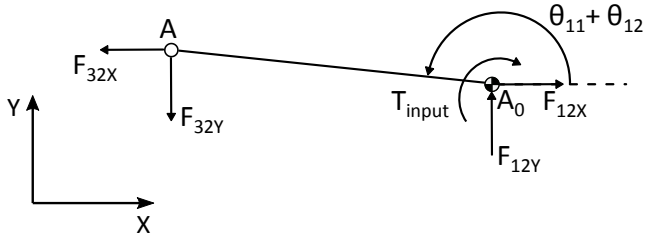

Figure 5.8. Free body diagram of link 2

$$\sum F_x = 0 \implies F_{12x} - F_{32x} = 0 \tag{5.12}$$

$$\sum F_y = 0 \implies F_{12y} - F_{32y} = 0 \tag{5.13}$$

$$\sum M_{A0} = 0 \implies F_{32y} r_2 \sin\left(\frac{3\pi}{2} - \theta_{11} - \theta_{12}\right) + F_{32x} r_2 \sin(\pi - \theta_{11} - \theta_{12}) + T_{input} = 0 \tag{5.14}$$

It is noted that $F_{ij} = -F_{ji}$ for the joint force. This equality is used to simplify the calculations.

$$F_{23x} = -F_{32x} \tag{5.15}$$

$$F_{23y} = -F_{32y} \tag{5.16}$$

$$-F_{23y} r_2 \sin\left(\frac{3\pi}{2} - \theta_{11} - \theta_{12}\right) - F_{23x} r_2 \sin(\pi - \theta_{11} - \theta_{12}) + T_{input} = 0 \tag{5.17}$$

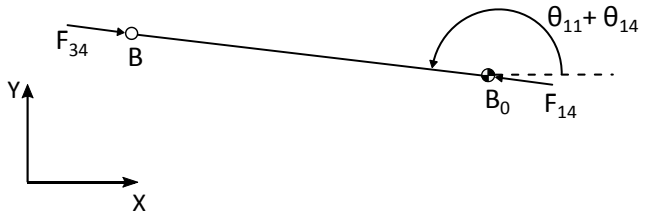

Figure 5.9. Free body diagram of link 4 (Two-force member)

$$F_{34} = -F_{14} \tag{5.18}$$

Force acting on point P is moved to the midpoint of link 3 to simplify calculations.

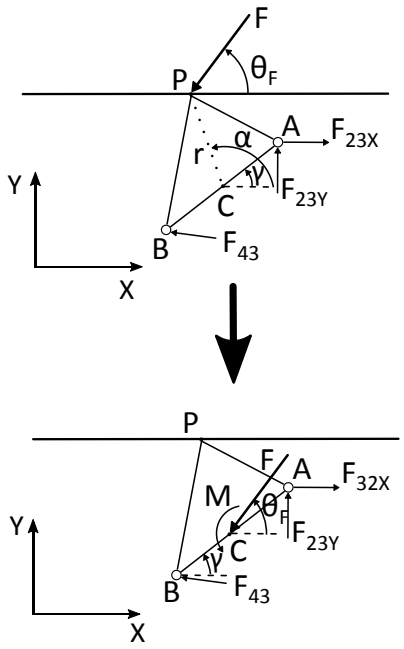

Figure 5.10. Free body diagram of link 3

$$\sum F_x = 0 \implies F_{23x} + F_{43}\cos(\theta_{11} + \theta_{14}) + Fcos(\theta_f) = 0 \tag{5.19}$$

$$\sum F_y = 0 \implies F_{23y} + F_{43}\sin(\theta_{11} + \theta_{14}) + Fsin(\theta_f) = 0 \tag{5.20}$$

$$\sum M_B = 0 \implies F_{23y} r_3 \sin\left(\frac{\pi}{2} - \gamma\right) + F_{23x} r_3 \sin(-\gamma) + M + F\frac{r_3}{2}\sin(\theta_f - \gamma) = 0 \tag{5.21}$$

Where,

$$M = Frsin\left(\theta_f - \beta - \gamma\right) \tag{5.22}$$

$$\alpha = \text{atan}\left((P_y - C_y), (P_x - C_x)\right) : constant \tag{5.23}$$

$$\gamma = \theta_{11} + \theta_{13} - \pi \tag{5.24}$$

$$\beta = \alpha - \gamma \tag{5.25}$$

The set of equations given above can be written in matrix form as follows:

$$[A] \cdot [x] = [b] \tag{5.26}$$

Where [A] is the coefficient matrix, [x] is a variable matrix consists of unknown forces and [b] is a constant matrix. Each side of Eq. (5.26) is multiplied with $[A]^{-1}$ to find the solution of [x].

$$[x] = [A]^{-1} \cdot [b] \tag{5.27}$$

Where

$$[x] = \begin{bmatrix} F_{23x} \\ F_{23y} \\ F_{43} \\ T_{input} \end{bmatrix} \tag{5.28}$$

$$[A] = \begin{bmatrix} 1 & 0 & \cos(\theta_{11} + \theta_{14}) & 0 \\ 0 & 1 & \sin(\theta_{11} + \theta 14) & 0 \\ r_3 \sin(-\gamma) & r_3 \sin(\frac{\pi}{2} - \gamma) & 0 & 0 \\ -r_2 \sin(\pi - \theta_{11} - \theta_{12}) & -r_2 \sin(\frac{3\pi}{2} - \theta_{11} - \theta_{12}) & 0 & 1 \end{bmatrix} \tag{5.29}$$

$$[b] = \begin{bmatrix} -F\cos(\theta_f) \\ -F\sin(\theta_f) \\ -M - F\frac{r_3}{2}\sin(\theta_f - \gamma) \\ 0 \end{bmatrix} \tag{5.30}$$

Variable matrix, [x] can be calculated by using Eq. (5.27) to find unknown forces and required driving torque.

5.2.2. Kinematic Synthesis and Analysis of Concept D5

The schematic view of Concept D5 and variables are shown in Figure 5.11. The fixed link is A_0B_0. The door is rigidly connected to coupler link AB. The graphical approach and analytical method explained previously are applied to solve this mechanism.

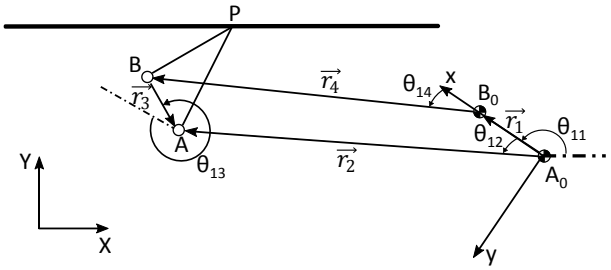

Figure 5.11. Schematic of Concept D5

5.2.2.1. Kinematic Synthesis

i. Graphical Approach

In this part, the graphical approach for the two-position synthesis given in Appendix A is applied to Concept D5 to find a solution. Figure 5.12 shows the initial and final positions of the door.

Figure 5.12. Initial and final positions of the door

The synthesized mechanism using the graphical approach is shown in Figure 5.13.

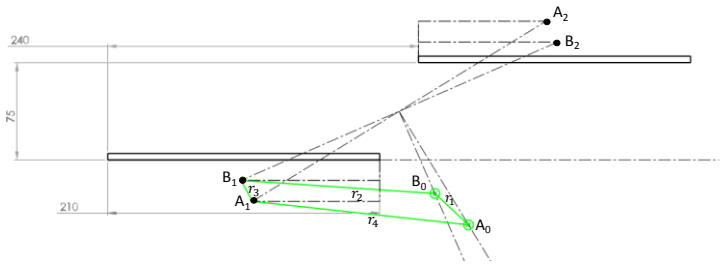

Figure 5.13. Synthesized Concept D5 schematic (Graphical Approach)

Calculated parameter values are given in Table 5.5.

Table 5.5. Calculated parameter values for Concept D5 (Graphical Approach)

1	2	3	4	5	6
r_1(mm)	r_2(mm)	r_3(mm)	r_4(mm)	θ_{12} (deg)	θ_{11} (deg)
35,43	167,89	18,35	150,09	36,77	137,04

ii. Analytical Method

Three-position synthesis with specified fixed pivots is also applied to synthesize Concept D5. Equations given in Appendix B are used to calculate unknown parameters.

Three positions of the door are given in Figure 5.14. Unlike the first and final position, mid-position is arbitrarily selected because there is no restriction for this position.

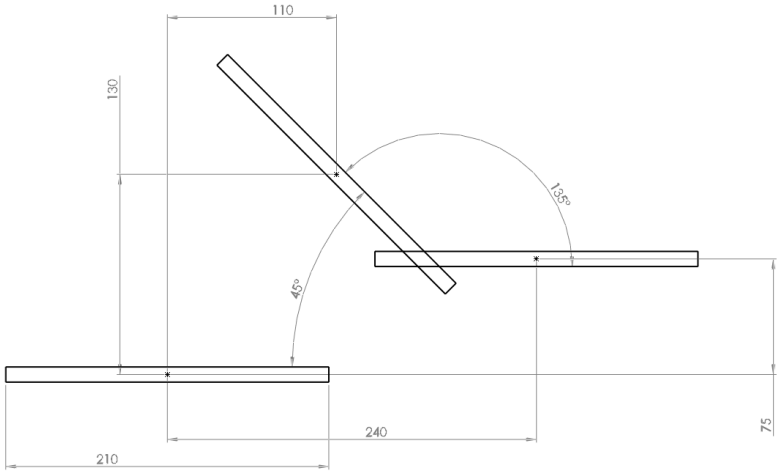

Figure 5.14. Three-Position of the door

Figure 5.15 shows the dyads of Concept D5.

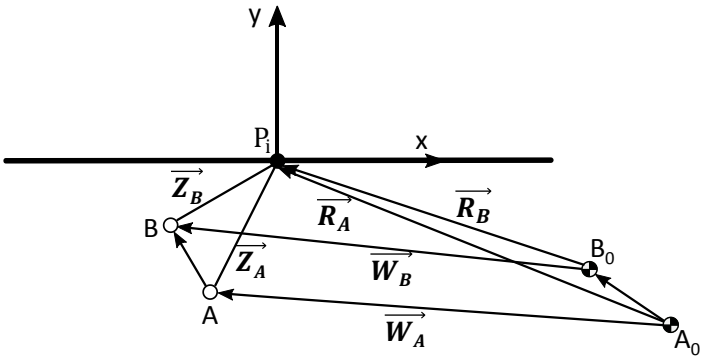

Figure 5.15. Dyads of Concept D5

Specified input parameters, which are positions and orientations of the door and positions of fixed points, are given in Table 5.6.

Table 5.6. *Input parameters of Concept D5*

Inputs								
	mm			**deg**	**rad**		**mm**	
δ_2	110	130	α_2	-45	-0,785	$\mathbf{R_A}$	175	-50
δ_3	240	75	α_3	-180	-3,142	$\mathbf{R_B}$	155	-35

Then, Vectors **W** and **Z** can be found by using Eqs. set (A.1) to (A.13). Calculated unknown parameters are given in Table 5.7.

Table 5.7. *Results of Concept D5*

	x	**y**
$\mathbf{W_A}$	-201,216	-4,407
$\mathbf{Z_A}$	26,216	54,407
$\mathbf{W_B}$	-187,101	-0,928
$\mathbf{Z_B}$	32,101	35,928
AB	-5,884	18,480
$\mathbf{A_0B_0}$	-20,000	15,000

Now, link lengths and orientation of the first position can be determined by using vectors **W** and **Z**. The results are given in Table 5.8.

Table 5.8. *Calculated parameters of Concept D5 by using the analytical method*

1	2	3	4	5	6
r_1(mm)	r_2(mm)	r_3(mm)	r_4(mm)	θ_{12} (deg)	θ_{11} (deg)
25,00	201,26	19,39	187,10	38,12	143,13

The synthesized mechanism is given in Figure 5.16.

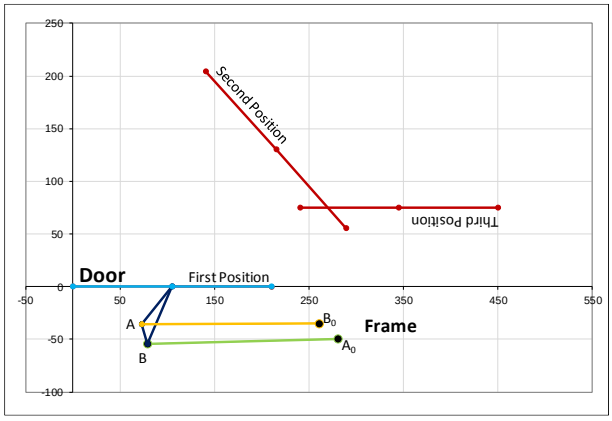

Figure 5.16. Representation of Concept D5 (Analytical Method)

5.2.2.2. Kinematic Analysis

After the synthesis study of Concept D5, Freudenstein's equation explained in Appendix C is used to perform kinematic analysis and to obtain positions of the mechanism for every specified input joint variable. The loop closure equation of the Concept D5 is given in the Eq. (5.31).

$$\overrightarrow{r_2} + \overrightarrow{r_3} - \overrightarrow{r_4} - \overrightarrow{r_1} = 0 \tag{5.31}$$

Complex number notation is given in the Eq. (5.32).

$$r_2 e^{i\theta_{12}} + r_3 e^{i\theta_{13}} - r_4 e^{i\theta_{14}} - r_1 = 0 \tag{5.32}$$

By solving the Eq. (5.32), the unknown joint variables are θ_{13} and θ_{14} can be found by using the below equations.

$$\theta_{13} = 2 \times atan(\frac{-B + \sigma\sqrt{B^2 - 4AC}}{2A}) \tag{5.33}$$

$$\theta_{14} = \text{atan}(\frac{r_2 sin\theta_{12} + r_3 sin\theta_{13}}{r_2 cos\theta_{12} + r_3 cos\theta_{13} - r_1}) \tag{5.34}$$

Where;

$$A = (K_1 + K_2 cos\theta_{12} - K_3 + cos\theta_{12}) \tag{5.35}$$

$$B = -2sin\theta_{12} \tag{5.36}$$

$$C = K_1 + K_2 cos\theta_{12} + K_3 - cos\theta_{12} \tag{5.37}$$

$$K_1 = \frac{r_4^2 - r_1^2 - r_2^2 - r_3^2}{2r_3 r_2} \tag{5.38}$$

$$K_2 = \frac{r_1}{r_3} \tag{5.39}$$

$$K_3 = \frac{r_1}{r_2} \tag{5.40}$$

$$\sigma = +1 \tag{5.41}$$

These equations are used to find joint variables for every crank angle and check the motion of the synthesized mechanism.

5.2.2.3. Static Force Analysis

Static force analysis is performed for Concept D5 to calculate the required driving torque. The free-body diagram of each link is drawn, and unknown forces are identified. Force equilibrium equations are written for each link. Free body diagrams and equations are given below.

The system given in Figure 5.17 is in equilibrium under the action of the external force F and driving torque, T_{input}. The magnitude and direction of external force F are estimated and known. Driving torque and the forces acting at joints can be determined.

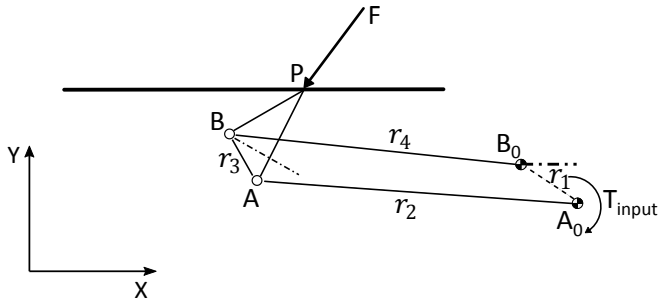

Figure 5.17. External force, F and input torque, T_{input} acting on Concept D5

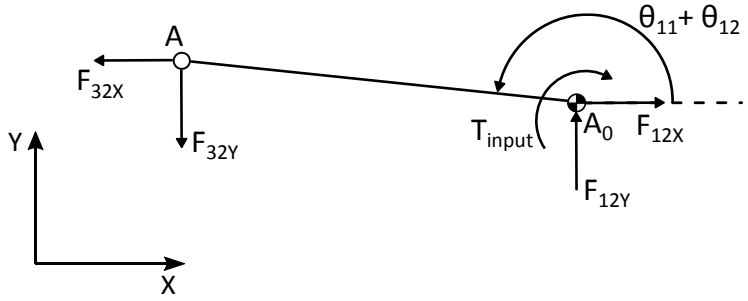

Figure 5.18. Free body diagram of link 2

$$\sum F_x = 0 \implies F_{12x} - F_{32x} = 0 \tag{5.42}$$

$$\sum F_y = 0 \implies F_{12y} - F_{32y} = 0 \tag{5.43}$$

$$\sum M_{A0} = 0 \implies F_{32y} r_2 \sin\left(\frac{3\pi}{2} - \theta_{11} - \theta_{12}\right) + F_{32x} r_2 \sin(\pi - \theta_{11} - \theta_{12)} + T_{input} = 0 \tag{5.44}$$

It is noted that $F_{ij} = -F_{ji}$ for the joint force. This equality is used to simplify the calculations.

$$F_{23x} = -F_{32x} \tag{5.45}$$

$$F_{23y} = -F_{32y} \tag{5.46}$$

$$-F_{23y} r_2 \sin\left(\frac{3\pi}{2} - \theta_{11} - \theta_{12}\right) - F_{23x} r_2 \sin(\pi - \theta_{11} - \theta_{12}) + T_{input} = 0 \tag{5.47}$$

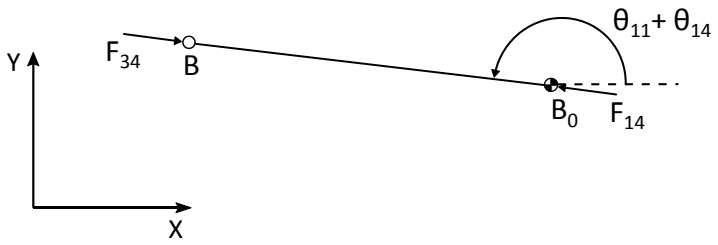

Figure 5.19. Free body diagram of link 4 (Two-force member)

$$F_{34} = -F_{14} \tag{5.48}$$

Force acting on point P is moved to the midpoint of link 3 to simplify calculations.

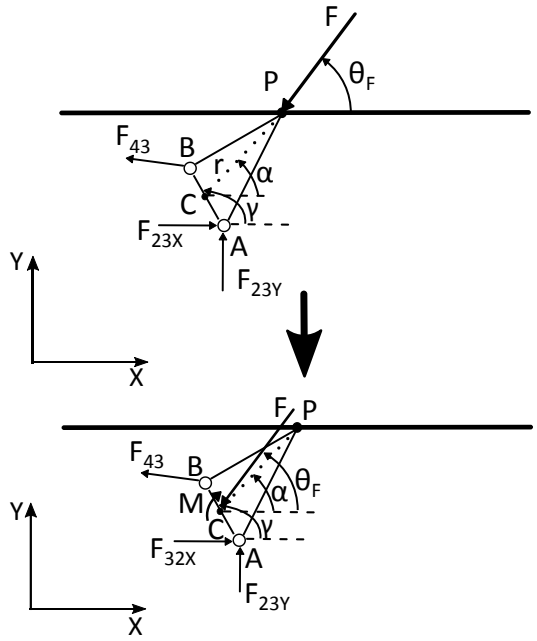

Figure 5.20. Free body diagram of link 3

$$\sum F_x = 0 \implies F_{23x} + F_{43}\cos(\theta_{11} + \theta_{14}) + F\cos(\theta_f) = 0 \tag{5.49}$$

$$\sum F_y = 0 \implies F_{23y} + F_{43}\sin(\theta_{11} + \theta_{14}) + F\sin(\theta_f) = 0 \tag{5.50}$$

$$\sum M_B = 0 \implies F_{23y} r_3 \sin\left(\frac{\pi}{2} - \gamma\right) + F_{23x} r_3 \sin(-\gamma) - M + F\frac{r_3}{2}\sin(\theta_f - \gamma) = 0 \tag{5.51}$$

Where,

$$M = Fr\sin\left(\theta_f - \beta - \gamma\right) \tag{5.52}$$

$$\alpha = \text{atan}\left((P_y - C_y), (P_x - C_x)\right) : constant \tag{5.53}$$

$$\gamma = \theta_{11} + \theta_{13} \tag{5.54}$$

$$\beta = -\alpha + \gamma \tag{5.55}$$

The set of equations given above can be written in matrix form as follows:

$$[A] \cdot [x] = [b] \tag{5.56}$$

Where [A] is the coefficient matrix, [x] is a variable matrix consists of unknown forces and [b] is a constant matrix. Each side of Eq. (5.56) is multiplied with $[A]^{-1}$ to find the solution of [x].

$$[x] = [A]^{-1} \cdot [b] \tag{5.57}$$

Where

$$[x] = \begin{bmatrix} F_{23x} \\ F_{23y} \\ F_{43} \\ T_{input} \end{bmatrix} \tag{5.58}$$

$$[A] = \begin{bmatrix} 1 & 0 & \cos(\theta_{11}+\theta_{14}) & 0 \\ 0 & 1 & \sin(\theta_{11}+\theta 14) & 0 \\ r_3\sin(-\gamma) & r_3\sin(\frac{\pi}{2}-\gamma) & 0 & 0 \\ -r_2\sin(\pi-\theta_{11}-\theta_{12}) & -r_2\sin(\frac{3\pi}{2}-\theta_{11}-\theta_{12}) & 0 & 1 \end{bmatrix} \quad (5.59)$$

$$[b] = \begin{bmatrix} -F\cos(\theta_f) \\ -F\sin(\theta_f) \\ +M - F\frac{r_3}{2}\sin(\theta_f-\gamma) \\ 0 \end{bmatrix} \quad (5.60)$$

Variable matrix, [x] can be calculated by using Eq. (5.57) to find unknown forces and required driving torque.

5.3. Kinematic Synthesis and Analysis of the Actuation Mechanisms

In this part, selected actuation mechanism concepts are synthesized by using a graphical approach based on an iterative process [14]. After synthesized studies are completed, kinematic analysis and force analysis are performed. In this section, only Concept A1 and Concept A3 are synthesized and analyzed. On the other hand, Concept A8 consists of a rotary actuator, which is directly connected to the driving link of the door mechanism. Therefore, there is no need to perform kinematic synthesis and analysis for Concept A8.

5.3.1. Kinematic Synthesis and Analysis of Concept A1

The schematic view of Concept A1 and variables are shown in Figure 5.21. The fixed link is A_0B_0. The output link, r_4 is rigidly connected to the driving link of the door mechanism. Two sides are symmetric; therefore, only one side is synthesized and analyzed.

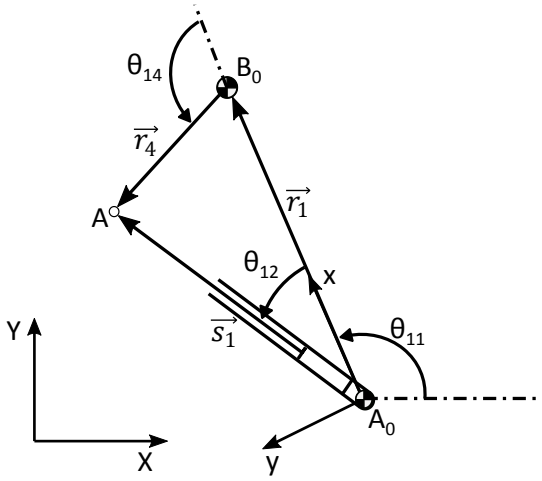

Figure 5.21. Schematic of Concept A1

5.3.1.1. Kinematic Synthesis

i. Graphical Approach

In this part, an iterative-based graphical approach is applied to find a solution to Concept A1. Required rotation of the output link should be equal to door mechanism driving link rotation between initial and final positions. For this purpose, the Concept D1 of the door mechanism found by a graphical approach is used. The required driving link rotation is calculated as -131,96 degrees. Therefore, the total rotation of the Concept A1 output link should be equal to -131,96 degrees.

After applying the graphical approach, a suitable mechanism shown in Figure 5.22 is synthesized. Initial and final positions are also given in this figure.

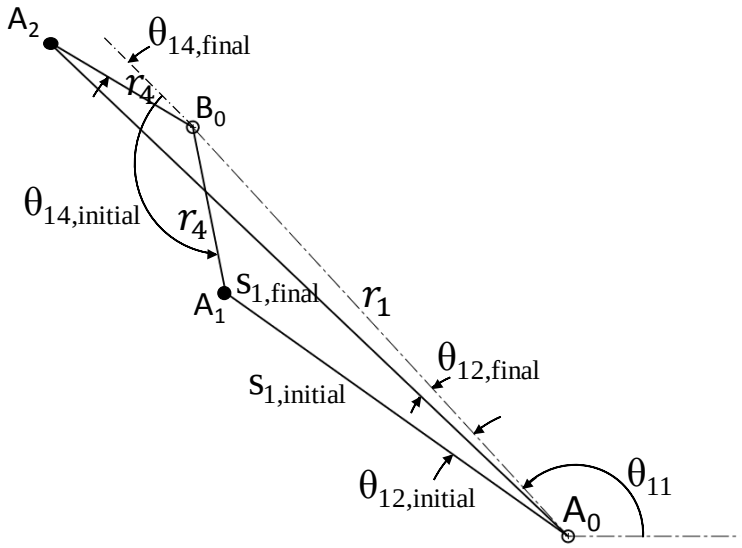

Figure 5.22. Synthesized Concept A1 schematic (Graphical Approach)

The calculated parameter values are given in Table 5.9.

Table 5.9. *Calculated parameter values for Concept A1 (Graphical Approach)*

1	2	3	4	5
r_1(mm)	r_4(mm)	s_1(mm)	θ_{11} (deg)	Δ_{stroke} (mm)
230,00	70,00	174,00	132,50	123,70

5.3.1.2. Kinematic Analysis

After the synthesis study of Concept A1, Freudenstein's equation explained in Appendix C is used to perform kinematic analysis and to obtain the position of the mechanism for every specified input joint variable. The loop closure equation in the vectorial form of Concept A1 is given in the Eq. (5.61).

$$\overrightarrow{s_1} - \overrightarrow{r_1} - \overrightarrow{r_4} = 0 \tag{5.61}$$

Complex number notation is given in the Eq. (5.62).

$$s_1 e^{i\theta_{12}} - r_1 - r_4 e^{i\theta_{14}} = 0 \tag{5.62}$$

By solving the Eq. (5.62), the unknown joint variables are θ_{12} and θ_{14} can be found as given below.

$$\theta_{12} = 2 \times atan\left(\sigma\sqrt{-\frac{C}{A}}\right) \tag{5.63}$$

$$\theta_{14} = \text{atan}\left(\frac{s_1 sin\theta_1}{s_1 cos\theta_1 - r_1}\right) \tag{5.64}$$

Where;

$$A = (K_1 + K_2 cos\theta_{12} - K_3 + cos\theta_{12}) \tag{5.65}$$

$$B = -2sin\theta_{12} \tag{5.66}$$

$$C = K_1 + K_2 cos\theta_{12} + K_3 - cos\theta_{12} \tag{5.67}$$

$$K_1 = \frac{r_4^2 - r_1^2 - r_2^2 - r_3^2}{2r_3 r_2} \tag{5.68}$$

$$K_2 = \frac{r_1}{r_3} \tag{5.69}$$

$$K_3 = \frac{r_1}{r_2} \tag{5.70}$$

$$\sigma = +1 \tag{5.71}$$

These equations are used to find joint variables for every stroke of the piston-cylinder and check the motion of the synthesized mechanism.

5.3.1.3. Static Force Analysis

Static force analysis is performed for Concept A1 to calculate the required driving force. The free-body diagram of each link is drawn, and unknown forces are identified. Force equilibrium equations are written for each link. Free body diagrams and equations are given below.

The system given in Figure 5.23 is in equilibrium under the action of the driving torque of the door mechanism, T_{input}, and driving force, $F_{actuator}$. The magnitude and direction of driving torque, T_{input} is previously calculated and known. Driving force, $F_{actuator}$, and the forces acting at joints can be determined.

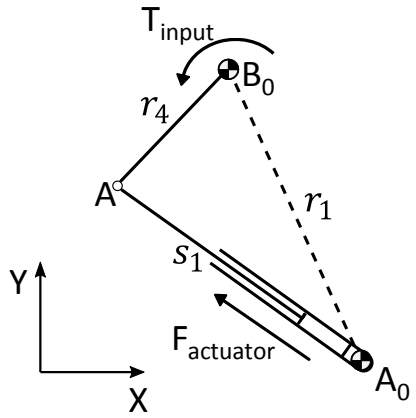

Figure 5.23. Driving force, $F_{actuator}$ and driving torque of door mechanism, T_{input} acting on Concept A1

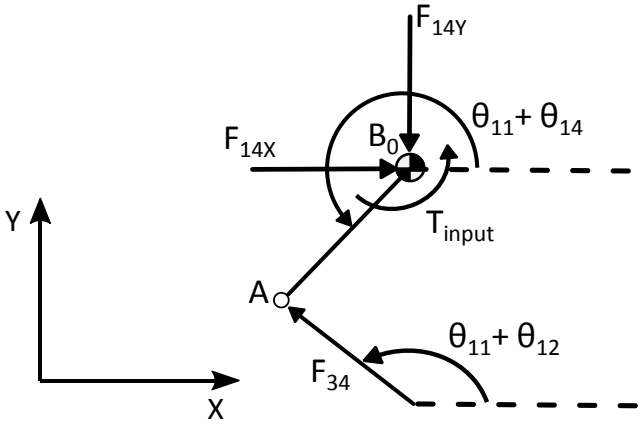

Figure 5.24. Free body diagram of link 4

$$\sum F_x = 0 \implies F_{14x} + F_{34}\cos(\theta_{12} + \theta_{11}) = 0 \tag{5.72}$$

$$\sum F_y = 0 \implies -F_{14y} + F_{34}\sin(\theta_{12} + \theta_{11}) = 0 \tag{5.73}$$

$$\sum M_{A0} = 0 \implies F_{34} r_4 \sin(\theta_{13} - \theta_{14}) + T_{input} = 0 \tag{5.74}$$

It is noted that $F_{ij} = -F_{ji}$ for the joint force. This equality is used to simplify the calculations.

$$F_{34} = -F_{43} \tag{5.75}$$

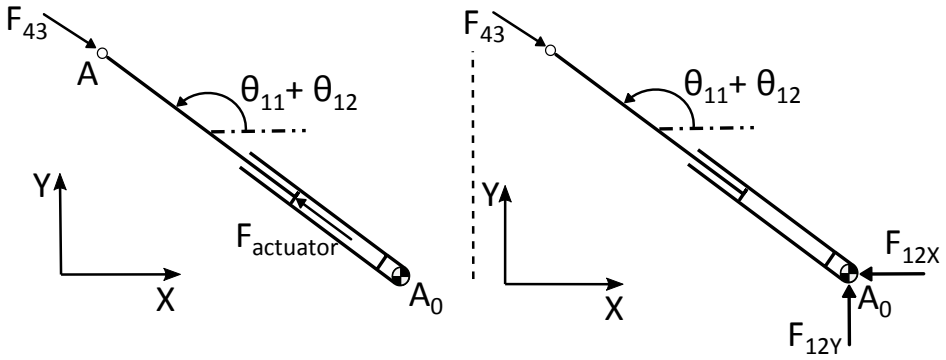

Figure 5.25. Free body diagram of link Piston-Cylinder (Two-force member)

$$-F_{43} = F_{actuator} = F_{34} \tag{5.76}$$

$$\sum F_x = 0 \implies -F_{12x} - F_{34}\cos(\theta_{12} + \theta_{11} + \pi) = 0 \tag{5.77}$$

$$\sum F_y = 0 \implies F_{12y} - F_{34}\sin(\theta_{12} + \theta_{11} + \pi) = 0 \tag{5.78}$$

The set of equations given above can be written in matrix form as follows:

$$[A] \cdot [x] = [b] \tag{5.79}$$

Where [A] is the coefficient matrix, [x] is a variable matrix consists of unknown forces and [b] is a constant matrix. Each side of Eq. (5.79) is multiplied with $[A]^{-1}$ to find the solution of [x].

$$[x] = [A]^{-1} \cdot [b] \tag{5.80}$$

Where

$$[x] = \begin{bmatrix} F_{14x} \\ F_{14y} \\ F_{34} \\ F_{actuator} \\ F_{12x} \\ F_{12y} \end{bmatrix} \tag{5.81}$$

$$[A] = \begin{bmatrix} 1 & 0 & \cos(\theta_{11} + \theta_{12}) & 0 & 0 & 0 \\ 0 & 1 & \sin(\theta_{11} + \theta_{12}) & 0 & 0 & 0 \\ 0 & 0 & r_4 \sin(\theta_{12} - \theta_{14}) & 0 & 0 & 0 \\ 0 & 0 & 1 & -1 & 0 & 0 \\ -1 & 0 & -\cos(\theta_{12} + \theta_{11} + \pi) & 1 & 0 & 0 \\ 0 & 1 & -\sin(\theta_{12} + \theta_{11} + \pi) & 0 & 0 & 0 \end{bmatrix} \tag{5.82}$$

$$[b] = \begin{bmatrix} 0 \\ 0 \\ -T_{input} \\ 0 \\ 0 \\ 0 \end{bmatrix} \tag{5.83}$$

Variable matrix, [x] can be calculated by using Eq. (5.80) to find unknown forces and required driving force, $F_{actuator}$.

5.3.2. Kinematic Synthesis and Analysis of Concept A3

Concept A3 is a multi-loop mechanism. The schematic view of Concept A3 and variables are shown in Figure 5.26 and Figure 5.27. The fixed link is A_0B_0. The output links, $r_4^{(2)}$ and $r_4^{(3)}$ are rigidly connected to driving links of the door mechanisms.

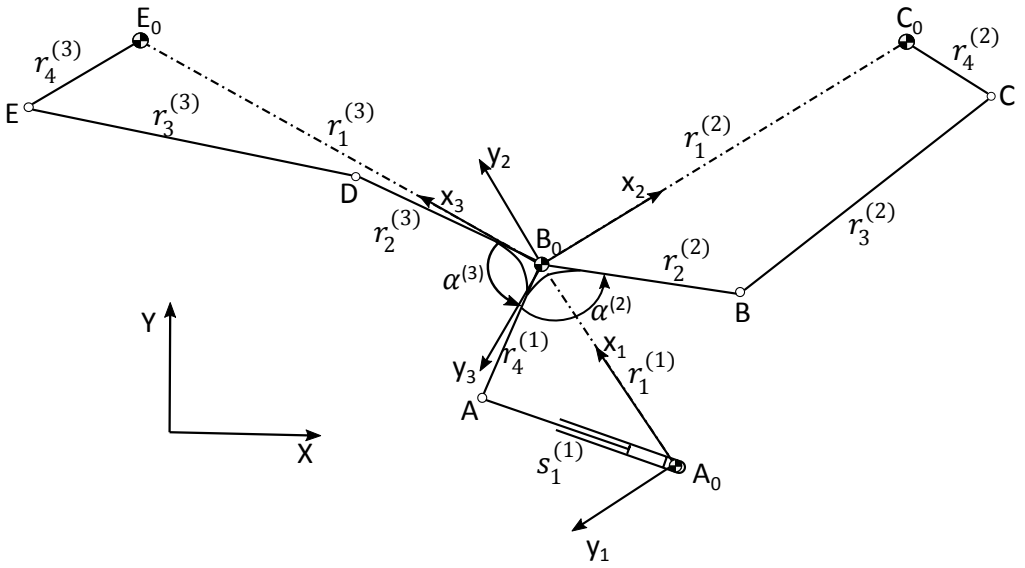

Figure 5.26. Schematic of Concept A3

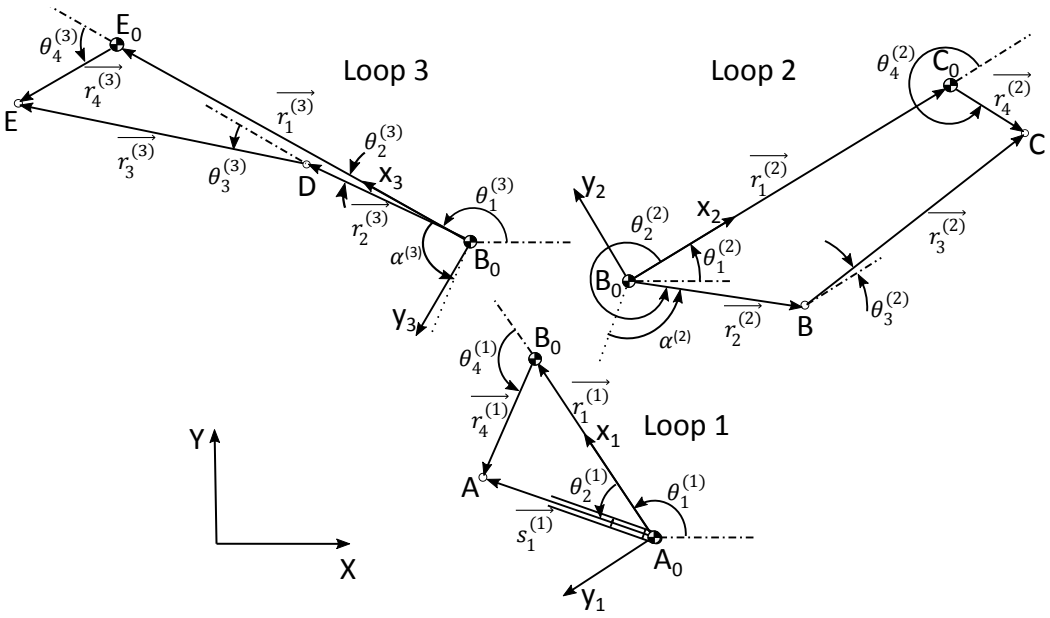

Figure 5.27. Loops and variables of Concept A3

5.3.2.1. Kinematic Synthesis

i. Graphical Approach

In this part, an iterative-based graphical approach is applied to find a solution to Concept A3. Required rotation of the output link should be equal to the door mechanism driving link rotation between initial and final positions. For this purpose, the Concept D1 of the door mechanism is previously determined by a graphical approach is used. The required driving link rotation is calculated as -131,96 degrees. Therefore, the total rotation of the Concept A3 output links should be equal to -131,96 degrees.

After applying the graphical approach, a suitable mechanism shown in Figure 5.28 is synthesized. Initial and final positions are also given in this figure.

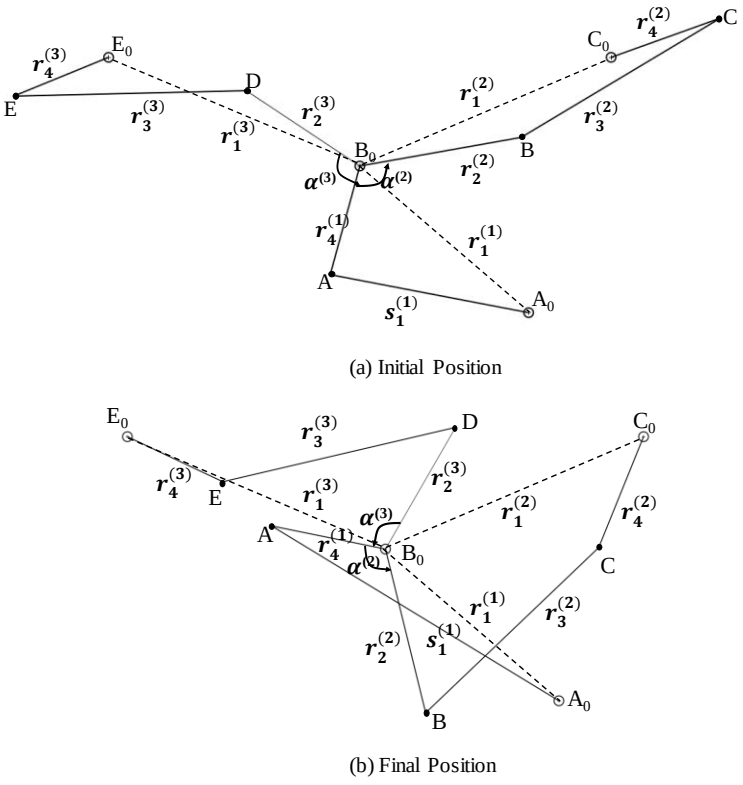

Figure 5.28. Synthesized Concept A3 schematic (Graphical Approach)

Calculated parameter values are given in Table 5.10.

Table 5.10. *Calculated parameter values for Concept A3 (Graphical Approach)*

1	**2**	**3**	**4**	**5**
$r_1^{(1)}$**(mm)**	$r_4^{(1)}$**(mm)**	s_0**(mm)**	$\theta_{11}^{(1)}$**(deg)**	Δ_{stroke} **(mm)**
205,17	135,00	185,00	138,87	142,18
6	**7**	**8**	**9**	**10**
$r_1^{(2)}$**(mm)**	$r_2^{(2)}$**(mm)**	$r_3^{(2)}$**(mm)**	$r_4^{(2)}$**(mm)**	$\theta_{11}^{(2)}$**(deg)**
250,80	150,00	213,00	106,50	23,50
11	**12**	**13**	**14**	**15**
$\alpha^{(2)}$**(deg)**	$r_2^{(3)}$**(mm)**	$r_3^{(3)}$**(mm)**	$r_4^{(3)}$**(mm)**	$\alpha^{(3)}$**(deg)**
-111,00	125,00	213,00	94,00	108,50

5.3.2.2. Kinematic Analysis

After the synthesis study of Concept A3, Freudenstein's equation explained in Appendix C is used to perform kinematic analysis and to obtain the position of the mechanism for every specified input joint variable. The loop closure equation in the vectorial form of the Loop 1-Concept A3 is given in the Eq. (5.84).

$$\overrightarrow{s_1} - \overrightarrow{r_1^{(1)}} - \overrightarrow{r_4^{(1)}} = 0 \tag{5.84}$$

Complex number notation is given in the Eq. (5.85).

$$s_1 e^{i\theta_{12}^{(1)}} - r_1^{(1)} - r_4^{(1)} e^{i\theta_{14}^{(1)}} = 0 \tag{5.85}$$

By solving the Eq. Eq. (5.85), the unknown joint variables are θ_{12} and θ_{14} can be found as given below.

$$\theta_{12}^{(1)} = 2 \times atan\left(\sigma^{(1)} \sqrt{-\frac{C^{(1)}}{A^{(1)}}}\right) \tag{5.86}$$

$$\theta_{14}^{(1)} = ata\,n\left(\frac{s_1 sin\theta_{11}^{(1)}}{s_1 cos\theta_{11}^{(1)} - r_1^{(1)}}\right) \tag{5.87}$$

Where;

$$A^{(1)} = (K_1^{(1)} + K_2^{(1)} cos\theta_{12}^{(1)} - K_3^{(1)} + cos\theta_{12}^{(1)}) \tag{5.88}$$

$$B^{(1)} = -2sin\theta_{12}^{(1)} \tag{5.89}$$

$$C^{(1)} = (K_1^{(1)} + K_2^{(1)} cos\theta_{12}^{(1)} + K_3^{(1)} - cos\theta_{12}^{(1)}) \tag{5.90}$$

$$K_1^{(1)} = \frac{(r_4^{(1)})^2 - (r_1^{(1)})^2 - (r_2^{(1)})^2 - (r_3^{(1)})^2}{2r_3^{(1)} r_2^{(1)}} \tag{5.91}$$

$$K_2^{(1)} = \frac{r_1^{(1)}}{r_3^{(1)}} \tag{5.92}$$

$$K_3^{(1)} = \frac{r_1^{(1)}}{r_2^{(1)}} \tag{5.93}$$

$$\sigma^{(1)} = +1 \tag{5.94}$$

These equations are used to find unknowns of loop 1, $\theta_{12}^{(1)}$ and $\theta_{14}^{(1)}$. Then, $\theta_{12}^{(2)}$ and $\theta_{12}^{(3)}$ are found by using the given equations below.

$$\theta_{12}^{(i)} = \theta_{14}^{(1)} - \alpha^{(i)} \; where \; i = 2,3 \tag{5.95}$$

After calculation of $\theta_{12}^{(2)}$ and $\theta_{12}^{(3)}$, Freudenstein's equation explained in Appendix C is used to calculate the unknowns of Loop 2 and Loop 3 to obtain the position of the mechanism for every specified input joint variable. Loop closure equation in the vectorial form of the Loop 2 and Loop 3 are given in the Eq. (5.96).

$$\overrightarrow{r_2^{(i)}} + \overrightarrow{r_3^{(i)}} - \overrightarrow{r_4^{(i)}} - \overrightarrow{r_1^{(i)}} = 0 \tag{5.96}$$

Complex number notation is given in the Eq. (5.97).

$$r_2^{(i)} e^{i\theta_{12}^{(i)}} + r_3^{(i)} e^{i\theta_{13}^{(i)}} - r_4^{(i)} e^{i\theta_{14}^{(i)}} - r_1^{(i)} = 0 \tag{5.97}$$

By solving the Eq. (5.97), the unknown joint variables are $\theta_{13}^{(i)}$ and $\theta_{14}^{(i)}$ can be found by using the below equations.

$$\theta_{13}^{(i)} = 2 \times atan\left(\frac{-B^{(i)} + \sigma\sqrt{(B^{(i)})^2 - 4A^{(i)}C^{(i)}}}{2A^{(i)}}\right) \tag{5.98}$$

$$\theta_{14}^{(i)} = \text{atan}\left(\frac{r_2^{(i)} sin\theta_{12}^{(i)} + r_3^{(i)} sin\theta_{13}^{(i)}}{r_2^{(i)} cos\theta_{12}^{(i)} + r_3^{(i)} cos\theta_{13}^{(i)} - r_1^{(i)}}\right) \tag{5.99}$$

Where;

$$A^{(i)} = (K_1^{(i)} + K_2^{(i)} cos\theta_{12}^{(i)} - K_3^{(i)} + cos\theta_{12}^{(i)}) \tag{5.100}$$

$$B^{(i)} = -2sin\theta_{12}^{(i)} \tag{5.101}$$

$$C^{(i)} = (K_1^{(i)} + K_2^{(i)} cos\theta_{12}^{(i)} + K_3^{(i)} - cos\theta_{12}^{(i)}) \tag{5.102}$$

$$K_1^{(i)} = \frac{(r_4^{(i)})^2 - (r_1^{(i)})^2 - (r_2^{(i)})^2 - (r_3^{(i)})^2}{2r_3^{(i)} r_2^{(i)}} \tag{5.103}$$

$$K_2^{(i)} = \frac{r_1^{(i)}}{r_3^{(i)}} \tag{5.104}$$

$$K_3^{(i)} = \frac{r_1^{(i)}}{r_2^{(i)}} \tag{5.105}$$

$$\sigma^{(2)} = +1, \sigma^{(3)} = -1 \tag{5.106}$$

These equations are used to find joint variables for every stroke of the piston-cylinder and check the motion of the synthesized mechanism.

5.3.2.3. Static Force Analysis

Static force analysis is performed for Concept A3 to calculate the required driving force. The free-body diagram of each link is drawn, and unknown forces are identified. Force equilibrium equations are written for each link. Free body diagrams and equations are given below.

The system given in Figure 5.29 is in equilibrium under the action of the driving torques of the door mechanisms, $T_{input,1}$ and $T_{input,2}$ and driving force, $F_{actuator}$. The magnitude and direction of driving torques, $T_{input,1}$ and $T_{input,2}$ are previously calculated and known. Driving force, $F_{actuator,}$ and the forces acting at joints can be determined.

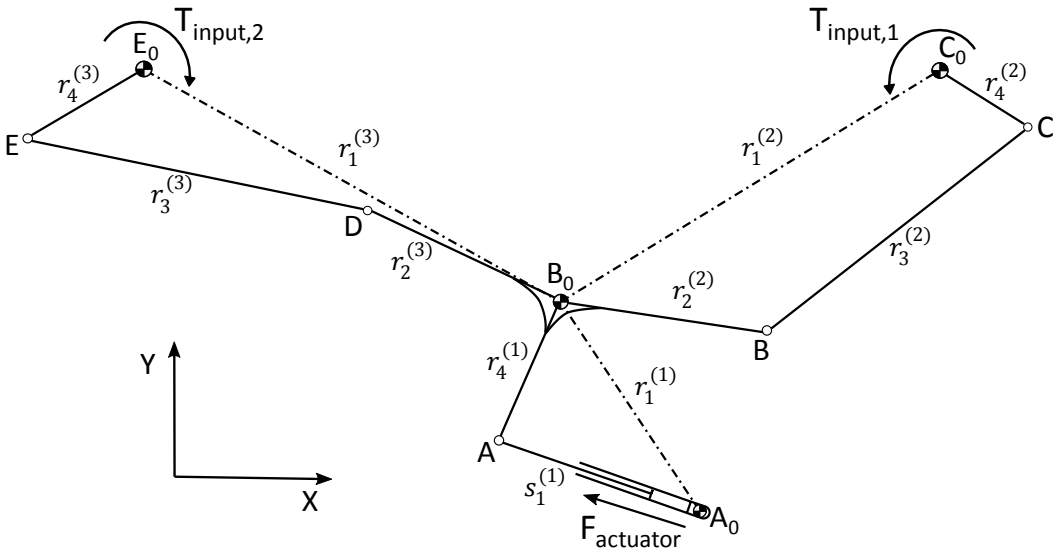

Figure 5.29. Driving force, $F_{actuator}$ and driving torques of door mechanism, $T_{input,1}$ and $T_{input,2}$ acting on Concept A3

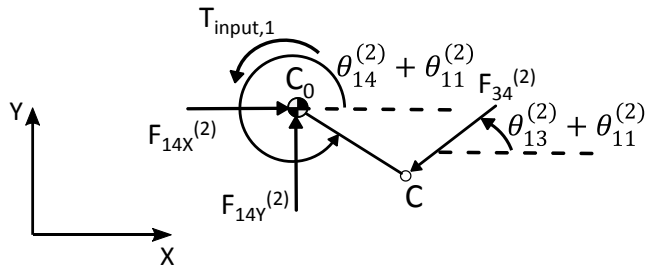

Figure 5.30. Free body diagram of link 4 of Loop 2

$$\sum F_x = 0 \implies F_{14x}^{(2)} + F_{34}^{(2)}\cos(\theta_{13}^{(2)} + \theta_{11}^{(2)} + \pi) = 0 \qquad (5.107)$$

$$\sum F_y = 0 \implies F_{14y}^{(2)} + F_{34}^{(2)}\sin(\theta_{13}^{(2)} + \theta_{11}^{(2)} + \pi) = 0 \qquad (5.108)$$

$$\sum M_{A0} = 0 \implies F_{34}^{(2)} r_4^{(2)} \, sin\left(\theta_{13}^{(2)} - \theta_{14}^{(2)}\right) + T_{input,1} = 0 \qquad (5.109)$$

It is noted that $F_{ij} = -F_{ji}$ for the joint force. This equality is used to simplify the calculations.

$$F_{34}^{(2)} = -F_{43}^{(2)} \qquad (5.110)$$

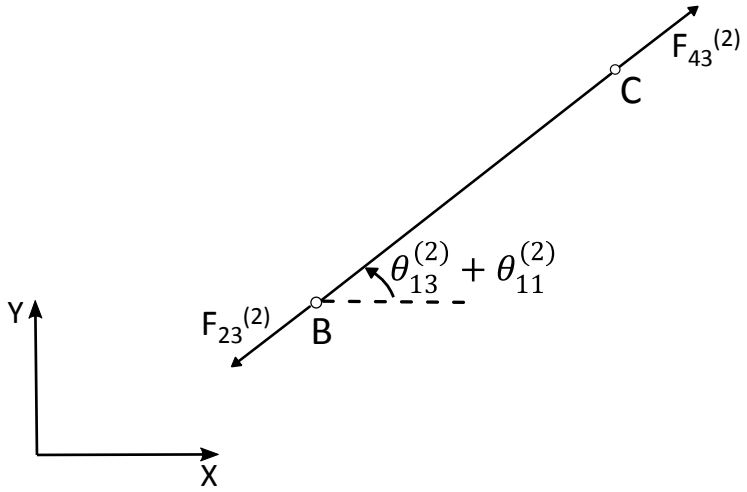

Figure 5.31. Free body diagram of link 3 of Loop 2 (Two-force member)

$$F_{43}^{(2)} = -F_{23}^{(2)} = -F_{34}^{(2)} = F_{32}^{(2)} \tag{5.111}$$

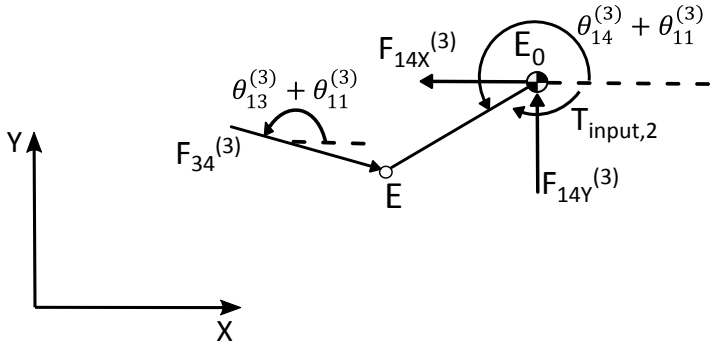

Figure 5.32. Free body diagram of link 4 of Loop 3

$$\sum F_x = 0 \implies -F_{14x}^{(3)} + F_{34}^{(3)} cos(\theta_{13}^{(3)} + \theta_{11}^{(3)} + \pi) = 0 \tag{5.112}$$

$$\sum F_y = 0 \implies F_{14y}^{(3)} + F_{34}^{(3)} sin(\theta_{13}^{(3)} + \theta_{11}^{(3)} + \pi) = 0 \tag{5.113}$$

$$\sum M_{A0} = 0 \implies F_{34}^{(3)} r_4^{(3)} \, sin\left(\theta_{13}^{(3)} - \theta_{14}^{(3)}\right) - T_{input,2} = 0 \tag{5.114}$$

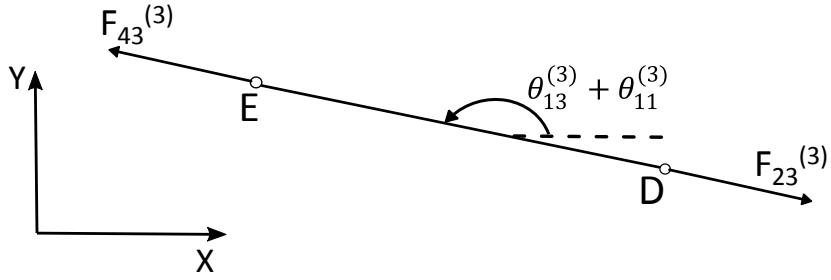

Figure 5.33. Free body diagram of link 3 of Loop 3 (Two-force member)

$$F_{43}^{(3)} = -F_{23}^{(3)} = -F_{34}^{(3)} = F_{32}^{(3)} \tag{5.115}$$

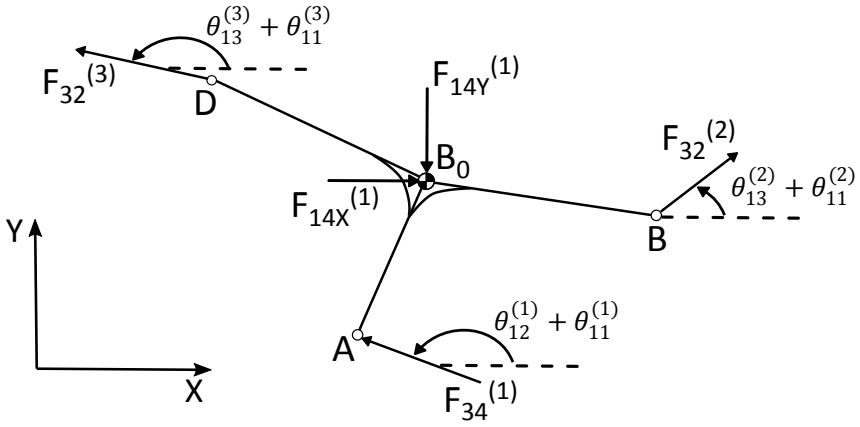

Figure 5.34. Free body diagram of the bellcrank

$$\sum F_x = 0 \implies F_{14x}^{(1)} - F_{34}^{(2)} \cos\left(\theta_{13}^{(2)} + \theta_{11}^{(2)}\right) - F_{34}^{(3)} \cos\left(\theta_{13}^{(3)} + \theta_{11}^{(3)}\right) = 0 \tag{5.116}$$

$$\sum F_y = 0 \implies -F_{14y}^{(1)} - F_{34}^{(2)} \sin\left(\theta_{13}^{(2)} + \theta_{11}^{(2)}\right) - F_{34}^{(3)} \sin\left(\theta_{13}^{(3)} + \theta_{11}^{(3)}\right) = 0 \tag{5.117}$$

$$\begin{aligned}\sum M_{B0} = 0 \implies & -F_{34}^{(2)} r_2^{(2)} \sin\left(\theta_{13}^{(2)} - \theta_{12}^{(2)}\right) - F_{34}^{(3)} r_2^{(3)} \sin\left(\theta_{13}^{(3)} - \theta_{12}^{(3)}\right) \\ & + F_{34}^{(1)} \mathrm{r}_4^{(1)} \sin(\theta_{12}^{(1)} - \theta_{14}^{(1)}) = 0\end{aligned} \tag{5.118}$$

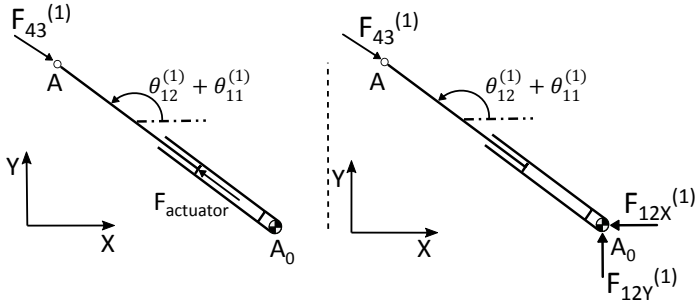

Figure 5.35. Free body diagram of Piston-Cylinder (Two-force member)

$$-F_{43}^{(1)} = F_{actuator} = F_{34}^{(1)} \tag{5.119}$$

$$\sum F_x = 0 \implies -F_{12x}^{(1)} - F_{34}^{(1)} \cos(\theta_{12}^{(1)} + \theta_{11}^{(1)} + \pi) = 0 \tag{5.120}$$

$$\sum F_y = 0 \implies F_{12y}^{(1)} - F_{34}^{(1)} \sin(\theta_{12}^{(1)} + \theta_{11}^{(1)} + \pi) = 0 \tag{5.121}$$

The set of equations given above can be written in matrix form as follows:

$$[A] \cdot [x] = [b] \tag{5.122}$$

Where [A] is the coefficient matrix, [x] is a variable matrix consists of unknown forces and [b] is a constant matrix. Each side of Eq. (5.122) is multiplied with $[A]^{-1}$ to find the solution of [x].

$$[x] = [A]^{-1} \cdot [b] \tag{5.123}$$

Where

$$[x] = \begin{bmatrix} F_{14x}^{(2)} \\ F_{14y}^{(2)} \\ F_{34}^{(2)} \\ F_{14x}^{(2)} \\ F_{14y}^{(2)} \\ F_{34}^{(2)} \\ F_{14x}^{(1)} \\ F_{14y}^{(1)} \\ F_{34}^{(1)} \\ F_{actuator} \\ F_{12x}^{(1)} \\ F_{12y}^{(1)} \end{bmatrix} \tag{5.124}$$

$$[A] = \begin{bmatrix} 1 & 0 & \cos(\theta_{13}^{(2)} + \theta_{11}^{(2)} + \pi) & 0 & 0 & 0 & 0 & 0 & 0 & 0 & 0 & 0 \\ 0 & 1 & \sin(\theta_{13}^{(2)} + \theta_{11}^{(2)} + \pi) & 0 & 0 & 0 & 0 & 0 & 0 & 0 & 0 & 0 \\ 0 & 0 & r_4^{(2)} \sin(\theta_{13}^{(2)} - \theta_{14}^{(2)}) & 0 & 0 & 0 & 0 & 0 & 0 & 0 & 0 & 0 \\ 0 & 0 & 0 & -1 & 0 & \cos(\theta_{13}^{(3)} + \theta_{11}^{(3)} + \pi) & 0 & 0 & 0 & 0 & 0 & 0 \\ 0 & 0 & 0 & 0 & 1 & \sin(\theta_{13}^{(3)} + \theta_{11}^{(3)} + \pi) & 0 & 0 & 0 & 0 & 0 & 0 \\ 0 & 0 & 0 & 0 & 0 & r_4^{(3)} \sin(\theta_{13}^{(3)} - \theta_{14}^{(3)}) & 0 & 0 & 0 & 0 & 0 & 0 \\ 0 & 0 & -\cos(\theta_{13}^{(2)} + \theta_{11}^{(2)}) & 0 & 0 & -\cos(\theta_{13}^{(3)} + \theta_{11}^{(3)}) & 1 & 0 & 0 & 0 & 0 & 0 \\ 0 & 0 & -\sin(\theta_{13}^{(2)} + \theta_{11}^{(2)}) & 0 & 0 & -\sin(\theta_{13}^{(3)} + \theta_{11}^{(3)}) & 0 & -1 & 0 & 0 & 0 & 0 \\ 0 & 0 & -r_2^{(2)} \sin(\theta_{13}^{(2)} - \theta_{12}^{(2)}) & 0 & 0 & -r_2^{(3)} \sin(\theta_{13}^{(3)} - \theta_{12}^{(3)}) & 0 & 0 & r_4^{(1)} \sin(\theta_{12}^{(1)} - \theta_{14}^{(1)}) & 0 & 0 & 0 \\ 0 & 0 & 0 & 0 & 0 & 0 & 0 & 0 & -1 & 1 & 0 & 0 \\ 0 & 0 & 0 & 0 & 0 & 0 & 0 & 0 & -\cos(\theta_{12}^{(3)} + \theta_{11}^{(3)} + \pi) & 0 & 1 & 0 \\ 0 & 0 & 0 & 0 & 0 & 0 & 0 & 0 & -\sin(\theta_{12}^{(3)} + \theta_{11}^{(3)} + \pi) & 0 & 0 & 1 \end{bmatrix} \tag{5.125}$$

$$[b] = \begin{bmatrix} 0 \\ 0 \\ -T_{input,1} \\ 0 \\ 0 \\ T_{input,2} \\ 0 \\ 0 \\ 0 \\ 0 \\ 0 \\ 0 \end{bmatrix} \tag{5.126}$$

Variable matrix, [x] can be calculated by using Eq. (5.123) to find unknown forces and required driving force, $F_{actuator}$.

CHAPTER 6

APPLICATION OF GENETIC ALGORITHM

In this section, both selected door mechanism concepts and actuation mechanism concepts are optimized by using the Genetic Algorithm Method. MATLAB Software is used to apply the Genetic Algorithm. MATLAB Software contains the Genetic Algorithm function and allows users to change Genetic Algorithm options easily. Different options exist, so an iterative process is applied to determine the best options. After the optimization is performed, concepts are compared to select the best concept for both the door mechanism and the actuation mechanism.

The used notation of the variables is given as $a_{i,k}^{(j)}$.

Where, index a : variable, i : variable number, j: loop number, and k: step number. The loop number is only used for multi-loop mechanisms.

Genetic Algorithm options are given in Table 6.1. These options are used in both the optimization process of door mechanism concepts and actuation mechanism concepts.

Table 6.1. *Options of the Genetic Algorithm optimization method*

Population Size	Maximum Generation	Crossover Function	Crossover Fraction	Mutation Function
2250	500	Heuristic 1.2	0.8	Uniform 0.1

6.1. Optimization of Door Opening Mechanisms

In this part, selected door mechanism concepts are synthesized and optimized based on different requirements and constraints. The open position clearance and the space envelope constraints of the door mechanism are defined for each door mechanism

concept. The door opening mechanism concepts are optimized by considering these limitations. When two doors open, the required clearance is minimum 400mm. Therefore, for a single door, the minimum clearance is 200mm. Figure 6.1 shows the required final position of doors.

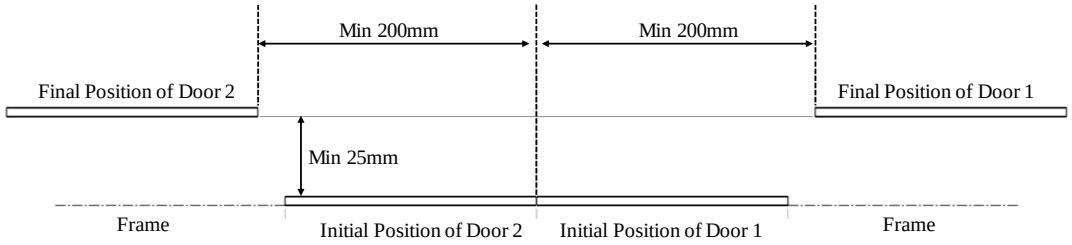

Figure 6.1. Final position requirements of doors

The allowable space envelope for the door opening mechanism is given in Figure 6.2.

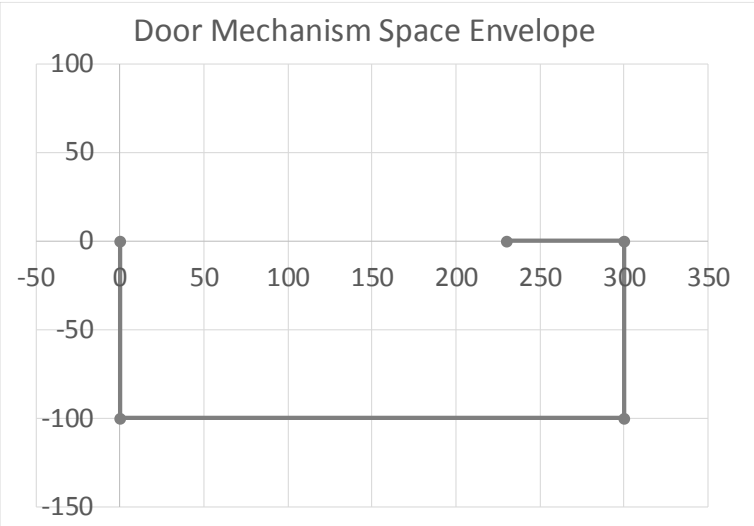

Figure 6.2. Allowable space envelope of the door mechanism

6.1.1. Optimization of Concept D1

The Concept D1 is shown in Figure 6.3. Firstly, the door hinge mechanism is designed by using a graphical approach and an analytical method (three positions synthesis methods with specified fixed pivots) to find a solution of mechanism and determine the boundary conditions of the design variables. Finally, a Multi-Objective Genetic Algorithm is applied to find an optimized mechanism solution according to motion and force characteristics.

The design variables of this system are $r_1, r_2, r_3, r_4, \theta_{12,initial}, \theta_{11}, \Delta_\theta$ also, unknowns of this system are θ_{13}, θ_{14}. All geometric variables are given in Figure 6.3. When applying the Genetic Algorithm optimization method, Eqs. set (5.1) to (5.11) is used to analyze the mechanism and find unknowns of the system and Eqs. set (5.12) to (5.30) is used for static force analysis and optimization of force characteristics.

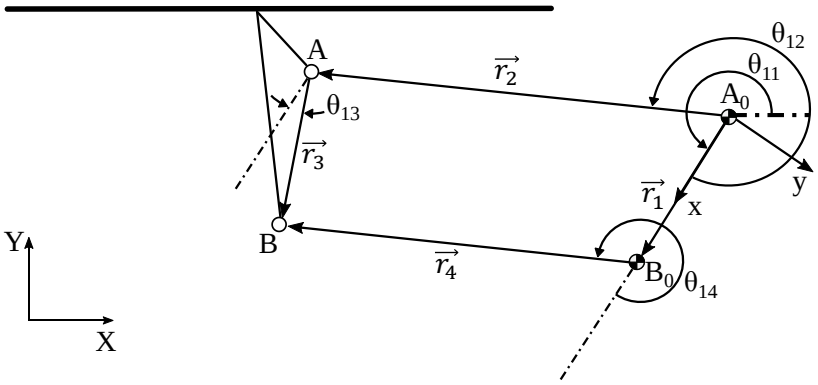

Figure 6.3. Schematic of Concept D1

The input variable, $\theta_{12,k}$ is calculated every step by using the given equation below.

$$\theta_{12,k} = \theta_{12,initial} + \Delta_\theta \times (i - 1) \tag{6.1}$$

Where, $k = 2,3 \ldots, N$. In this problem step number taking as $N = 50$.

6.1.1.1. Goal Functions

In this problem, a laterally opening hinge mechanism is to be designed. Therefore, the first goal function is the orientation of the door. Desired rotation of the door is zero degrees between closed and open positions. The door is rigidly connected to the coupler link hence the goal function is given as:

$$f(1) = abs\left(abs\left(\theta_{3,\text{initial}} - \theta_{3,\text{final}}\right)\right) G \tag{6.2}$$

Where G is a penalty function and used to verify that the mechanism is working properly at every step of the mechanism motion. If the mechanism works correctly at every step, then it is defined as $G = 1$. On the other hand, if the mechanism does not work correctly at any step, the value of $G = 1000000$ is assigned to penalize the solution.

The second objective function is the optimization of the input torque. The purpose of this objective function is to reduce the required input torque of the door hinge mechanism to decrease the required actuator power. Eqs. set (5.12) to (5.30) is used to calculate input torque. This objective function is given as;

$$f(2) = maximum\left(T_{input}\right) \times G \tag{6.3}$$

6.1.1.2. Constraints of Concept D1

Concept D1 is constrained according to different limitations.

The first limitation is the orientation of the first position of mechanism to find a suitable mechanism. These constraints are given in Eq. (6.4) and Eq. (6.5).

$$175° \geq \theta_{11} + \theta_{12,initial} \geq 165° \tag{6.4}$$

$$absolute(\theta_{12,initial} - \theta_{13,initial}) > 5° \tag{6.5}$$

The second limitation is the open position clearance of the doors given in Figure 6.1. The constraint is given in the Eq. (6.6) is defined to satisfy required final position.

$$r_2 \times \cos(\theta_{11} + \theta_{12,final}) - r_2 \times \cos(\theta_{11} + \theta_{12,initial}) - 200mm > 0 \quad (6.6)$$

Also, the allowable space envelope for door opening mechanism is given in Figure 6.2. Other constraints are defined based on the given space envelope restriction. Fixed point, A_0 is located at (230,-50). Therefore, these constraints are defined according to the given A_0 location.

Constraint about the initial position of the fixed point, B_0 is given in the Eq. (6.7).

$$r_1 \times \sin(\theta_{11}) > -50mm \quad (6.7)$$

Constraints about the initial and final position of moving points, A_0 and B_0 are defined to prevent collision between the moving point and frame/door at initial and final positions and obtain suitable mechanism. Eq. (6.8) and Eq. (6.9) constrain the initial and final position of the moving point, A. Constraints of the moving point, B are given in the Eq. (6.10), Eq. (6.11), and Eq. (6.12).

$$r_2 \times sin(\theta_{11} + \theta_{12,initial}) < 30mm \quad (6.8)$$

$$120mm > r_2 \times sin(\theta_{11} + \theta_{12,final}) > 70mm \quad (6.9)$$

$$r_1 \times \sin(\theta_{11}) + r_4 \times \sin(\theta_{11} + \theta_{14,initial}) < 30mm \quad (6.10)$$

$$r_1 \times \cos(\theta_{11}) + r_4 \times \cos(\theta_{11} + \theta_{14,initial}) > -180mm \quad (6.11)$$

$$170mm > r_1 \times \sin(\theta_{11}) + r_4 \times \cos(\theta_{11} + \theta_{14,final}) > 70mm \quad (6.12)$$

These constraints are applied in the optimization code. If these constraints are not satisfied, the penalty function, G is taken as G = 1000000 to penalize and eliminate this solution.

The final limitation is the range for design variables. Design variables are determined according to design space limitations. The initial range of design variables is found by using graphical and analytical approaches. After finding initial ranges, an iterative process is applied to find the final suitable range of the design variables. The limits of the design variables are given in Table 6.2.

Table 6.2. *Upper and lower boundaries of Concept D1's design variables*

	1	2	3	4	5	6	7
	r_1(mm)	r_2(mm)	r_3(mm)	r_4(mm)	θ_{12} (deg)	θ_{11} (deg)	Δ_θ (deg)
Minimum	20	100	30	100	-65	180	-2,90
Maksimum	100	200	125	200	65	230	-1,60

6.1.1.3. Results of Concept D1 Optimization

After the optimization process, the optimized mechanism is determined. The calculated parameters are given in Table 6.3.

Table 6.3. *Optimized parameter values of Concept D1*

1	2	3	4	5	6	7
r_1(mm)	r_2(mm)	r_3(mm)	r_4(mm)	θ_{12} (deg)	θ_{11} (deg)	Δ_θ (deg)
42,12	119,89	36,57	139,39	-63,31	228,92	-2,40

The computation time is 637 seconds for Concept D1 optimization process. The position error is evaluated as 3,25E-06 radians. Also, the maximum required input torque is calculated as 24,48 Nm. The initial and final positions of the optimized mechanism are given in Figure 6.4.

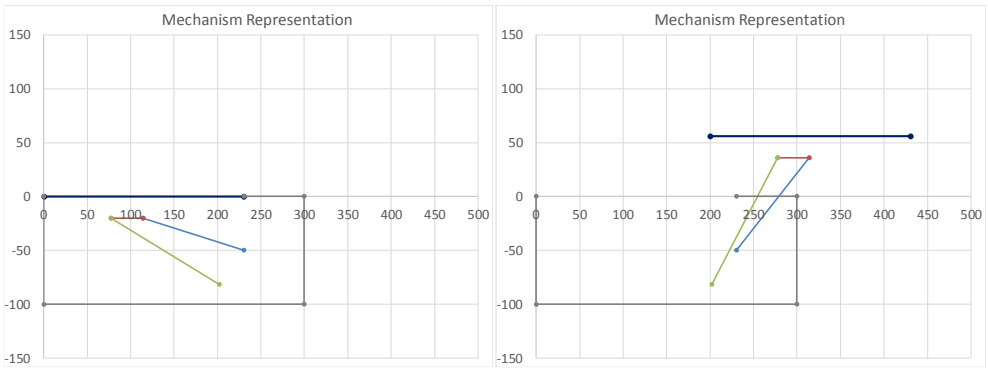

Figure 6.4. The initial and final position of optimized Concept D1

The MSC ADAMS model is created in order to verify the calculation of input torque. Concept D1 MSC ADAMS model is given in Figure 6.5. This figure shows the revolute joints, applied forces, and given motion.

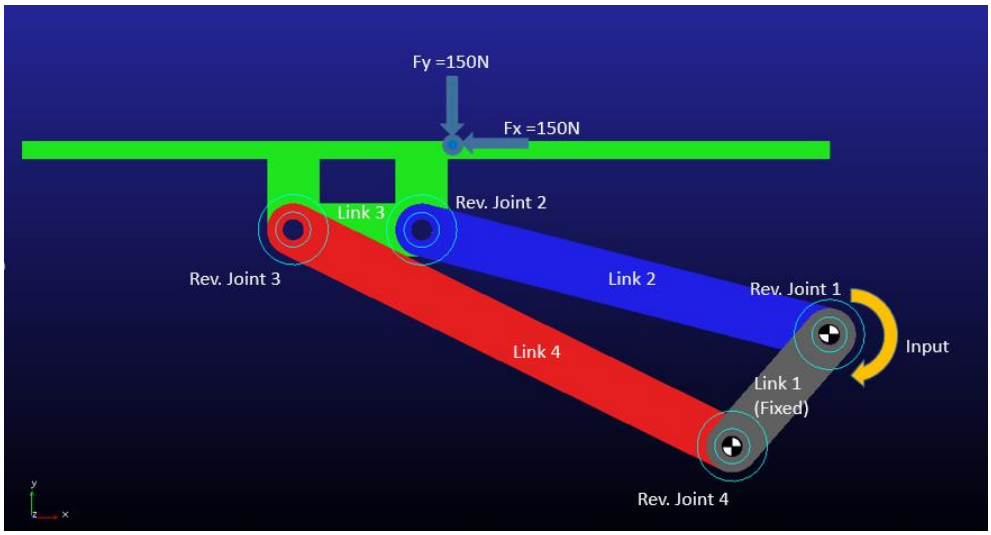

Figure 6.5. MSC ADAMS model of optimized Concept D1

Figure 6.6 shows the calculated required input torque by using MSC ADAMS and Genetic Algorithm with respect to crank angle rotation. Additionally, the percentage error between MSC ADAMS and Genetic Algorithm results is given in Figure 6.7.

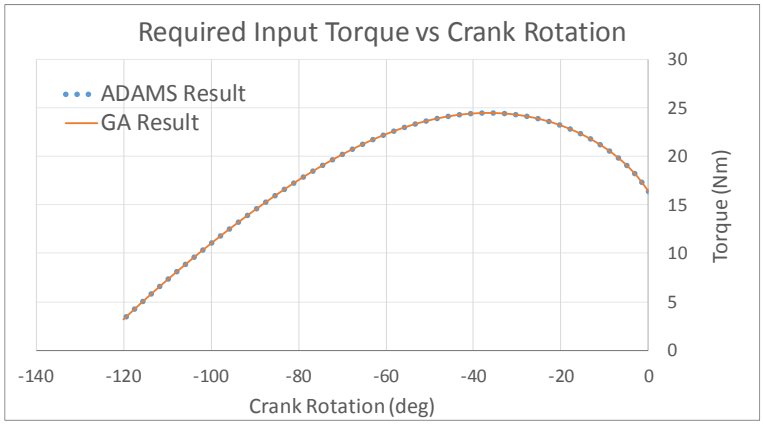

Figure 6.6. Required driving torque of Concept D1

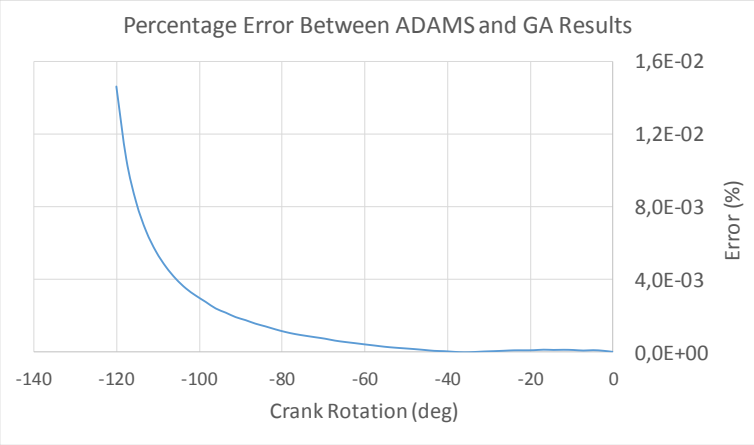

Figure 6.7. Percentage error between MSC ADAMS and Genetic Algorithm

It should be noted that mechanisms, which are synthesized by using graphical and analytical approaches, are also analyzed by using MSC ADAMS to compare the results of the Genetic Algorithm method. Calculated driving torque by using various methods difference is given in Figure 6.8. Required maximum input torque calculated by using the Genetic Algorithm is the smallest as seen in this figure.

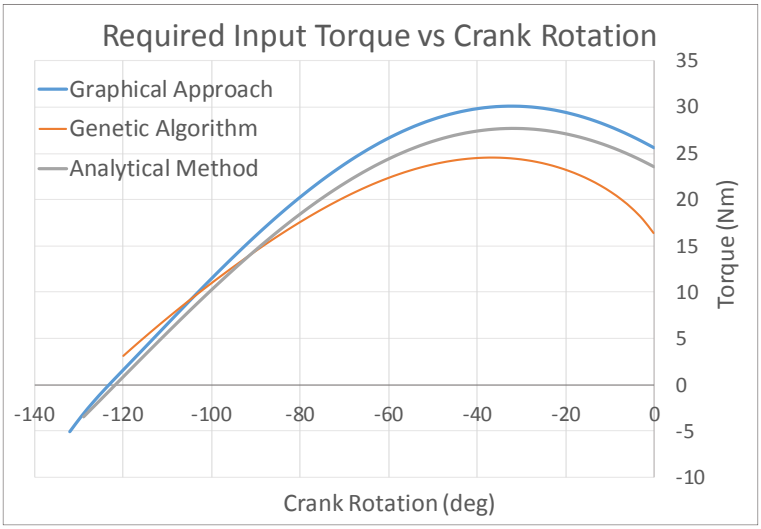

Figure 6.8. Calculated driving torque of different methods

Table 6.4 shows the maximum input torque of different methods and percentage improvement of the Genetic Algorithm method compared to analytical and graphical methods.

Table 6.4. *Maximum required driving torques of Concept D1 and percent improvements*

	METHODS		
	Genetic Algorithm	**Analytical Method**	**Graphical Approach**
Maximum Driving Torque	24,48	27,65	30,08
Percent Improvement		11,47%	18,59%

6.1.2. Optimization of Concept D5

The second selected concept of the door mechanism is shown in Figure 6.9. Firstly, the door hinge mechanism is designed by using a graphical approach and an analytical method (three positions synthesis methods with specified fixed pivots) to find a solution of mechanism and determine the boundary conditions of the design variables. Finally, a Multi-Objective Genetic Algorithm is applied to find an optimized mechanism solution according to motion and force characteristics.

The design variables of this system are $r_1, r_2, r_3, r_4, \theta_{12,initial}, \theta_{11}, \Delta_\theta$, and unknowns of this system are θ_{13}, θ_{14}. All geometric variables are given in Figure 6.9. When applying the Genetic Algorithm optimization method, Eqs. set (5.31) to (5.41) is used to analyze the mechanism and find unknowns of the system and Eqs. set (5.42) to (5.60) is used for static force analysis and optimization of force characteristics.

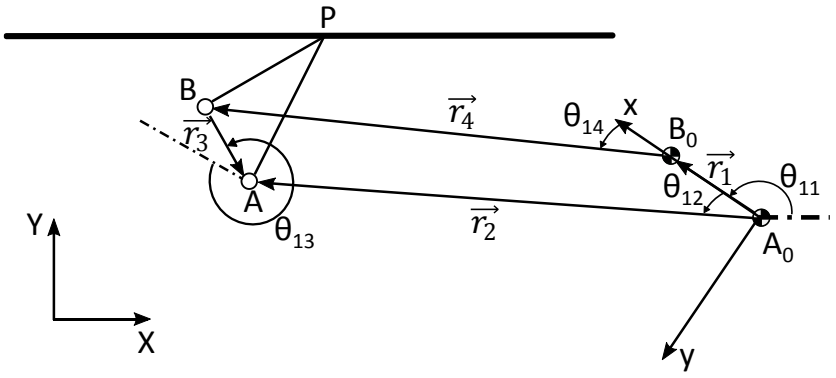

Figure 6.9. Schematic of Concept D5

The input variable, $\theta_{12,k}$ is calculated every step by using the given equation.

$$\theta_{12,k} = \theta_{12,initial} + \Delta_\theta \times (k-1) \tag{6.13}$$

Where, $k = 2,3 \ldots, N$. In this problem step number taking as $N = 50$.

6.1.2.1. Goal Functions

In this problem, a 180-degree rotation hinge mechanism is to be designed. Therefore, the first goal function is the orientation of the door. The desired rotation of the door is 180 degrees between closed and open positions. The door is rigidly connected to the coupler link hence the goal function is given as:

$$f(1) = abs\left(abs\left(\theta_{13,\text{initial}} - \theta_{13,\text{final}}\right) - 180°\right)G \tag{6.14}$$

Where G is a penalty function and used to verify that the mechanism is working properly at every step of the mechanism motion. If the mechanism is working properly at every step, then $G = 1$. If one of the loops is not working properly at any step, the value of $G = 1000000$ is assigned to penalize the solution.

The second objective function is the optimization of the input torque. The purpose of this objective function is to reduce the required input torque of the door hinge mechanism to decrease the required actuator power. Eqs. set (5.42) to (5.60) is used to calculate input torque. This objective function is given as;

$$f(2) = maximum\left(T_{input}\right) \times G \tag{6.15}$$

6.1.2.2. Constraints of Concept D5

Concept D5 is constrained according to different limitations.

The first limitation is the orientation of the first position of the mechanism to find a suitable mechanism. These constraints are given in Eq. (6.16) and Eq.(6.17).

$$\theta_{11} + \theta_{12,initial} \geq 155° \tag{6.16}$$

$$\theta_{11} + \theta_{14,initial} \geq 165° \tag{6.17}$$

The second limitation is the open position clearance of the doors given in Figure 6.1, and the allowable space envelope for the door mechanism is given in Figure 6.2.

These constraints are applied in the optimization code. If these constraints are not satisfied, the penalty function, G is taken as G = 1000000 to penalize and eliminate this solution.

The third limitation is the range for design variables. Design variables are determined according to design space limitations. The initial range of design variables is found by using graphical and analytical approaches. After finding initial ranges, an iterative process is applied to find the final suitable range of the design variables. The limits of the design variables are given in Table 6.5.

Table 6.5. *Upper and lower boundaries of Concept D5's design variables*

	1	**2**	**3**	**4**	**5**	**6**	**7**
	r_1(mm)	**r_2(mm)**	**r_3(mm)**	**r_4(mm)**	**$\theta_{12,initial}$ (deg)**	**θ_{11} (deg)**	**Δ_θ (deg)**
Minimum	20	135	15	135	2	170	-1,50
Maksimum	50	210	60	200	45	100	-3,00

6.1.2.3. Results of Design 2 Optimization

After the optimization process, the optimized mechanism is determined. The calculated parameters are given in Table 6.6.

Table 6.6. *Optimized parameter values of Concept D5*

1	2	3	4	5	6	7
r_1(mm)	r_2(mm)	r_3(mm)	r_4(mm)	$\theta_{12,initial}$ (deg)	θ_{11} (deg)	Δ_θ (deg)
25,69	209,68	28,20	184,20	16,14	160,57	-2,10

The computation time is 491 seconds for Concept D5 optimization process. The position error is evaluated as 4,32E-09 radians. Also, the maximum required input torque is calculated as 37,91 Nm. The initial and final positions of the optimized mechanism are given in Figure 6.10.

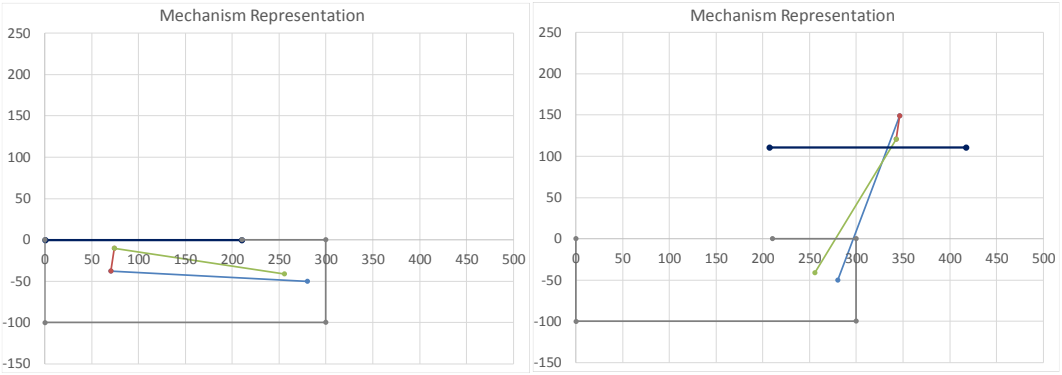

Figure 6.10. The initial and final position of optimized Concept D1

Also, the MSC ADAMS model is created in order to verify the calculation of input torque. Concept D5 MSC ADAMS model is given in Figure 6.11. This figure shows the revolute joints, applied forces, and given motion.

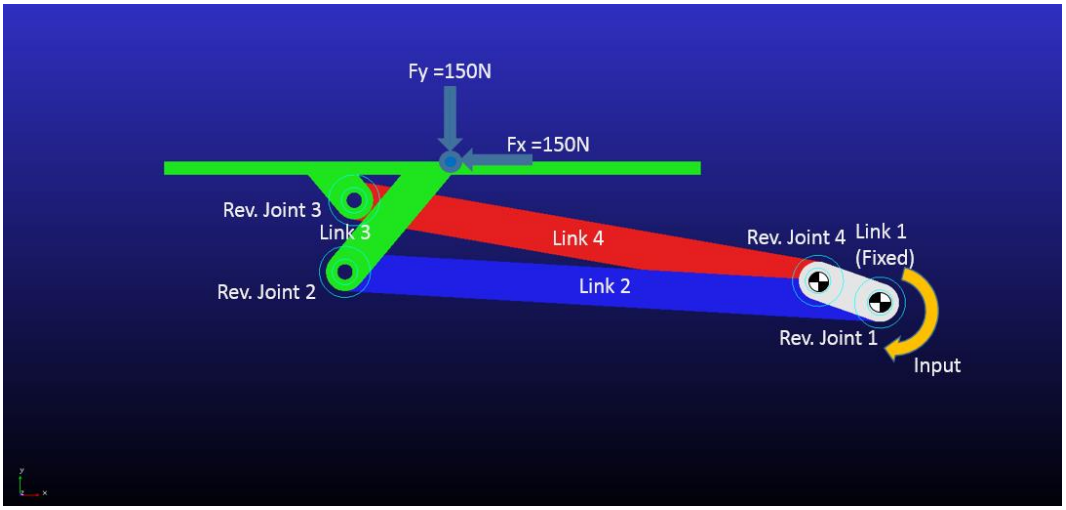

Figure 6.11. MSC ADAMS model of optimized Concept D5

Figure 6.12 shows the calculated required input torque by using MSC ADAMS and Genetic Algorithm with respect to crank angle rotation. Additionally, the percentage error between MSC ADAMS and Genetic Algorithm results is given in Figure 6.13.

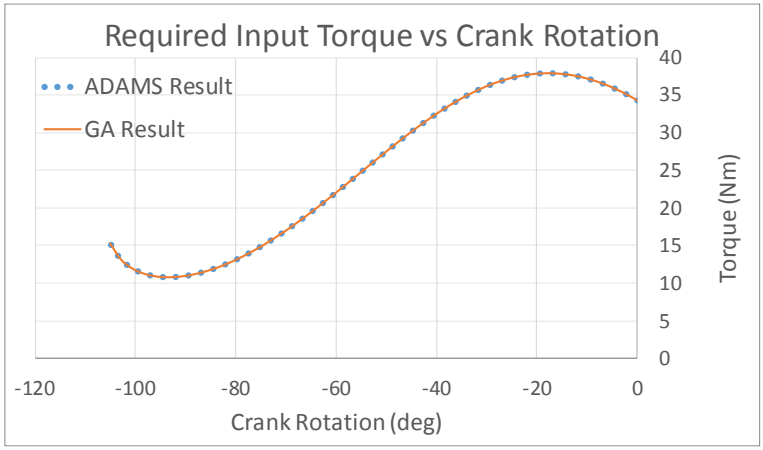

Figure 6.12. Required driving torque of Concept D5

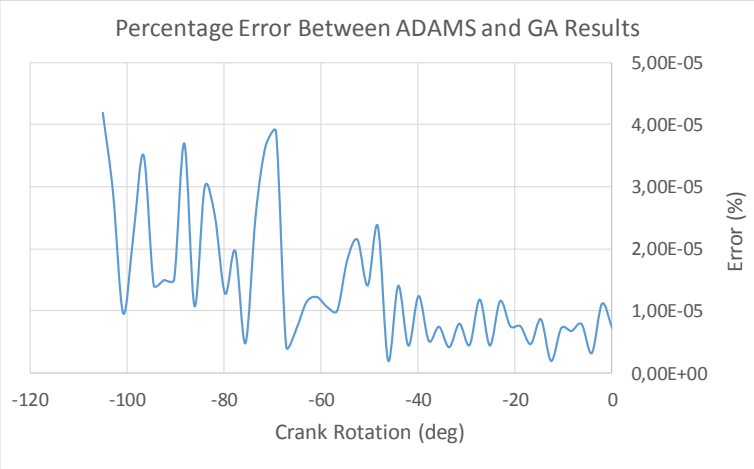

Figure 6.13. Percentage error between MSC ADAMS and Genetic Algorithm

The mechanisms, which are synthesized by using graphical and analytical approaches, are also analyzed by using MSC ADAMS to compare the results of the Genetic Algorithm method. The calculated driving torque by using various methods is given in Figure 6.14. The required maximum input torque calculated by using the Genetic Algorithm is the smallest as seen in this figure.

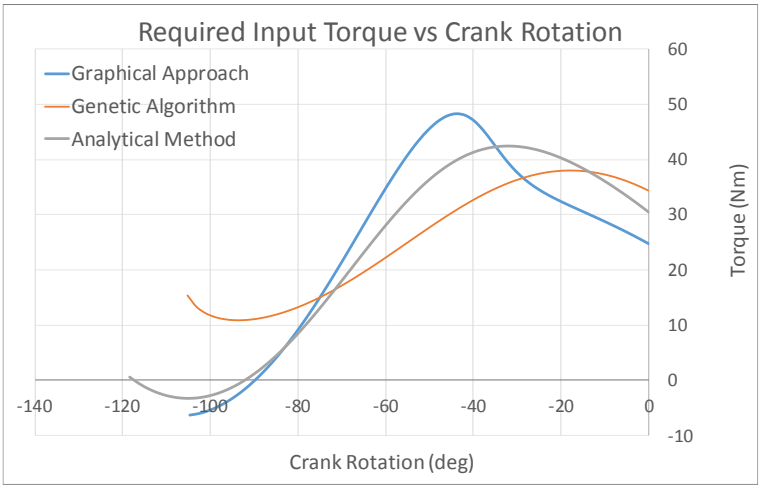

Figure 6.14. Calculated driving torque of different methods

Table 6.7 shows the maximum input torque of different methods and percentage improvement of the Genetic Algorithm method compared to analytical and graphical methods.

Table 6.7. *Maximum required driving torques of Concept D5 and percent improvements*

	METHODS		
	Genetic Algorithm	**Analytical Method**	**Graphical Approach**
Maximum Driving Torque(Nm)	37,91	42,38	48,26
Percent Improvement		10,54%	21,43%

6.2. Comparison of Selected Door Mechanism Concepts

In this part, Concept D1 and Concept D5 are compared, and one of the door opening mechanism is selected in order to reduce the number of door opening design options to one.

The first criterion is the required input torque. Figure 6.15 shows the optimized driving torque graph of Concept D1 and Concept D5.

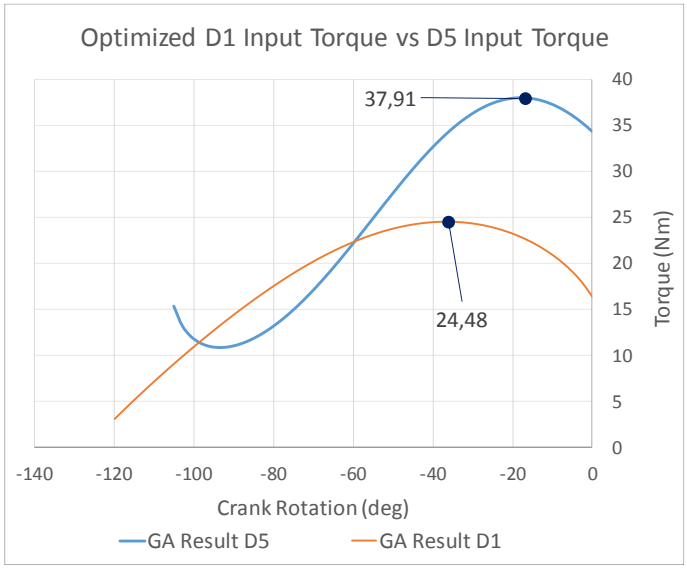

Figure 6.15. Driving torque comparison of Concept D1 and Concept D5

The percent difference between these designs is given in the below equation.

$$\frac{T_{D1,max} - T_{D2,max}}{\left(\frac{T_{D1,max} + T_{D2,max}}{2}\right)} \times 100 = 43{,}05\% \tag{6.18}$$

Figure 6.15 and Eq. (6.18) show that the percent difference between the maximum input torque of Concept D1 and Concept D5 is significant. The required input torque directly affects actuator size, mass, and power consumption; therefore, using Concept D1 is more favorable, compared with Concept D5. Additionally, Concept D1 width is smaller than Concept D5; therefore, Concept D1 is more suitable to combine with an actuation mechanism concept where space is a constraint. Based on these results, Concept D1 is selected to combine with the selected actuation mechanism concepts.

6.3. Optimization of Actuation Mechanism Concepts

In this part, the selected actuation mechanism concepts are synthesized and optimized based on outputs of the door opening mechanism, requirements, and constraints. The output link of the selected actuation mechanism concepts, which are Concept A1 and Concept A3, are rigidly connected to the crank of the door opening mechanism. Therefore, the crank rotation of the door opening mechanism is equal to the output link of these actuation mechanisms. On the other hand, rotary actuators are used in Concept A8 and directly connected to the driving links of the door mechanism. Therefore, there is no need to optimize Concept A8. In this section, only Concept A1 and Concept A3 are optimized.

Concept D1 is selected as the preferred door mechanism. Therefore, Concept D1 outputs are used. The first input of actuation mechanisms is calculated Concept D1 crank rotation between initial and final positions. The second input is required driving torque to actuate Concept D1. Figure 6.16 shows an input-output flow chart of the problem.

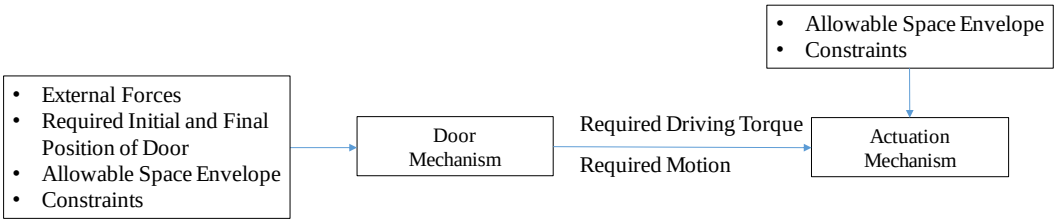

Figure 6.16. Input-output flow chart of the problem

An order three polynomial trend-line of required input torque is generated, and the required crank rotation between initial and final position is calculated by using Concept D1 results. The generated trend-line equation is given in the Eq. (6.19). Figure 6.17 shows the generated trend-line and required crank rotation, $(\Delta_{\theta_{12}})_{Design1}$ calculated as -120 degree.

$$T(\Delta_{\theta_{12}}) = -2 \times 10^{-5}(\Delta_{\theta_{12}})^3 - 0{,}0068(\Delta_{\theta_{12}})^2 - 0{,}4289(\Delta_{\theta_{12}}) + 17{,}029 \qquad (6.19)$$

Where

$$\begin{aligned} \Delta_{\theta_{12}} &= \left(\theta_{12}^{i} - \theta_{12}^{initial}\right)_{door\ opening\ mech.} \\ &= \left(\theta_{14}^{i} - \theta_{14}^{initial}\right)_{actuation\ mech.} \end{aligned} \qquad (6.20)$$

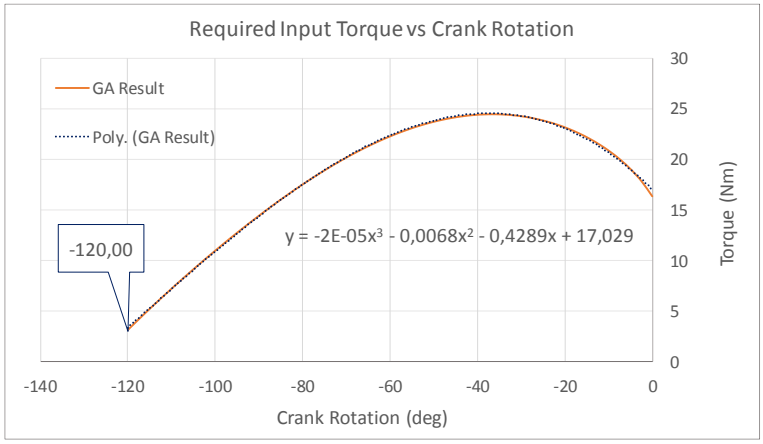

Figure 6.17. Trend-line of Concept D1's driving torque

Also, the total allowable space envelope constraint of the actuation mechanisms and door mechanism is defined. The actuation mechanism concepts are optimized by considering this limitation given in Figure 6.18.

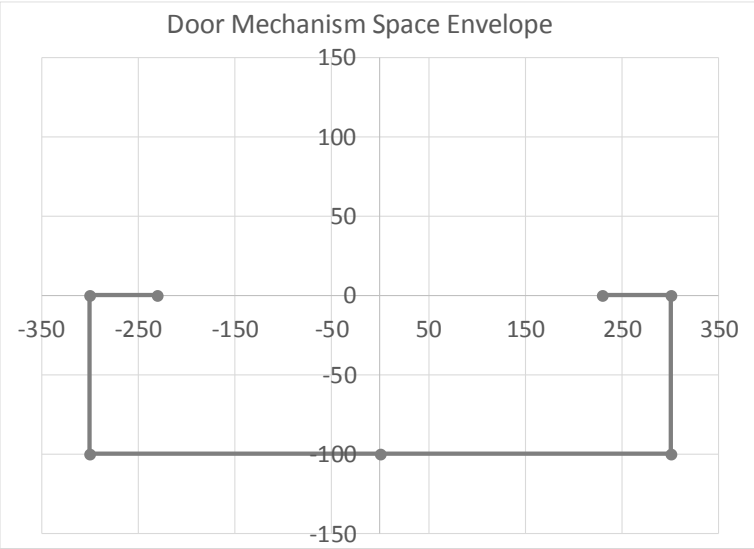

Figure 6.18. Allowable space envelope of the in-flight door actuation mechanism

6.3.1. Optimization of Concept A1

The first concept is shown in Figure 6.19. A Genetic Algorithm is applied to find an optimized mechanism according to motion and force characteristics.

The design variables of this system are $r_1, r_4, s_0,\ \theta_{11}, \Delta_{stroke}$ .Unknowns of this system are $\theta_{12}\ and\ \theta_{14}$. All geometric variables are given in Figure 6.19. When applying the Genetic Algorithm optimization method, Eqs. set (5.61) to (5.71) is used to analyze the mechanism and find unknowns of the system and Eqs. set (5.72) to (5.83) is used for static force analysis and optimization of force characteristics.

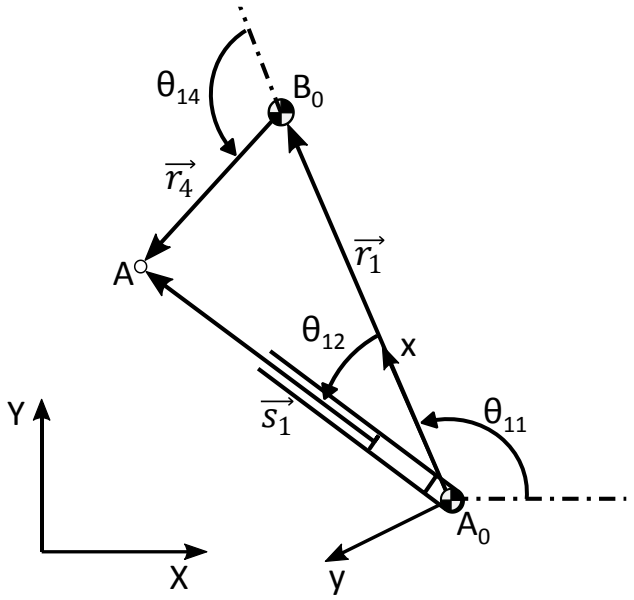

Figure 6.19. Schematic of Concept A1

The input stroke, $s_{1,k}$ is calculated every step by using the given equation.

$$s_{1,k} = s_0 + \Delta_{stroke} \times (k-1) \tag{6.21}$$

Where, $k = 2,3 \dots, N$. In this problem step number taking as $N = 50$.

6.3.1.1. Goal Functions

In this problem, the actuation mechanism is developed to combine with Concept D1. The actuation mechanism provides motion to the door mechanism in order to open or close the doors. Required crank rotation, $(\Delta_{\theta_{12}})_{Design1}$ between the initial and final position of the door mechanism is previously calculated. The first goal function of the actuation mechanism is providing the required motion to rotate the crank of the door mechanism from the initial position to the final position. The actuation mechanism output link is rigidly connected to the crank of the door mechanism; hence, the rotation of these links is considered equal. The goal function is given below.

$$f(1) = abs\left(abs\left(\theta_{14,\text{initial}} - \theta_{14,\text{final}}\right) - (\Delta_{\theta_{12}})_{Design1}\right)G \tag{6.22}$$

Where G is a penalty function and used to verify that the mechanism works correctly at every step of motion. If the mechanism works correctly at every step, then $G = 1$. If one of the loops is not working correctly at any step, the value of $G = 1000000$ is assigned to penalize the solution.

The second objective function is the optimization of the actuation force. The purpose of this objective function is to reduce the required actuation force of the actuation mechanism to decrease the required power. Eqs. set (5.72) to (5.83) is used to calculate the actuator force. This objective function is given as;

$$f(2) = maximum(F_{actuator}) \times G \tag{6.23}$$

6.3.1.2. Constraints of Concept A 1

Concept A1 is constrained according to different limitations.

The first limitation is the transmission angle to find a suitable mechanism. This constraint is given in Eq. (6.24).

$$140° \geq \mu \geq 20° \tag{6.24}$$

The second limitation is the total allowable space envelope given in Figure 6.18 for the door opening mechanism and actuation mechanism. The door opening mechanism fixed pivot, A_0 is located at (230,50). Therefore, these constraints are given in the Eq. (6.25), Eq. (6.26), and Eq. (6.27) are defined based on the total allowable space envelope, and door-opening mechanism fixed pivot, A_0.

$$r_1 \times sin(\theta_{11}) < 300mm \tag{6.25}$$

$$r_1 \times cos(\theta_{11}) < 170mm \tag{6.26}$$

$$s_{1,final} \times sin\left(\theta_{11} + \theta_{12,final}\right) - r_1 \times sin(\theta_{11}) < 45 \tag{6.27}$$

These constraints are applied in the optimization code. If these constraints are not satisfied, the penalty function, G is taken as G = 1000000 to penalize and eliminate this solution.

The final limitation is the range for design variables. Design variables are determined according to design space limitations. The initial range of design variables is determined by using graphical and analytical approaches. After finding the initial ranges, an iterative process is applied to find the final suitable range of the design variables. The limits of the design variables are given in Table 6.8.

Table 6.8. *Upper and lower boundaries of Concept A1's design variables*

	1	**2**	**3**	**4**	**5**
	r_1**(mm)**	r_4**(mm)**	s_0**(mm)**	θ_{11} **(deg)**	Δ_{stroke} **(mm)**
Minimum	50	30	50	50	1
Maksimum	300	130	250	200	3,2

6.3.1.3. Results of Concept A1

Following the optimization process, the optimized mechanism is determined. The calculated parameters are given in Table 6.9.

Table 6.9. *Optimized parameter values of Concept A1*

1	**2**	**3**	**4**	**5**
r_1**(mm)**	r_4**(mm)**	s_0**(mm)**	θ_{11} **(deg)**	Δ_{stroke} **(mm)**
249,99	78,39	189,94	131,44	2,65

The computation time is 193 seconds for Concept A1 optimization process. The position error is evaluated as 3,96E-06 radians. The maximum required input force is calculated as 313,18 N. The simulation of the optimized mechanism is given in Figure 6.20.

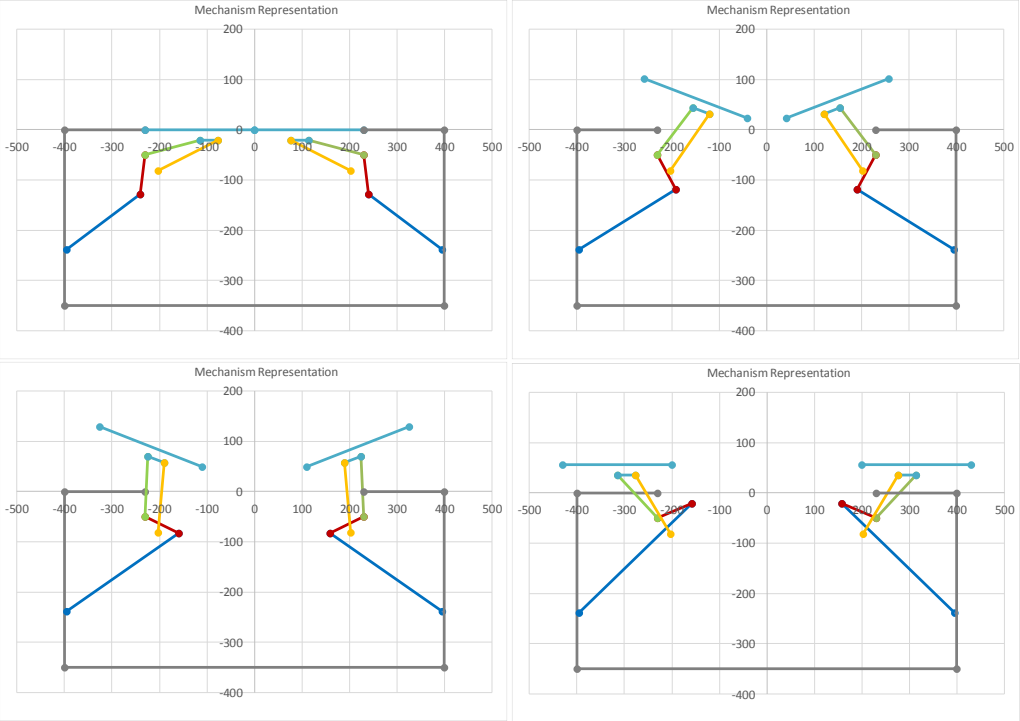

Figure 6.20. Simulation of the Concept A1 combined with Concept D1

In addition, the MSC ADAMS model is created in order to verify the calculation of the actuator force. The combination of door mechanism (Concept D1) and actuation mechanism (Concept A1) MSC ADAMS model is given in Figure 6.21. This figure shows joints, applied forces, and given motion of the combined mechanism.

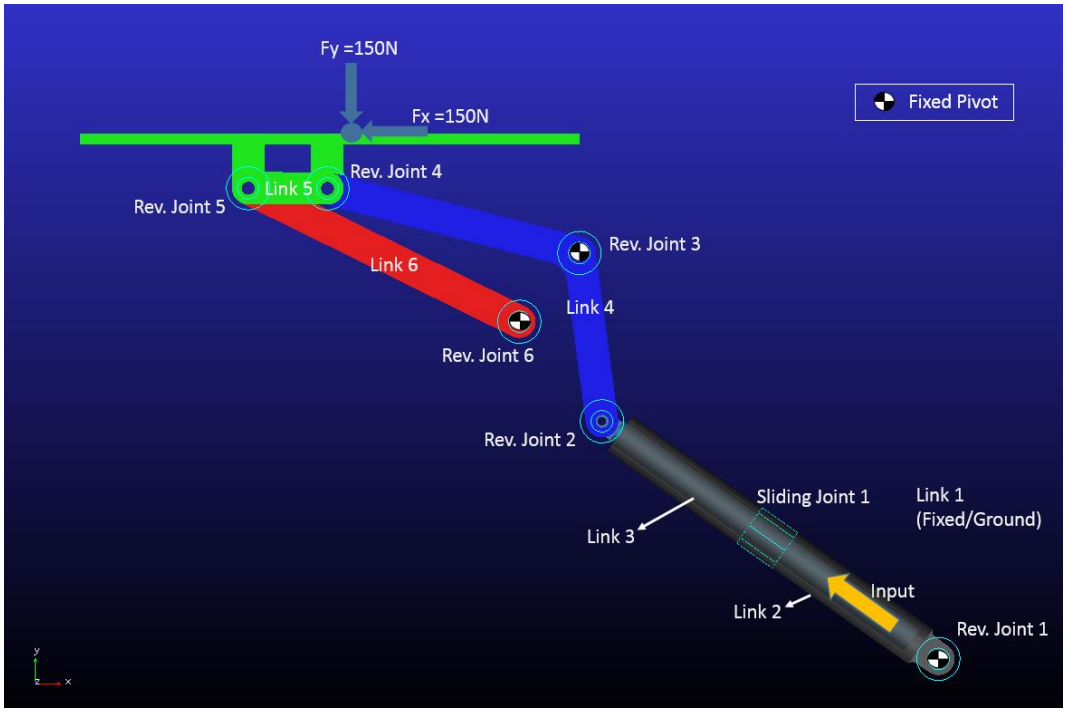

Figure 6.21. MSC ADAMS model of optimized Concept A1

Figure 5.27 shows the calculated required input torque by using MSC ADAMS and the Genetic Algorithm with respect to the stroke of the actuator.

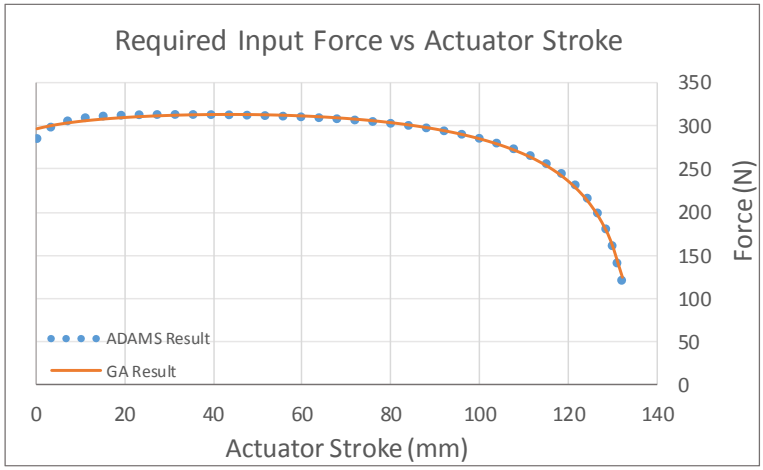

Figure 6.22. Required actuator force of Concept A1 (One side)

In addition, mechanism, which is synthesized by using a graphical approach, is also analyzed by using MSC ADAMS to compare the results of the Genetic Algorithm method. The calculated input forces by using various methods are given in Figure 6.23.

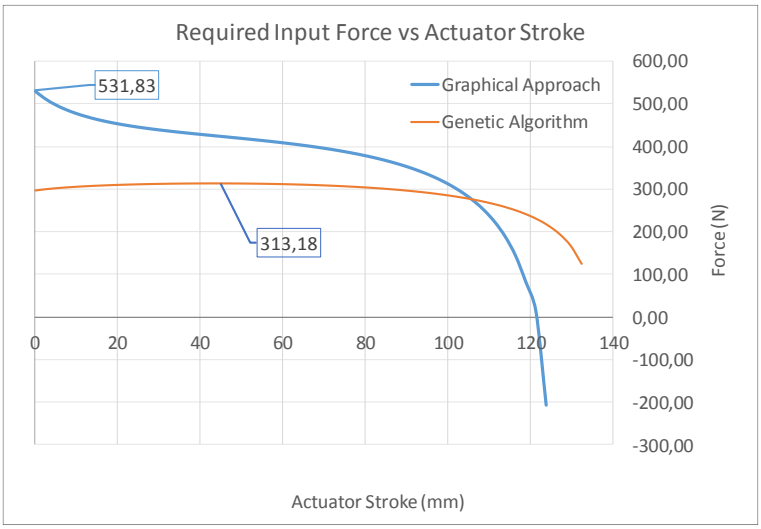

Figure 6.23. Calculated actuator forces comparison of different methods

Table 6.10 shows the maximum input force of different methods and the percentage improvement of the Genetic Algorithm method compared to the graphical method.

Table 6.10. *Maximum actuator forces of Concept A1 and percent improvement*

	METHODS	
	Genetic Algorithm	**Graphical Approach**
Maximum Actuator Force (N)	313,18	531,83
Percent Improvement		41,11%

6.3.2. Optimization of Concept A3

The second actuation mechanism concept is shown in Figure 6.24. The Genetic Algorithm is applied to find an optimized mechanism according to motion and force characteristics.

The design variables of this system are $r_1^{(1)}, r_4^{(1)}, s_0,\ \theta_{11}^{(1)},\ \Delta_{stroke},\ r_1^{(2)},\ r_2^{(2)}, r_3^{(2)}, r_4^{(2)}, \theta_{11}^{(2)}, \alpha^{(2)}, r_1^{(3)}, r_2^{(3)},\ r_3^{(3)}, r_4^{(3)}, \theta_{11}^{(3)}, \alpha^{(3)}$. Also, the unknowns of this system are $\theta_{12}^{(1)}, \theta_{14}^{(1)},\ \theta_{13}^{(2)}, \theta_{14}^{(2)},\ \theta_{13}^{(3)}\ and\ \theta_{14}^{(3)}$. All geometric variables are given in Figure 6.24. When applying the Genetic Algorithm optimization method, Eqs. set (5.84) to (5.106) is used to analyze the mechanism and find unknowns of the system and Eqs. set (5.107) to (5.126) is used for static force analysis and optimization of force characteristics.

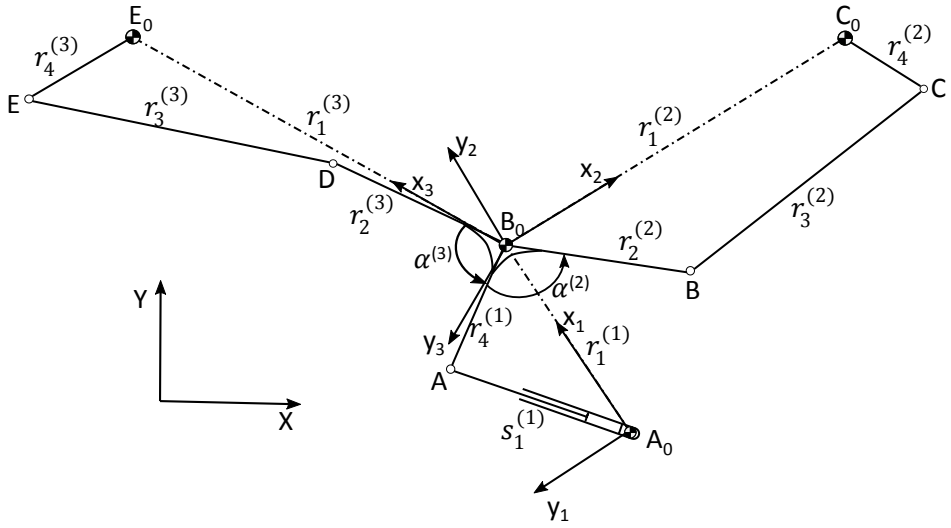

Figure 6.24. Schematic of Concept A3

The input stroke, Δ_{stroke} is given and $s_1^{(1)}$ is calculated every step by using the given equation.

$$s_{1,i}^{(1)} = s_0 + \Delta_{stroke} \times (i-1) \tag{6.28}$$

Where, $i = 1,2 \ldots, N$ and $N: Step\ Number$. In this problem step number taking as $N = 50$.

6.3.2.1. Goal Functions

In this problem, the actuation mechanism is developed to combine with Concept D1. The Actuation mechanism provides the motion required to open or close doors. The required crank rotation, $(\Delta_{\theta_{12}})_{Design1}$ between the initial and final position of the door mechanism is calculated. The first goal function of the actuation mechanism is to provide the required motion to rotate the crank of the door mechanism from the initial position to the final position. The actuation mechanism output link is rigidly connected to the crank of the door mechanism hence rotation of these links is considered equal. The goal function is given in the Eq. (6.29).

$$f(1) = abs\left(abs\left(\theta^{(2)}_{4,\text{initial}} - \theta^{(2)}_{4,\text{final}}\right) - (\Delta_{\theta_{12}})_{Design1}\right) G \qquad (6.29)$$

Where G is the penalty function and used to confirm the mechanism is working correctly throughout every step of the motion. If the mechanism is working correctly at every step, then $G = 1$. If one of the loops is not working correctly at any step, the value of $G = 1000000$ is assigned to penalize the solution.

The second objective function is the optimization of the actuation force. The purpose of this objective function is to reduce the required actuation force of the actuation mechanism to decrease the required power. Eqs. set (5.107) to (5.126) is used to calculate actuator force. This objective function is given as;

$$f(2) = maximum(F_{actuator}) \times G \qquad (6.30)$$

The third objective function is the symmetry error. The actuation mechanism will actuate both side door mechanisms to open doors symmetrically.

$$f(3) = abs\left(abs\left(\theta^{(2)}_{4,\text{initial}} - \theta^{(2)}_{4,\text{final}}\right) - abs\left(\theta^{(3)}_{4,\text{initial}} - \theta^{(3)}_{4,\text{final}}\right)\right) G \qquad (6.31)$$

6.3.2.2. Constraints of Concept A3

Concept A3 is constrained according to different limitations.

The first limitation is the transmission angle to find a suitable mechanism. These constraints are given in Eq. (6.32), Eq. (6.33), and (6.34).

$$156° \geq \mu^{(1)} \geq 30° \tag{6.32}$$

$$156° \geq \mu^{(2)} \geq 30° \tag{6.33}$$

$$156° \geq \mu^{(3)} \geq 30° \tag{6.34}$$

The second limitation is the total allowable space envelope given in Figure 6.18 for the door opening mechanism and actuation mechanism. The door opening mechanism fixed pivot, A_0 is located at (230, 50). Therefore, these constraints given in the Eq. (6.35), Eq. (6.36), and (6.37) are defined based on the total allowable space envelope, and door opening mechanism fixed pivot, A_0.

$$229.99mm < r_1^{(2)} \times cos\left(\theta_{11}^{(2)}\right) < 230.01mm \tag{6.35}$$

$$s_{1,final} \times sin\left(\theta_{11}^{(1)} + \theta_{12,final}^{(1)}\right) - r_1^{(1)} \times sin\left(\theta_{11}^{(1)}\right) - r_1^{(2)} \times \sin\left(\theta_{11}^{(2)}\right) < 40 \tag{6.36}$$

$$r_2^{(3)} \times sin\left(\theta_{11}^{(3)} + \theta_{12,final}^{(3)}\right) - r_1^{(2)} \times \sin\left(\theta_{11}^{(2)}\right) < 40 \tag{6.37}$$

Other constraints are defined to obtain symmetrical motion.

$$r_1^{(3)} = r_1^{(2)} \tag{6.38}$$

$$\theta_{11}^{(3)} = 180° - \theta_{11}^{(2)} \tag{6.39}$$

These given constraints are applied in the optimization code. If these constraints are not satisfied, the penalty function, G is taken as G = 1000000 to penalize and eliminate this solution.

The final limitation is the range for design variables. Design variables are determined according to design space limitations. The initial range of design variables is found by using graphical and analytical approaches. After finding initial ranges, an iterative process is applied to find the final suitable range of the design variables. The limits of

the design variables are given in Table 6.11. $r_1^{(3)}\ and\ \theta_{11}^{(3)}$ are calculated by using Eq. (6.38) and Eq. (6.39) therefore not given in Table 6.11.

Table 6.11. *Upper and lower boundaries of Concept A3's design variables*

	1	**2**	**3**	**4**	**5**
	$r_1^{(1)}$**(mm)**	$r_4^{(1)}$**(mm)**	s_0**(mm)**	$\theta_{11}^{(1)}$**(deg)**	Δ_{stroke} **(mm)**
Minimum	125	75	165	60	2,40
Maksimum	250	170	215	150	5
	6	**7**	**8**	**9**	**10**
	$r_1^{(2)}$**(mm)**	$r_2^{(2)}$**(mm)**	$r_3^{(2)}$**(mm)**	$r_4^{(2)}$**(mm)**	$\theta_{11}^{(2)}$**(deg)**
Minimum	200	75	185	65	20
Maksimum	275	110	260	90	45
	11	**12**	**13**	**14**	**15**
	$\alpha^{(2)}$**(deg)**	$r_2^{(3)}$**(mm)**	$r_3^{(3)}$**(mm)**	$r_4^{(3)}$**(mm)**	$\alpha^{(3)}$**(deg)**
Minimum	-130	85	190	65	60
Maksimum	-75	135	240	100	125

6.3.2.3. Results of Concept A3

After the optimization process, the optimized mechanism is synthesized. The calculated parameters are given in Table 6.12.

Table 6.12. *Optimized parameter values of Concept A3*

1	**2**	**3**	**4**	**5**
$r_1^{(1)}$**(mm)**	$r_4^{(1)}$**(mm)**	s_0**(mm)**	$\theta_{11}^{(1)}$**(deg)**	Δ_{stroke} **(mm)**
230,12	165,73	214,34	137,73	3,27
6	**7**	**8**	**9**	**10**
$r_1^{(2)}$**(mm)**	$r_2^{(2)}$**(mm)**	$r_3^{(2)}$**(mm)**	$r_4^{(2)}$**(mm)**	$\theta_{11}^{(2)}$**(deg)**
249,95	96,41	231,83	71,16	23,05
11	**12**	**13**	**14**	**15**
$\alpha^{(2)}$**(deg)**	$r_2^{(3)}$**(mm)**	$r_3^{(3)}$**(mm)**	$r_4^{(3)}$**(mm)**	$\alpha^{(3)}$**(deg)**
-99,34	102,64	228,42	77,03	124,91

The computation time is 485 seconds for Concept A3 optimization process. The position error is evaluated as 2,89E-04 radians. Also, the maximum required input torque is calculated as 503,841 N and symmetry error is calculated as 8,9E-06 radian. The simulation of the optimized mechanism is given in Figure 6.25.

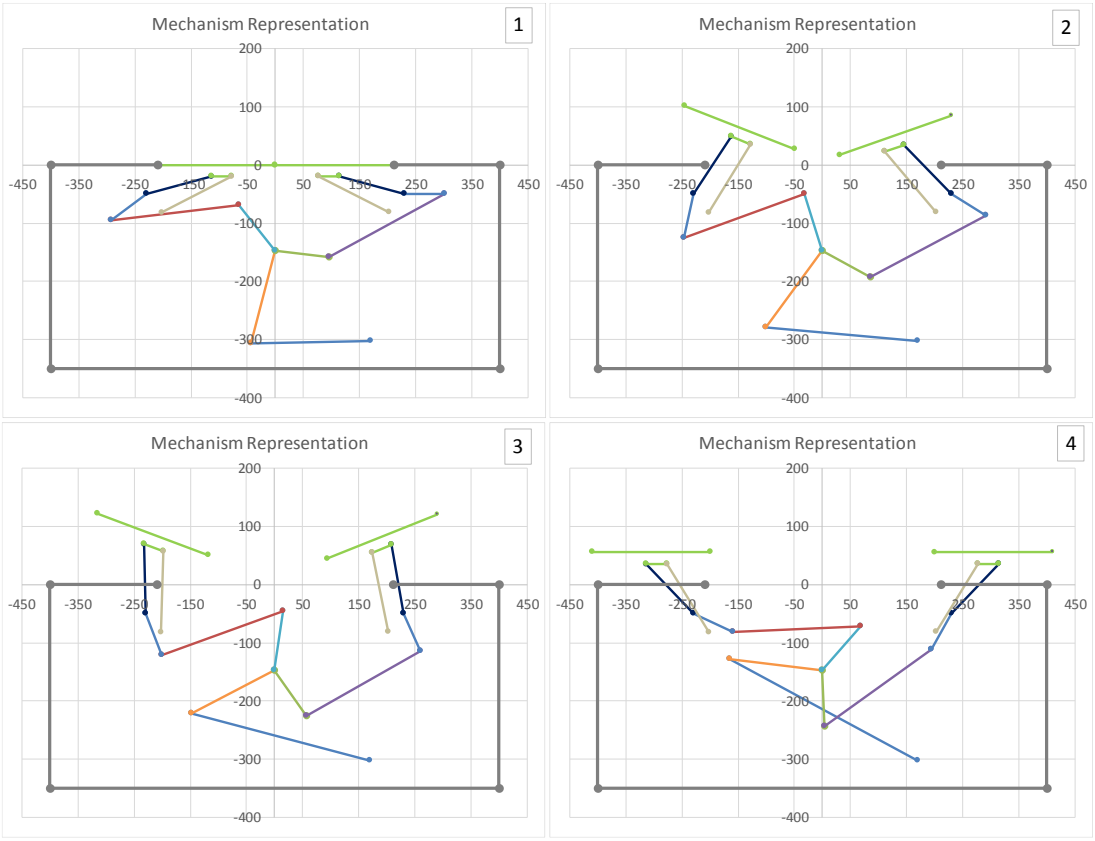

Figure 6.25. Simulation of the Concept A3 combined with Concept D1

The MSC ADAMS model is created in order to verify the calculation of the actuator force. The combination of the door mechanism (Concept D1) and the actuation mechanism (Concept A3) MSC ADAMS model is given in Figure 6.26. This figure shows joints, applied forces, and the given motion of the combined mechanism.

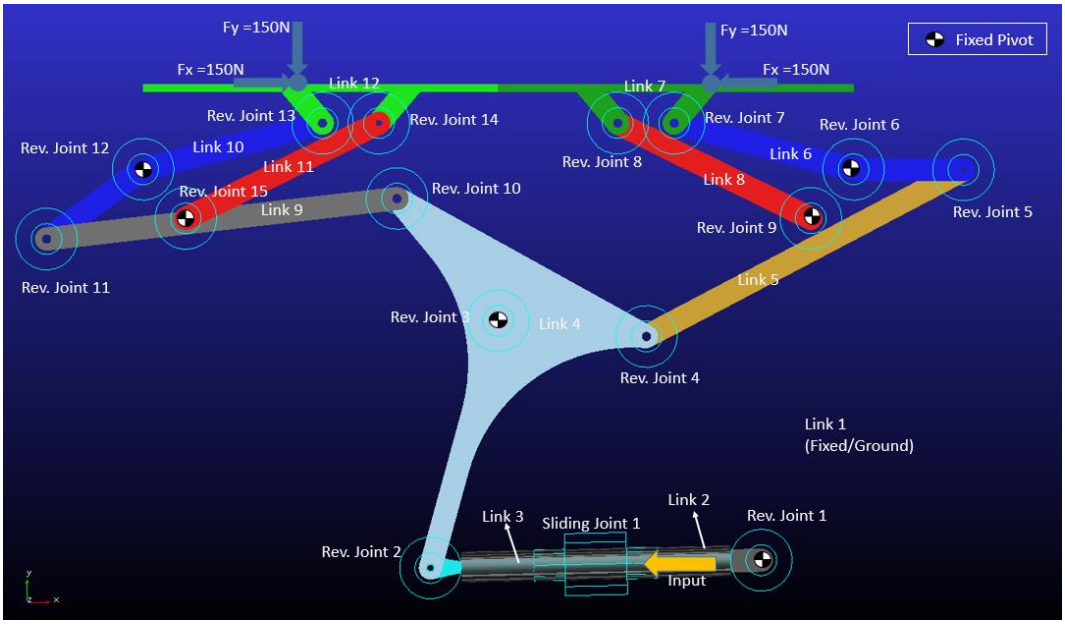

Figure 6.26. MSC ADAMS model of optimized Concept A3

Figure 6.27 shows the calculated required input torque by using MSC ADAMS and Genetic Algorithm with respect to the stroke of the actuator.

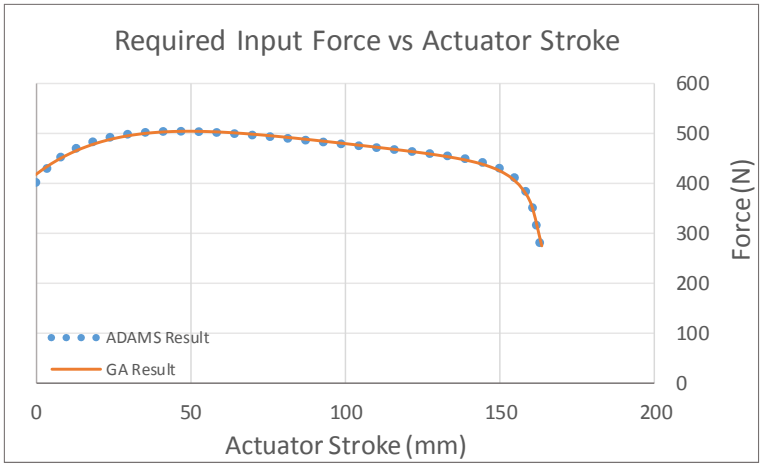

Figure 6.27. Required actuator force of Concept A3

The mechanism, which is synthesized by using the graphical approach, is also analyzed by using MSC ADAMS to compare the results of the Genetic Algorithm method. The calculated input force by using various methods is given in Figure 6.28.

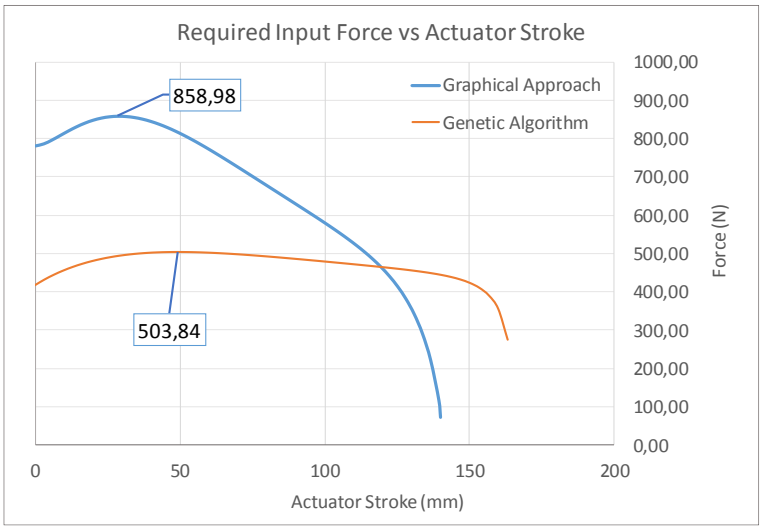

Figure 6.28. Calculated actuator forces comparison of different methods

Table 6.13 shows the maximum input forces of different methods and the percentage improvement of the Genetic Algorithm method compared to the graphical method.

Table 6.13. *Maximum actuator forces of Concept A3 and percent improvement*

	METHODS	
	Genetic Algorithm	**Graphical Approach**
Maximum Actuator Force (N)	503,84	858,98
Percent Improvement		41,34%

6.4. Comparison of Selected Actuation Mechanism Concepts

In this part, selected actuation mechanisms, Concept A1, Concept A3, and Concept A8 are compared among themselves, and one of the actuation mechanism is selected as the best concept.

The first criterion is the required power. Doors opening time is assumed as 5 seconds. Then, using ADAMS Software, the power consumption of the actuators are calculated. Figure 6.29 shows the total required power for the selected actuation mechanisms. According to the power requirement, Concept A1 and Concept A3 show better

characteristics than Concept A8 therefore, Concept A8 is eliminated, based on this criterion.

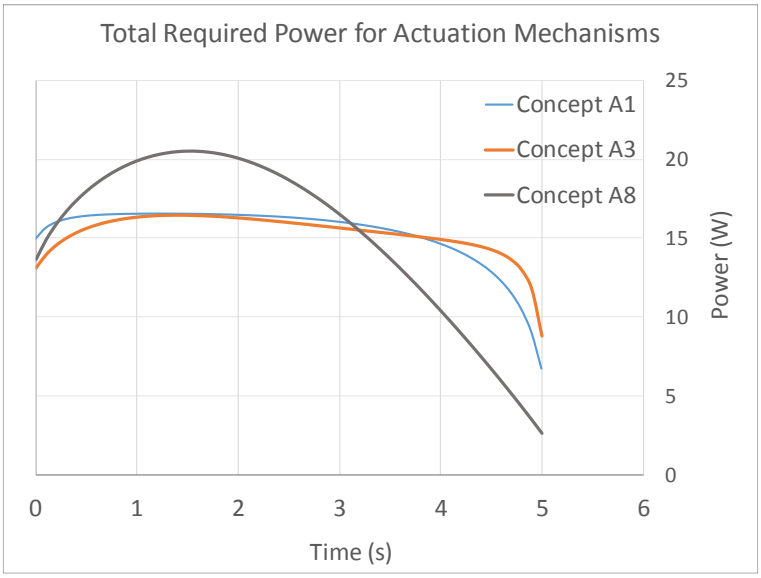

Figure 6.29. The required power of actuation concepts

Considering the optimized mechanisms, Concept A1 requires less space compare to Concept A3. In addition, a high number of links decrease rigidity and reliability. Therefore, Concept A1 is considered more rigid and reliable than Concept A3. Additionally, simplicity is another advantage of the Concept A1. For these reasons, Concept A1 is selected as the best actuation mechanism concept.

CHAPTER 7

DISCUSSION AND CONCLUSIONS

In this thesis, the preliminary design of an in-flight refueling door actuation mechanism is presented. Following a brief introduction and literature review to support this study, a method is defined to design an in-flight door actuation mechanism systematically. The design problem is divided into two sub-problems, which are door open/close function and actuation function.

Following the definition of the problem, different concepts were developed for each sub-problem according to requirements and constraints. In addition evaluation criteria were defined to evaluate and select the best suitable concepts systematically for each sub-problem. Six different mechanical engineers subjectively perform the evaluation process. After the evaluation process, two concepts were selected for the door mechanism, and three concepts were selected for the actuation mechanism.

Kinematic synthesis for each concept was performed by using graphical and analytical methods to obtain suitable mechanisms. In addition, the obtained results were used to determine the initial upper and lower boundaries of design parameters for the optimization process. Thereafter position analysis was executed by using Freudenstein's equation to check the motion of the synthesized mechanisms. Additionally, force analysis was performed to obtain the required actuation force and joint forces of the concepts. In this study, external forces acting on the system were estimated. Therefore, a detailed aerodynamic analysis is required to obtain more accurate actuator and joint forces in the detailed design stage. Also, it was assumed that masses of the components were negligible and inertia forces were ignored because the effect of the masses and inertia forces were relatively smaller than applied external forces. Axial forces were not taken into consideration. However, these forces may

increase joint forces and friction forces and affect the system force characteristic. In future works, the effects of the masses, inertial forces, and axial forces could be considered.

Finally, chosen concepts are optimized by using the Multi-objective Genetic Algorithm Optimization Method. Before the optimization process, the lower and upper boundaries of design parameters, objective functions, and constraints are specified. Then, for each sub-problem concept, the optimization process is performed, and optimized concepts are compared with each other to select the best concept. In this study, Concept D1 and Concept A1 are chosen as the best concepts. After determining the best concepts for each sub-problem, these concepts are combined to obtain the preliminary design of the in-flight refueling door actuation system mechanism.

REFERENCES

[1] W. Alyafie, “Automatic Door System of Bus Door,” 2012. [Online]. Available: https://www.slideshare.net/WaleedAlyafie/automatic-door-of-bus-door.

[2] B. Baykus, E. Anli, and I. Ozkol, “Design and Kinematics Analysis of a Parallel Mechanism to be Utilized as a Luggage Door by an Analogy to a Four-Bar Mechanism,” vol. 2011, no. April, pp. 411–421, 2011.

[3] N. D. Thang, “Mechanism.” [Online]. Available: https://www.youtube.com/user/thang010146/about.

[4] J. Soss, “Hinge,” US1484093A, 1924.

[5] J. A. M. Eng, A. Toropov, and R. Ad, “Kinematics of Invisible Hinge,” J. Appl. Mech. Eng., vol. 6, no. 4, pp. 4–11, 2017.

[6] C. Lanni and M. Ceccarelli, “An Optimization Problem Algorithm for Kinematic Design of Mechanisms for Two-Finger Grippers,” Open Mech. Eng. J., vol. 3, no. 1, pp. 49–62, 2009.

[7] A. J. G. Nuttall and A. J. Klein Breteler, “Compliance Effects in a Parallel Jaw Gripper,” Mech. Mach. Theory, vol. 38, no. 12, pp. 1509–1522, 2003.

[8] K. Youssefi, “Synthesis of Mechanism.” Augusta Stafford, p. 10, 2018.

[9] G. N. Sandor and A. G. Erdman, “Advanced Mechanism Design”, Volume 2., Prentice-Hall International, Inc., London, 1984, pp. 76–90.

[10] A. Kunjur and S. Krishnamurty, “Genetic Algorithms in Mechanism Synthesis,” J. Appl. Mech. Robot., vol. 4, no. 2, pp. 18–24, 1997.

[11] J. A. Cabrera, A. Simon, and M. Prado, “Optimal Synthesis of Mechanisms with Genetic Algorithms,” Mech. Mach. Theory, vol. 37, no. 10, pp. 1165–1177, 2002.

[12] M. A. Laribi, A. Mlika, L. Romdhane, and S. Zeghloul, “A Combined Genetic Algorithm-Fuzzy Logic Method (GA-FL) in Mechanisms Synthesis,” Mech. Mach. Theory, vol. 39, no. 7, pp. 717–735, 2004.

[13] L. İpek, “Optimization Of Backhoe-Loader Mechanisms,” METU, 2006.

[14] L. G. Reifschneider, “Teaching Kinematic Synthesis of Linkages without Complex Mathematics,” J. Ind. Technol., vol. 21, no. 4, pp. 17–32, 2005.

[15] F. Freudenstein, “An Analytical Approach to the Design of Four-Link Mechanisms,” Trans. ASME, vol. 76, pp. 483–492, 1954.

[16] G. Pahl, W. Beitz, J. Feldhusen, and K.-H. Grote, Engineering Design A Systematic Approach. 2015.

[17] M. Özsipahi, “Design of a Car Door Window Regulator,” METU, 2009.

APPENDICES

Appendix A. Graphical Approach

The graphical approach [9] is a simple method to synthesize a planar mechanism. The procedure of this approach is explained by using Concept D1 case. The methodology for two-position synthesis is explained below;

The initial and final positions of the door are given in Figure A.1.

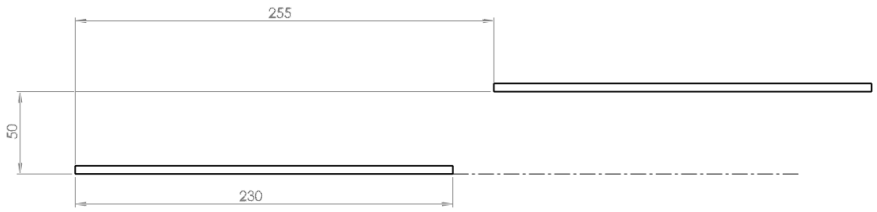

Figure A.1. Initial and final positions of the door

Then, two moving points, A1 and B_1 are selected on the door. These points are shown in Figure A.2.

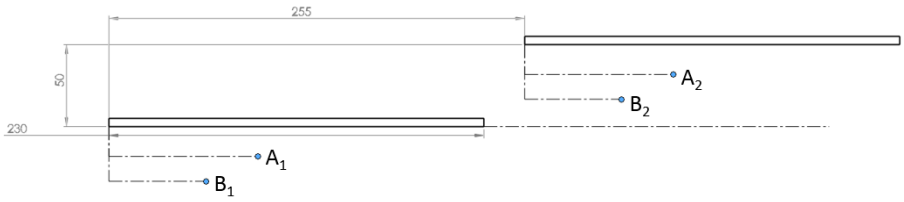

Figure A.2. Selection of moving points A_1 and B_1

The next step is to connect A_1 to A_2 and B_1 to B2. Figure A.3 shows this step.

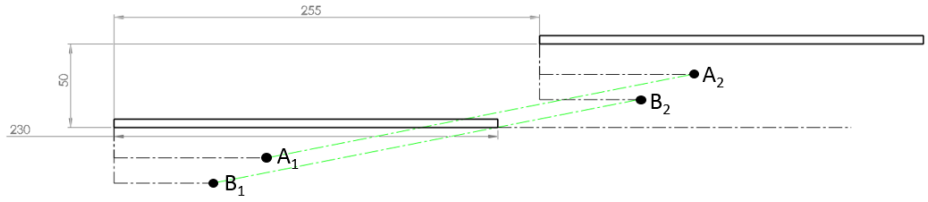

Figure A.3. A_1A_2 and B_1B_2 lines

Two lines are drawn a perpendicular to A_1A_2 and B_1B_2 at the midpoint.

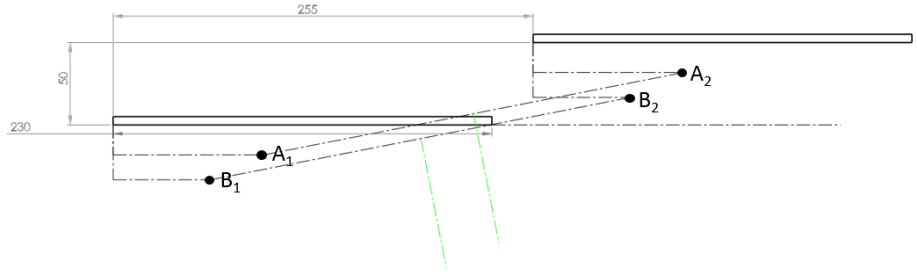

Figure A.4. Mid-normal of A_1A_2 and B_1B_2 lines

Two fixed pivot points, A_0 and B_0 are selected anywhere on the two mid-normal. A_0 and B_0 are shown in Figure A.5.

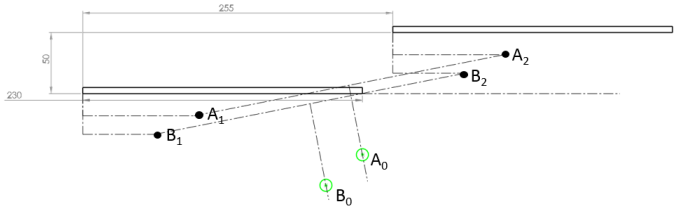

Figure A.5. Selection of fixed points A_0 and B_0

The synthesized mechanism using the graphical approach is shown in Figure A.6.

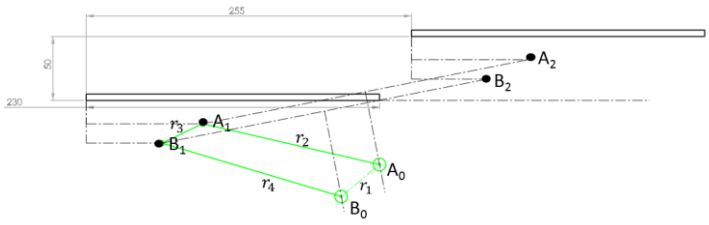

Figure A.6. Synthesized Concept D1 schematic (Graphical Approach)

Appendix B. Analytical Method

In the dyadic approach introduced by Erdman [9], planar linkages are considered as a combination of vector pairs called dyads, each of all realizes the motion independently thorough the prescribed positions. For example, the four-bar linkage in Figure B.7 can be seen as two dyads. The left side of the linkage represented as a vector pair ($\mathbf{W_A}$ and $\mathbf{Z_A}$) and the right side of the linkage represented as a vector pair ($\mathbf{W_B}$ and $\mathbf{Z_B}$). The vectors **AB** that represents coupler link and ground link, $\mathbf{A_0B_0}$ are determined by vector addition after these dyads are synthesized. All vector rotations are measured from the starting position. Angle β_2 represents the rotation of vector **W** from the initial position to the second position and β_3 represents rotation from the initial position to the third position. Similarly, angles α_j represent the rotation of vector **Z** from the initial position to the jth position. The dyads have to be solved separately. Then these dyads can be combined to form a whole mechanism. In the case of a four-bar mechanism, two dyads must be synthesized independently and must then be combined. In Figure B.7, the dyads of the four-bar mechanism are shown.

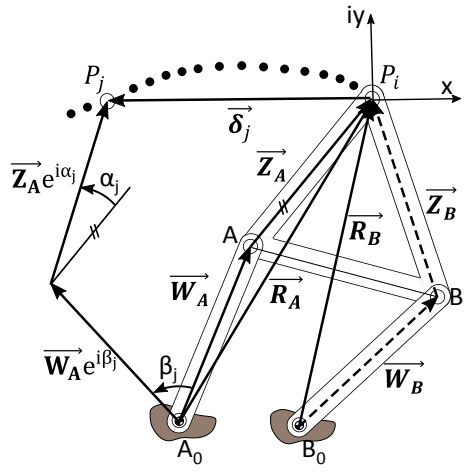

Figure B.7. Dyads of the four-bar mechanism

In the dyadic approach, the formulation gives the synthesis of a single dyad. The single dyad is shown in Figure B.8.

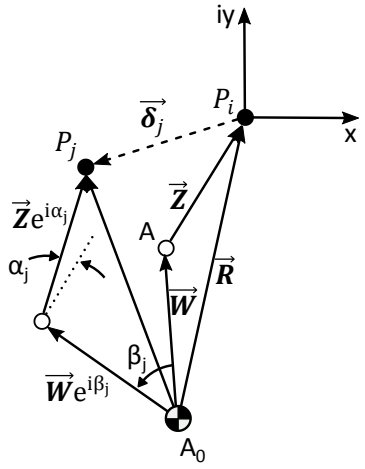

Figure B.8. Single dyad representation

Three-position synthesis with specified fixed pivots requires that $\boldsymbol{\delta_2 = (R_2 - R_1)}$, $\boldsymbol{\delta_3 = (R_3 - R_1)}$, α_2 , and α_3 be specified. It is noted that $\boldsymbol{\delta_j}$ represent displacement vectors. $\boldsymbol{R_1}$ has to be specified in order to specify the locations of center points. Synthesis equations for three finitely separated positions can be written as;

$$\boldsymbol{W + Z = R_1} \tag{A.1}$$

$$\boldsymbol{We^{i\beta_2} + Ze^{i\alpha_2} = R_2} \tag{A.2}$$

$$\boldsymbol{We^{i\beta_3} + Ze^{i\alpha_3} = R_3} \tag{A.3}$$

This set of the equation can be solved for $\boldsymbol{W}$ and $\boldsymbol{Z}$ only if the determinant of the coefficient matrix is identically zero.

$$\begin{vmatrix} 1 & 1 & \boldsymbol{R_1} \\ e^{i\beta_2} & e^{i\alpha_2} & \boldsymbol{R_2} \\ e^{i\beta_3} & e^{i\alpha_3} & \boldsymbol{R_3} \end{vmatrix} = 0 \tag{A.4}$$

Since the unknowns are in the first column, the determinant is expanded about this column:

$$\left(\boldsymbol{R_3}e^{i\alpha_2} - \boldsymbol{R_2}e^{i\alpha_3}\right) + e^{i\beta_2}\left(\boldsymbol{R_3} - \boldsymbol{R_1}e^{i\alpha_3}\right) + e^{i\beta_3}\left(\boldsymbol{R_2} - \boldsymbol{R_1}e^{i\alpha_2}\right) = 0 \tag{A.5}$$

Or

$$\boldsymbol{D_1} + \boldsymbol{D_2}e^{i\beta_2} + \boldsymbol{D_3}e^{i\beta_3} = 0 \tag{A.6}$$

Where

$$\boldsymbol{D_1} = \boldsymbol{R_3}e^{i\alpha_2} - \boldsymbol{R_2}e^{i\alpha_3} \tag{A.7}$$

$$\boldsymbol{D_2} = \boldsymbol{R_3} - \boldsymbol{R_1}e^{i\alpha_3} \tag{A.8}$$

$$\boldsymbol{D_3} = \boldsymbol{R_2} - \boldsymbol{R_1}e^{i\alpha_2} \tag{A.9}$$

Taking conjugate of Eq. (A.5):

$$\overline{\boldsymbol{D_1}} + \overline{\boldsymbol{D_2}}e^{-i\beta_2} + \overline{\boldsymbol{D_3}}e^{-i\beta_3} = 0 \tag{A.10}$$

Multiplying Eq. (A.6) and (A.10):

$$\boldsymbol{D_3}\overline{\boldsymbol{D_3}} = \boldsymbol{D_1}\overline{\boldsymbol{D_1}} + \boldsymbol{D_2}\overline{\boldsymbol{D_2}} + \overline{\boldsymbol{D_1}}\boldsymbol{D_2}e^{i\beta_2} + \boldsymbol{D_1}\overline{\boldsymbol{D_2}}e^{-i\beta_2} \tag{A.11}$$

Let

$$\Delta = \boldsymbol{D_1}\overline{\boldsymbol{D_1}} + \boldsymbol{D_2}\overline{\boldsymbol{D_2}} - \boldsymbol{D_3}\overline{\boldsymbol{D_3}} \;\; and \; t = e^{i\beta_2}, \frac{1}{t} = e^{-i\beta_2} \tag{A.12}$$

Then, a quadratic function is obtained as;

$$\overline{\boldsymbol{D_1}}\boldsymbol{D_2}t^2 + \Delta t + \boldsymbol{D_1}\overline{\boldsymbol{D_2}} = 0 \tag{A.13}$$

Eq. (A.13) is a quadratic function of the only t. One set of β solutions will be trivial (The trivial solution is $\beta_2 = \alpha_2$ & $\beta_3 = \alpha_3$). The non-trivial solution set of $\beta'S$ can be found by using Eq. (A.13). Plugging a nontrivial set of $\beta's$ into Eqs. (A.2) and (A.3) to find $\boldsymbol{W}\ and\ \boldsymbol{Z}$ by using Eqs. set (A.1) to (A.3). The same procedure can be applied for the second dyad. If both dyads are solved, unknowns are found, and the synthesis of the mechanism is completed.

Appendix C. Freudenstein's Equation

Four-bar Mechanism

Freudenstein's equation [15] approach is used when solving the four-bar mechanism for position analysis. The calculation steps are shown below.

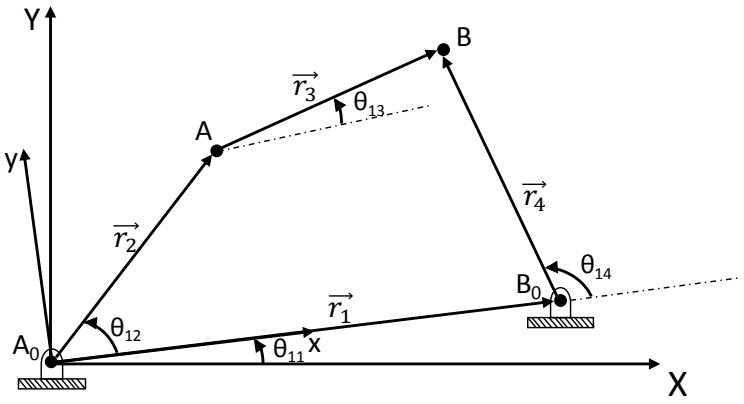

Figure A.9. Variables of the four-bar mechanism

The loop closure equation in vectorial form is given in the Eq. (A.14).

$$\overrightarrow{r_2} + \overrightarrow{r_3} - \overrightarrow{r_4} - \overrightarrow{r_1} = 0 \tag{A.14}$$

Complex number notation is given in the Eq. (A.15).

$$r_2 e^{i\theta_{12}} + r_3 e^{i\theta_{13}} - r_4 e^{i\theta_{14}} - r_1 = 0 \tag{A.15}$$

Real and imaginary parts are given in the Eq. (A.16) and Eq. (A.17).

$$r_2 cos\theta_{12} + r_3 cos\theta_{13} - r_1 = r_4 cos\theta_{14} \tag{A.16}$$

And

$$r_2 sin\theta_{12} + r_3 sin\theta_{13} = r_4 sin\theta_{14} \tag{A.17}$$

Then, adding squares of the Eq. (A.16) and Eq. (A.17) and dividing every term by $2r_3r_2$;

$$\frac{r_4^2 - r_1^2 - r_2^2 - r_3^2}{2r_3r_2} = -\frac{r_1}{r_3}cos\theta_{12} - \frac{r_1}{r_2}cos\theta_{13} + cos\theta_{12}cos\theta_{13} + sin\theta_{12}sin\theta_{13} \quad \text{(A.18)}$$

Or

$$K_1 = -K_2cos\theta_{12} - K_3cos\theta_{13} + cos\theta_{12}cos\theta_{13} + sin\theta_{12}sin\theta_{13} \quad \text{(A.19)}$$

Where,

$$K_1 = \frac{r_4^2 - r_1^2 - r_2^2 - r_3^2}{2r_3r_2} \quad \text{(A.20)}$$

$$K_2 = \frac{r_1}{r_3} \quad \text{(A.21)}$$

$$K_3 = \frac{r_1}{r_2} \quad \text{(A.22)}$$

Using half-angle identities and Eq. (A.19), θ_{13} can be found as

$$sin\theta_{13} = \frac{2\,tan\left(\frac{\theta_{13}}{2}\right)}{1 + tan^2\left(\frac{\theta_{13}}{2}\right)},\ cos\theta_{13} = \frac{1 - tan^2\left(\frac{\theta_{13}}{2}\right)}{1 + tan^2\left(\frac{\theta_{13}}{2}\right)} \quad \text{(A.23)}$$

Where

$$\tan\left(\frac{\theta_{13}}{2}\right) = W \quad \text{(A.24)}$$

Rearrange Eq. (A.19);

$$\begin{aligned} K_1 + K_1W^2 = {} & -K_2cos\theta_{12} - W^2K_2cos\theta_{12} - K_3 + cos\theta_{12} \\ & + (K_3 - cos\theta_{12})W^2 + 2Wsin\theta_{12} \end{aligned} \quad \text{(A.25)}$$

Then, grouping the tangent terms to form a quadratic form of the equation,

$$AW^2 + BW + C = 0 \quad \text{(A.26)}$$

Where,

$$A = (K_1 + K_2cos\theta_{12} - K_3 + cos\theta_{12}) \quad \text{(A.27)}$$

$$B = -2sin\theta_{12} \tag{A.28}$$

$$C = K_1 + K_2 cos\theta_{12} + K_3 - cos\theta_{12} \tag{A.29}$$

Then, the quadratic formula can be applied to find θ_{13}

$$\theta_{13} = 2 \times atan(\frac{-B + \sigma\sqrt{B^2 - 4AC}}{2A}) \tag{A.30}$$

Where $\sigma = \pm 1$

Then, from Eq. (A.16) and Eq. (A.17), θ_{14} can be calculated as;

$$\theta_{14} = \text{atan}(\frac{r_2 sin\theta_{12} + r_3 sin\theta_{13}}{r_2 cos\theta_{12} + r_3 cos\theta_{13} - r_1}) \tag{A.31}$$

Slider-crank Mechanism

Freudenstein's equation approach is also used when solving a slider-crank mechanism for position analysis. The only difference is that a prismatic joint is used instead of a revolute joint. Therefore, Freudenstein's equation cannot be used directly. The calculation steps are shown below for the slider-crank mechanism.

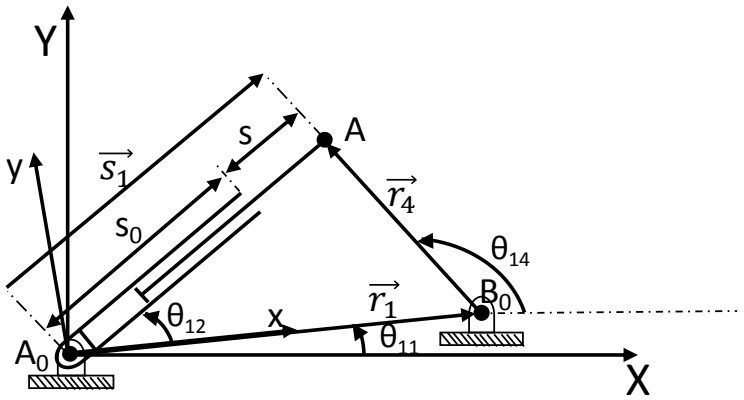

Figure A.10. Variables of piston-cylinder mechanism

The loop closure equation in vectorial form is given in the Eq. (A.32).

$$\overrightarrow{s_1} - \overrightarrow{r_1} - \overrightarrow{r_4} = 0 \tag{A.32}$$

Complex number notation is given in the Eq. (A.33).

$$s_1 e^{i\theta_{12}} - r_1 - r_4 e^{i\theta_{14}} = 0 \tag{A.33}$$

Real and imaginary parts are given in the Eq. (A.34) and Eq. (A.35).

$$s_1 cos\theta_{12} - r_1 = r_4 cos\theta_{14} \tag{A.34}$$

$$s_1 sin\theta_{12} = r_4 sin\theta_{14} \tag{A.35}$$

Then, adding squares of the Eq. (A.34) and Eq. (A.35) and dividing every term by $2s_1 r_1$;

$$\frac{r_4^2 - r_1^2}{2r_1} = \frac{s_1^2}{2r_1} - s_1 cos\theta_{12} \tag{A.36}$$

Where,

$$K_1 = \frac{r_4^2 - r_1^2}{2r_1} \tag{A.37}$$

Using half-angle identities,

$$sin\theta_{12} = \frac{2\,tan\left(\frac{\theta_{12}}{2}\right)}{1 + tan^2\left(\frac{\theta_{12}}{2}\right)}\,,\; cos\theta_{12} = \frac{1 - tan^2\left(\frac{\theta_{12}}{2}\right)}{1 + tan^2\left(\frac{\theta_{12}}{2}\right)} \tag{A.38}$$

And

$$\tan\left(\frac{\theta_{12}}{2}\right) = Z \tag{A.39}$$

Rearrange Eq. (A.36) by using Eqs. (A.37), (A.38), and (A.39), θ_{12} can be found as

$$(K_1 - \frac{s_1^2}{2r_1} - s_1)Z^2 + (K_1 - \frac{s_1^2}{2r_1} + s_1) = 0 \tag{A.40}$$

Eq. (A.41) can be written as

$$AZ^2 + C = 0 \tag{A.41}$$

Where,

$$A = K_1 - \frac{s_1^2}{2r_1} - s_1 \tag{A.42}$$

$$C = K_1 - \frac{s_1^2}{2r_1} + s_1 \tag{A.43}$$

Then, the quadratic equation formula can be applied to find θ_{12}

$$\theta_{12} = 2 \times atan\left(\sigma\sqrt{-\frac{C}{A}}\right) \tag{A.44}$$

Where, $\sigma = \pm 1$

Then, from Eq. (A.34) and Eq. (A.35), θ_{14} can be calculated as;

$$\theta_{14} = \text{atan}(\frac{s_1 sin\theta_1}{s_1 cos\theta_1 - r_1}) \tag{A.45}$$